Measuring
muscle and joint geometry parameters
for a shoulder model

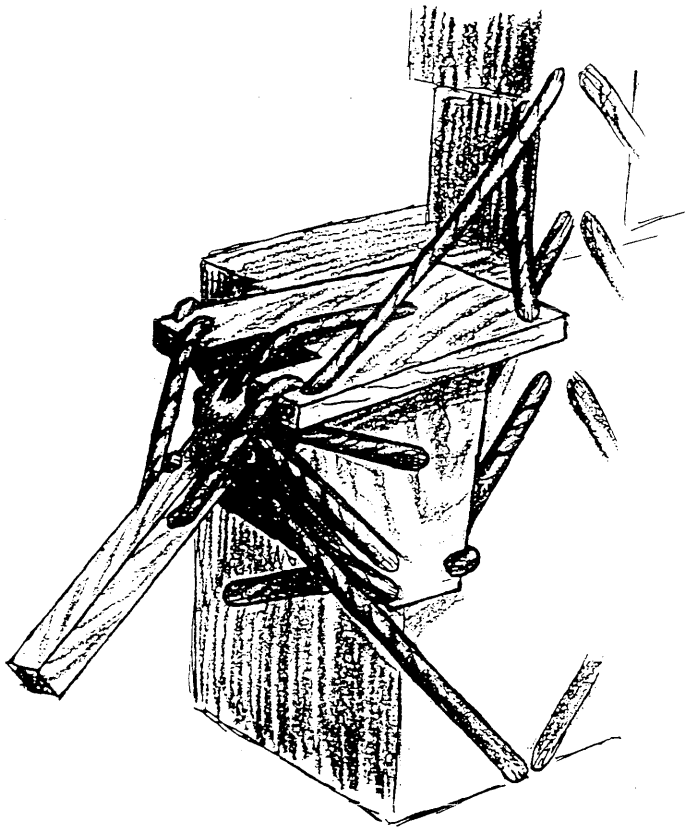

Vrije Universiteit
Faculty of human movement sciences
Department of: Functional anatomy
Research report and study of literature by:
Mary Klein Breteler
Supervisors: Spoor
Van der Helm
Huijing
Veeger

July, 1996

Contents

Abstract

An extensive set of muscle and joint geometry parameters is measured on the right shoulder of an embalmed 56-year-old male. The parameter set is needed for more accurate muscle and joint modelling of the shoulder.

Positions of palpable bony landmarks, muscle and ligament attachment sites and the articular surfaces were recorded with a very accurate (SD = 0.96 mm) 3-D digitizer, the "palpator". Muscles were manually divided in 2-15 muscle parts, depending on the size of the muscle. Muscle and fibre length of all muscle parts were measured with a ruler. The mass of all muscle parts was measured on a weighing device. Sarcomere lengths in all muscle parts were measured using laser diffraction. From the measured data the model parameters were calculated: joint rotation centres, segment centres of gravity, segment mass, rotational inertia, physiological cross-sections and mathematical descriptions of spheres, a cylinder and an ellipsoid around which muscles are curved.

Tendon length, optimum fibre length and the physiological cross-section were calculated. These parameters are needed to calculate the force-length relationship of a muscle, which determines the force that a muscle part maximally can exert.

Within a muscle only small differences in the sarcomere length were found in the position measured. For example in the m. deltoideus, a steady incline of sarcomere length in adjacent muscle parts was noticed.

After implementation of the model parameters in a computer model of the shoulder, an abduction of the arm was simulated with steps of 30°. For the simulations a computer model of the shoulder was used, which is developed at the Man-Machine Systems Group of the Laboratory of Measurement and Control at the Delft University of Technology. In each of these positions, actual sarcomere length was calculated from the muscle length (which is, among others, output of the model). With a curve that represents the sarcomere force-length relationship it can be seen how much force all muscle parts maximally can exert in each position. For most muscle parts it could be seen that the complete movement (the simulated abduction) takes place within the range in which force can be exerted. Muscle parts act on the ascending limb as well as on the plateau and on the descending limb.

The shape of the force-length relationship is discussed and also the influence of movement and stimulation frequency on the shape of the force-length curve. Other studies on sarcomere length range are compared with the sarcomere lengths measured and calculated in this study.

With these experiments a very complete dataset is created that is not only important for the development of the shoulder model, but also for functional analysis of shoulder movements in general.

Chapter 1: Introduction

The human shoulder is a very complex mechanism. Unlike quadrupeds the forelimbs of man are not used for support of the own body weight but for manipulation. For manipulation a stable base and a wide movement range are needed. Stability is provided for by three bones that form the shoulder girdle: thorax, clavicula and scapula (Figure 1). The thorax is assumed to be a rigid bone. Together this chain of bones functions as a moveable but stable base for support of the upper arm. The orientation of the glenoid cavity, which is part of the scapula, can be varied with the humerus orientation. The combined change of orientation of the glenoid cavity and rotation in the glenohumeral joint provide a wide movement range for the arm. The four bones are connected by sixteen muscles and five ligaments.

In order to study the complex movements of the shoulder mechanism a computer model is developed at the Man-Machine Systems group of the Laboratory for Measurement and Control at the Delft University of Technology. The computer model is based on the finite element theory (Pronk, 1991; Van der Helm, 1991; Van der Helm 1994b). Morphological structures are represented by elements of which the dynamical behaviour is well-known. A bone, for example, is represented by a rigid body, relative to which all points are defined. A muscle is represented by a truss with a variable length. Because the dynamic behaviour of the single elements is known, the dynamic behaviour of the whole system can be calculated by connecting the elements.

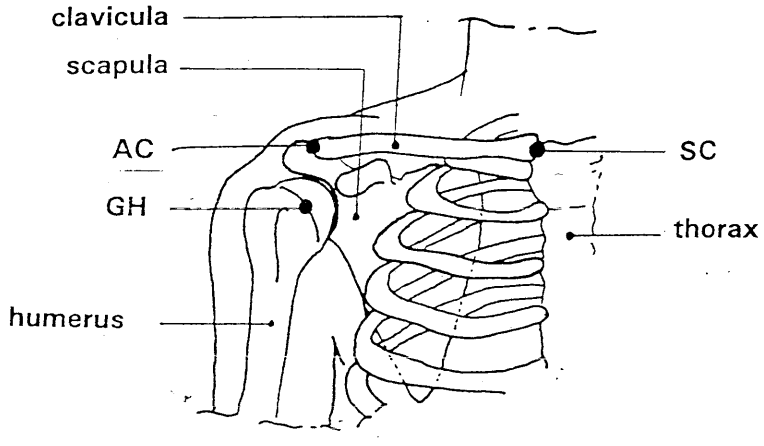

Figure 1.
Bones in the shoulder that are represented by rigid bodies. Frontal view of the right shoulder girdle.
SC = sternoclavicular joint
AC = acromioclavicular joint
GH = glenohumeral joint

Kinematic as well as dynamic situations can be simulated with the shoulder model. In a kinematic situation, for example, the shoulder model is used for analysis of a glenohumeral arthrodesis. This is a surgical operation in which the cartilage of the glenohumeral joint is removed and the hu-

merus and scapula are fused. The operation is done when someone is not able to elevate the humerus by a rotation in the glenohumeral joint because of a permanent paralysis of the shoulder muscles, caused by a brachial plexus injury. Once the scapula and humerus are fused, the humerus can be elevated by a rotation of the scapula. The importance of the computer model is to determine the optimal angle at which the scapula and humerus should be fused in order to obtain the desired motion range of the hand.

In a dynamic situation, the model is used for calculating the load in the shoulder during wheelchair propulsion. In different combinations of chair height and position of the chair with respect to the wheels, net joint moments in the shoulder can be calculated. From net joint moments, muscle forces can be calculated. The chair combination that causes the least muscle forces in the shoulder is the one most suitable for that particular person.

1.1 The shoulder model

For a better understanding of the purpose of this research, first a short description of the shoulder model is given.

In the finite element model of the shoulder, each morphological structure that contributes to the motions of the shoulder is represented by a simplified element that describes the behaviour of that particular structure. For an extensive description, see Van der Helm (1991), Van der Helm (1994a) and Van der Helm (1994b). Here follows a short description of each element.

1.1.1 Bones

The shoulder model consists of four bony structures (see Figure 1): the thorax, clavicula, scapula and humerus. The bones are represented by rigid MULTINODE elements. A local co-ordinate system through the MULTINODE element is defined in which all data points on the bone are expressed. Each MULTINODE element is subject to gravity and has inertial properties.

1.1.2 Joints

The bones are connected by joints. The sternoclavicular (SC) joint, the acromioclavicular (AC) joint and the glenohumeral (GH) joint are represented as a spherical joint by three perpendicular HINGE elements. The translational degrees of freedom are neglected.

The scapula is connected to the thorax by the scapulothoracic gliding plane. Displacement of the scapula is constrained, because the upper and lower points on the medial border of the scapula are forced to follow an ellipsoid SURFACE element, representing the surface of the thorax (Figure 2).

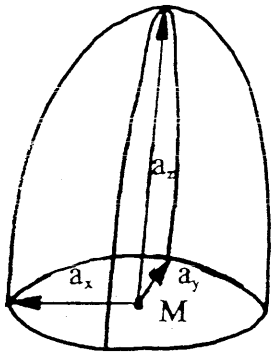

Figure 2.
An ellipsoid is fitted to the thorax. Parameters of the ellipsoid are the co-ordinates of the centre of the ellipsoid (M_x, M_y, M_z) and the lengths of the axes of the ellipsoid (a_x, a_y, a_z).

1.1.3 Ligaments

Ligaments are represented by TRUSS elements. The lig. conoideum has a fixed length, which determines the rotation angle of the clavicula about its long axis. The other ligaments can vary in length. Except for the lig. conoideum, the ligaments are unable to generate force. With inverse dynamics irrational forces would occur. With forward dynamics a passive force-length relationship would have to be known.

1.1.4 Muscles

Muscles are represented by TRUSS or CURVED-TRUSS elements with variable length. CURVED-TRUSS elements follow bony contours that are represented by a sphere, an ellipsoid or a cylinder. The shoulder model calculates the shortest way between origo and insertion around a bony contour. The ellipsoid SURFACE element that represents the thorax is also used as bony contour, to determine the curve of the m. serratus anterior. Two spheres are fitted through measured points on the surface of the proximal part of the humerus. One sphere is fitted to points on the articular surface to determine the position of the rotation centre of the GH-joint, and to determine the curve of the m. supraspinatus, m. subscapularis, m. teres minor and the long head of the m. biceps. The second sphere, through the tuberculum majus and tuberculum minus and the proximal dorsal humerus, is for determination of the curve of the m. deltoideus. A cylinder is estimated through the surface of the humerus shaft. This surface is used to calculate the curve of the m. latissimus dorsi, m. teres minor and m. pectoralis major.

A muscle is modelled by a muscle belly attached to the bones by tendons. The length of a tendon is assumed to be fixed. The muscle belly is allowed to shorten and lengthen. Force output depends on the physiological cross-section at optimum length, on the relative length of the muscle fibres and on the contraction velocity. The length dependency, the force-length relation, will be discussed in chapter 4.

1.1.5 Short description of the working of the model

Input variables are position co-ordinates of palpable bony structures at different positions during the movement that is to be simulated, namely the y- and z-co-ordinates of the acromioclavicular joint and the x-co-ordinate of the trigonum spinae, and also three rotations of the humerus and the direction of the external force, which in the case of gravitational force is directed downwards. The input variables are measured on the subject whose movements are to be simulated.

Model parameters are included in the shoulder model. The model parameters are measured on the cadaver: positions of palpable bony structures, positions of rotation centres, positions of attachment sites of all muscle parts and ligaments, physiological cross-sections of all muscle parts, weight of all bones and inertia of all modelled body segments. These parameters are included in the model.

In the inverse dynamic approach the model first calculates the full kinematic position, i.e. the orientation of the bones, while taking into account the given input variables and the motion constraints of the lig. conoideum and the scapulothoracic gliding plane. To this purpose the medial border of the scapula is pressed against the thorax. When the orientation of the bones is calculated, muscle length, the direction of muscle force, and moment arms can be calculated.

Then the dynamical part follows. Joint moments are calculated that are necessary to resist the gravitational and external forces. Muscle forces are then calculated by an optimization criterion. Since there are more muscle parts than degrees of freedom, muscle forces have to be calculated with an optimization procedure. This procedure minimizes the sum of squared muscle stresses in the entire system.

It is the optimization procedure for which more muscle parameters need to be known. The criterion for activation (or not) of a muscle part is not only a favourable moment arm. Also the maximum force of a muscle part, at maximum activation, is of importance. The maximum force depends, apart from the physiological cross-section, on the relative muscle length, which cannot be calculated without these additional muscle parameters.

1.2 Additional parameters for muscle and joint modelling

For a good description of the dynamic part of the shoulder model, some additional parameters are needed. The main purpose of this study is to measure these muscle geometry parameters so that a better muscle model can be implemented in the shoulder model. The most important parameters that are additionally measured in this research are sarcomere length and muscle fibre length.

Because these lengths have to be compatible with the dimensions of the cadaver, a complete new set of parameters had to be measured. A second goal of this research is to measure

some of the parameters in a more accurate and realistic way. These parameters are attachment sites and lines of action and rotation centres.

A third goal is to measure also the glenohumeral and sternoclavicular ligaments to study their dynamical behaviour.

1.2.1 Sarcomeres, fibres and tendons

The smallest functional part of the muscle is the sarcomere. In general a series of sarcomeres lined up in a chain form a muscle fibre. A collection of parallel muscle fibres form a muscle belly. The muscle belly is attached to the skeleton by two tendons. If the dynamical behaviour of the sarcomeres and the tendon is known, and the muscle geometry and pennation angle is known, a muscle model can be constructed. With this muscle model the maximal force output at a given muscle length can be calculated. The force output depends on the cross-section of the muscle belly and on the actual length of the sarcomeres. To calculate the actual sarcomere length, in addition to the actual total length of the muscle-tendon complex, the tendon length and optimum fibre length have to be known.

In this research sarcomere lengths, fibre lengths and muscle lengths are measured. Tendon length is assumed to be fixed, since a length change of about 4% in short tendons is negligible, and is the total length of the muscle-tendon complex minus the muscle fibre length. Optimum fibre length is the measured fibre length divided by the measured sarcomere length and multiplied with the optimum sarcomere length.

1.2.2 Determination of attachment sites and lines of action of muscles

Until now a muscle in the model was represented by a number of line segments that can lengthen and shorten and exert a certain amount of force. Six lines of action were assumed to be sufficient, because a joint which is crossed by the muscle can maximally have six degrees of freedom (three translations and three rotations).

For determination of the origo or insertion of a muscle, first many attachment points were measured (Veeger et al., 1991). To these points a surface or a line was fitted. If there was a clear round tendon, one point sufficed. The mathematical description of this surface, line or point is the origo or insertion of the muscle.

Next, the lines of action are to be divided over the origo and insertion. If there is a clear round tendon, a singular attachment site can be appointed, but if there is a large attachment area, the procedure is more complicated. In the earlier model one solved the problem by making a mathematical function that describes the distribution of the lines of action on a part of the origo or insertion. According to this function (with a so-called t-criterion) maximally six attachment sites were appointed (Van der Helm & Veenbaas, 1991; see Figure 3). Physiological cross-sections of

all six muscle parts were assumed to be equal.

In this study the mathematical division of six lines of action is thought to be too artificial. An attempt will be made to approach reality better by manually dividing the muscle in a few or more muscle parts, depending on the size and appearance of the muscle. An optical centroid of origo and insertion for each muscle part will be measured.

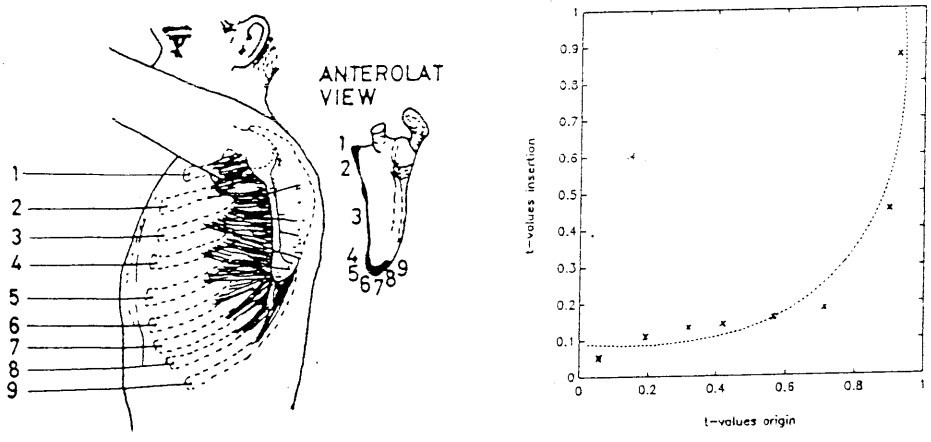

Figure 3.
Mapping of the t-values of the origin (t_0) to the t-values of the insertion (t_i), in order to obtain the direction of the muscle bundles of the m. serratus anterior. x = t-values of recorded attachment points. (Van der Helm and Veenbaas, 1991)

1.2.3 Position of rotation centres

In the former model it was assumed that there were no translational degrees of freedom in the sterno-clavicular joint and acromioclavicular joint. The rotation centre was positioned in the centre of the articular surface. In the present study a better estimation of the position of the rotation centres was made with the help of screw axes.

1.2.4 Ligaments

Attachment sites of a number of ligaments were measured (see Figure 4). Besides, for different orientations of the clavicula and scapula it was noted whether the ligaments between them were tight or slack. From these experiments the lengths of the unloaded ligaments can be derived.

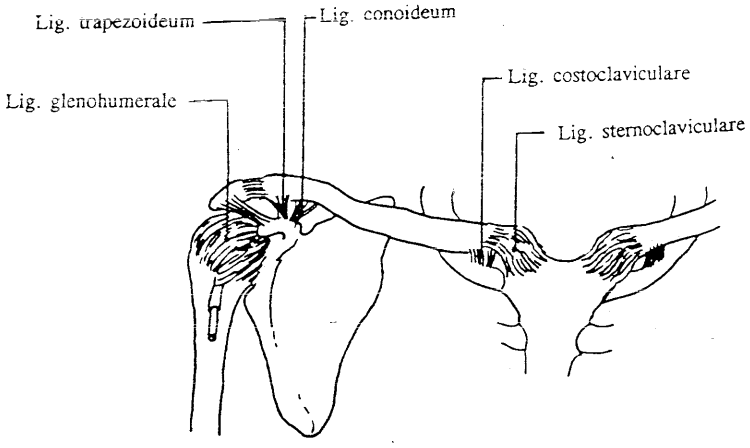

Figure 4
Ligaments in the shoulder.

1.3 In short

A whole new set of geometry parameters is measured. Since this is the most complete dataset of a human shoulder measured until now, applications will not be restricted to the present shoulder model. These parameters can also be used for muscle modelling in other applications, and for functional analysis of shoulder movements in general.

In the next chapter the recording and processing of the muscle and joint geometry parameters will be described and also a simulation of an abduction and anteflexion, followed in the third chapter by the results. In the fourth chapter the results will be discussed and also the shape of the force-length relationship of sarcomeres and muscles will be discussed. In the last chapter some concluding remarks and recommendations will be made.

Chapter 2: Methods

2.1 Morphology measurements

Measurements were performed on the right shoulder of the cadaver of a 57-year-old muscular man. Length and weight of the cadaver could not be determined since the legs were removed as the cadaver became available. Total body length was estimated to be 168 cm with the help of proportional dimensions, mentioned by Martin and Saller (1957). The cadaver was attached to a stainless steel frame with stainless steel pins so that the thorax was fixed rigidly to the frame. The cadaver could be easily put upright with the help of the frame.

In every part of the skeleton, i.e. head, thorax, clavicula, scapula, humerus, radius and ulna, four or five screws were driven. These screws were evenly and non-collinearly distributed over the bone, so that they could be used as reference points for measuring changes in position and orientation.

Before the dissection was started, the positions of four reference points on the frame, 18 palpable bony structures (see Figure 5) and all screws were measured. The positions of the skeletal parts as determined in this measurement were used as standard body posture.

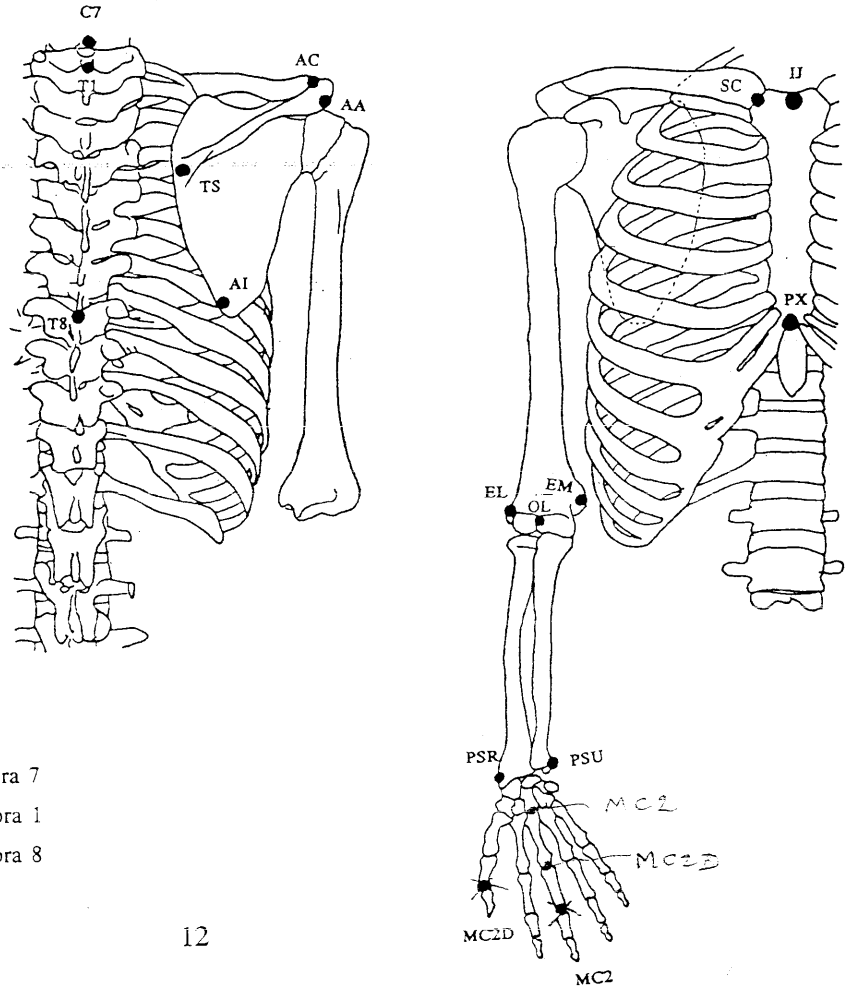

Figure 5.
All palpable bony contours:
IJ = Incisura Jugularis
PX = Processus Xiphoideus
SC = Sternoclavicular joint
AC = Acromioclavicular joint
AA = Angulus acromialis
TS = Trigonum Spinae
AI = Angulus Inferior
EL = Epicondylus lateralis
EM = Epicondylus medialis
PSU = Processus styloideus ulnae
PSR = Processus styloideus radii
MC2 = Metacarpale 2, cranial end
MC2D = Metacarpale 2, distal end
OL = Olecranon
C7 = Processus spinale of Cervical vertebra 7
T1 = Processus spinale of Thoracal vertebra 1
T8 = Processus spinale of Thoracal vertebra 8

2.1.1 The palpator

For measuring positions the palpator was used (Pronk & Van der Helm, 1991; Veeger et al., 1991). The palpator is a device that exists of four bars that are connected by hinge joints provided with potentiometers (see Figure 6). The potentiometers measure the rotations in the hinge joints. From the lengths of the bars and the rotations in the hinge joints the position of the end of the last bar can be calculated. The last bar has a sharp tip at the end with which a position can be pointed at. By pressing a button the position of the tip of the palpator is recorded. The palpator is a very accurate measurement device. The measurement error has a standard deviation of 1.43 mm in absolute distance (Pronk & Van der Helm, 1991).

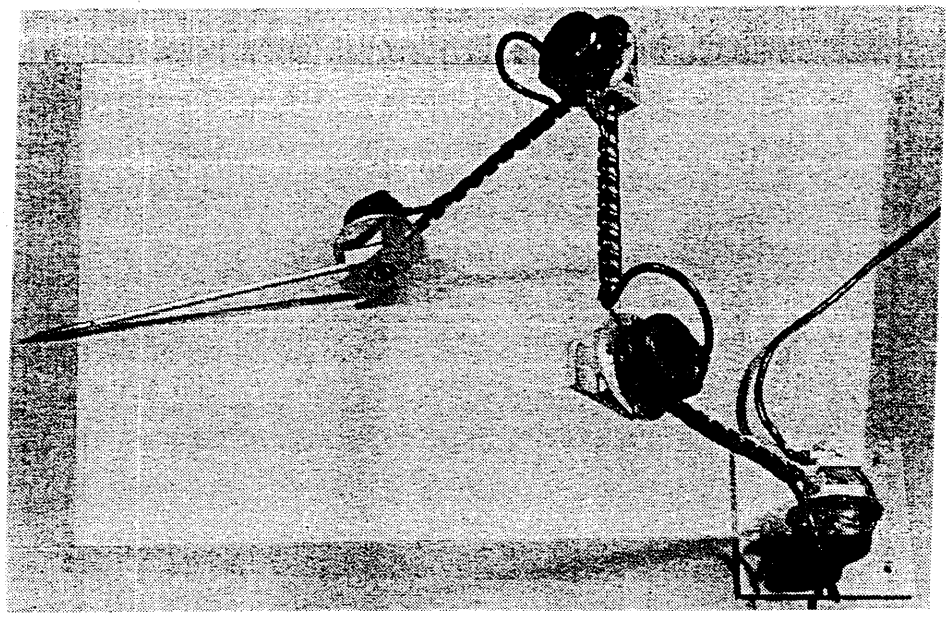

Figure 6.

The palpator is composed of four links,connected by four hinges with potentiometers placed on it. On the final link a sharp tip is attached. With the palpator three-dimensional co-ordinates can be recorded.

2.1.2 The dissection

First the skin and all the fatty tissues over and between the muscles was removed as good as possible. Every muscle was loosened from its surrounding without disconnecting the origo or insertion from the bone. For every muscle it was decided in how many parts it was to be divided. Criteria were: the size of the total muscle, attachment sites on different parts of the skeleton, difference in muscle fibre length, difference in the angle between muscle fibre and bone, attachment to another tendon plate or already existing gliding planes between parts of the muscle. For every muscle part, the beginning and end of an estimated representative muscle fibre were

marked. A numbered label was attached to the bone and another one to the muscle. The label was attached to the bone with a split pin or with a nail, depending on the thickness of the bone. Because bone tissue is too hard to hammer a nail in it, first a hole had to be drilled. The label on the muscle was sewn with needle and thread. For every attachment site it was noted which label on the bone belonged to which label on the muscle.

For most muscles (m. coracobrachialis, m. deltoideus, m. infraspinatus, m. pectoralis major, m. serratus anterior, m. subscapularis, m. supraspinatus, m. teres major, m. trapezius and m. triceps), it was not possible to divide the muscle in situ, because part of the muscle was hidden or because no separate parts could be distinguished from the outside. In that case the complete muscle was cut loose, meanwhile marking a lot of attachment sites on the muscle as well as on the bone and noting which label on the bone belonged to which label on the muscle. Then the muscle was divided into parts, without separating the muscle parts at the origo and insertion. Beginning and end of an estimated representative muscle fibre for every muscle part was marked on the muscle. The muscle was fitted back onto the bones with the help of the initially attached labels and the origos and insertions of the representative fibres were copied to the bone and labelled.

After all muscles had been removed from the cadaver, again measurements with the palpator were performed. For the acromioclavicular and sternoclavicular joint a number of extreme postures were measured. The postures were limited by ligaments or bony contact. In every posture the positions of the reference screws were measured. It was also noted down which ligaments were stretched or slack. For the SC-joint screw positions of the thorax, clavicula and scapula were measured as the scapula was held in a number of extreme positions. For the AC-joint first the SC-joint was cut loose. The clavicula and scapula were fixed to a frame in extreme postures and the screws were measured.

After the positions of origos and insertions of all ligaments had been measured, the ligaments were cut. The bones were separated. Positions of points all over the surfaces of the joints were measured, together with the reference screws.

Finally on every bone the reference screws and the attachment sites of all muscle parts were measured with the palpator.

2.1.3 Muscle length and muscle fibre length

The length of each muscle part was measured with the help of a string and a ruler. The string was laid tightly along the muscle and held at the positions of the labels that marked the beginning and end of the muscle part. This length was measured along the ruler. The muscle had to be laid down on a flat surface first, because some muscles were crinkled or ran over a curved surface.

From every muscle part three fibre bundles were taken, approximately 2 mm in diameter. The bundles were representative for that muscle part. If, for example, a muscle part consisted of long and some shorter muscle fibres, two long and one short fibre bundles were taken. Of each fibre

bundle the length was determined by laying the fibre bundle on the ruler. The mean length of the fibre bundles was considered to be the fibre length of that muscle part.

2.1.4 Sarcomere length and laser diffraction

Because of the striated character of skeletal muscles, sarcomere length can be measured by laser diffraction. A small part of a muscle fibre is regarded as a lattice, with the A-band with the thick myosin filaments and part of the actin filaments in between as bars, and the I-band with only the thinner actin filaments as slits in between through which the laser light can pass. The laser tube was positioned on a fixed distance from the wall (see Figure 7). On the wall a scale was attached in order to be able to directly read the sarcomere length.

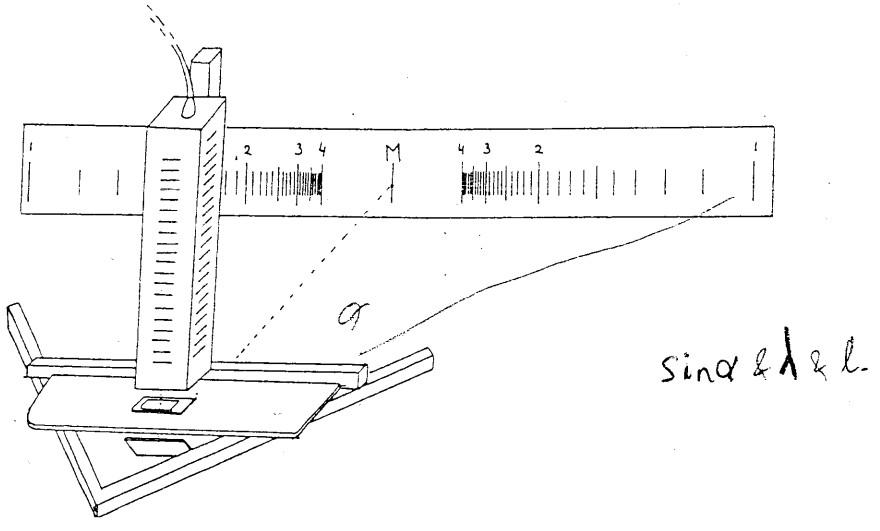

Figure 7. The laser diffraction line-up.
A vertical laser tube is mounted on a frame. Below the laser tube is a horizontal metal stage to support slides with muscle samples. The laser light passes through a hole in the stage, reflects in a 45°-mirror and is projected onto a scale on a wall.

The samples of the fibre bundle had to be quite thin, so that the laser light could shine through them. Samples were about 1 cm long and about 10 muscle fibres in cross-section. Viewing through an operation microscope, a number of thin muscle samples were cut from every fibre bundle. The samples were so thin that it was not really possible to cut them (The scalpel was thicker than the samples). The samples had to be eased apart.

Beforehand it was checked whether the sample preparation had any noticeable influence on the sarcomere length. A sample of about 4 cm long was loosened with as little pulling as possible. This fibre part was so long that it was possible to pull on both sides with tweezers.

Before pulling, the sarcomere length of the long sample was determined. While the sarcomere length could be read on the scale, the sample was pulled on both ends. The sarcomere length was seen to increase up to 4.2 μm. Then the sample broke. After releasing the sample, sarcomere length decreased to the starting length of 3.1 μm. From this experiment it was concluded that the sample preparation does not affect the sarcomere length as long as the sample is not being pulled during the measurements. The length change is probably not the result of sliding filaments since the filaments are tightly connected as a result of the embalming process. The lengthening might be caused by elasticity of the protein chains.

2.2 Data processing

2.2.1 The co-ordinate systems

Data are expressed in a global orthogonal co-ordinate system. The x-axis points laterally from the incisura jugularis (IJ), perpendicular to a plane fitted through C7, T8, IJ and PX (see Figure 5 for the abbreviations). The z-axis points upwards from the middle between PX and T8 towards the middle between IJ and C7, and the y-axis points forwards, perpendicular to the x- and z-axes.

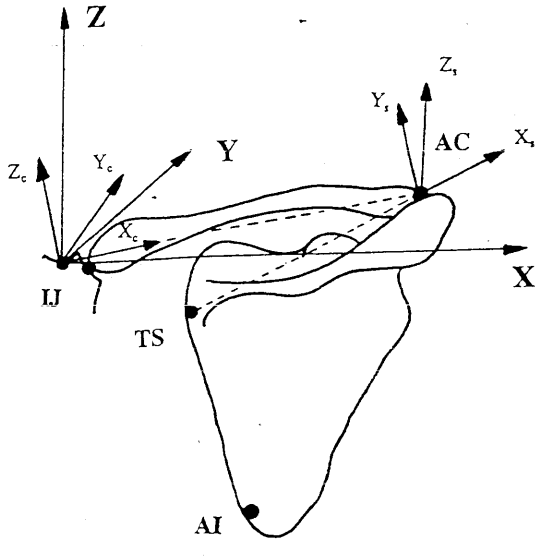

Figure 8.

The global and local co-ordinate systems.

For rotating the bones local co-ordinate systems are used:

thorax:	same as global co-ordinate system.
clavicula:	x-axis: IJ --> AC
	y-axis: $\perp$ x-axis and global z-axis, pointing forwards.
	z-axis: $\perp$ x-axis and y-axis.
scapula:	x-axis: TS --> AC
	y-axis: $\perp$ plane through AC, TS and AI, pointing forwards.
	z-axis: $\perp$ x-axis and y-axis.
humerus:	x-axis: $\pm$ EM --> EL, $\perp$ y- and z-axis.
	y-axis: $\perp$ plane through EM, EL and GH-joint, pointing forwards.
	z-axis: midpoint between EM and EL --> GH-joint.

2.2.2 Optimum fibre length

The number of sarcomeres in all three fibre bundles in a muscle part are calculated by dividing the fibre bundle length by the mean sarcomere length in that fibre bundle. Optimum fibre bundle length is obtained by multiplying the number of sarcomeres with the optimum sarcomere length of 2.7 μm (as measured by Walker & Schrodt (1974). Optimum fibre length of a muscle part is the mean of the three optimum fibre bundle lengths.

2.2.3 Physiological cross-section

The physiological cross-section of the muscle part at optimum length needs to be known. The calculations of the physiological cross-sections are based on the fact that the volume of a muscle remains constant. A contracted muscle is thicker and a relaxed muscle is thinner.

Of all muscle parts the mass of the muscle belly without the tendon was determined. The mass of all the labels that were still attached to the muscle part was subtracted from it. The volume of each muscle part was calculated by dividing the mass of the muscle part by the specific density of muscle tissue. The specific density of muscle tissue was determined by submerging a bunch of shoulder muscles suspended on a wire with a known mass in a can with water. The muscle volume follows from the weight change. The weight of the replaced water is the same as the volume of that bunch of muscle fibres. From the volume and the weight of that bunch the specific density was calculated. The physiological cross-section is calculated by dividing the volume of each muscle part by its optimum fibre length.

Total cross-section of each muscle was measured with a rectangular U-shape. The thickest part of a muscle was put into it. The height until which the U-shape was filled was determined with a slide. The muscles are supple enough to fill also the corners of the U-shape.

2.2.4 Screw axes

The rotation centres of the SC- and AC-joint were calculated with the help of screw axes. A screw axis is a rotation axis about which a set of data points rotates and translates. A method of expressing the one set of data points in the co-ordinate system of the other set of data points is by means of screw axes. Screw axis parameters are: the position of a point on the rotation axis, the direction of the rotation axis, the length of the displacement along this axis and the angle of rotation. It is called a screw axis because the execution of this action looks like a screw being driven into something.

For the determination of the rotation centres of the joints, the positions and directions of a few rotation axes are needed.

About ten orientations of the clavicula and the scapula were measured. For the SC-joint, for example, screw axes were calculated between any two orientations of the clavicula. Since the SC-joint is not a joint with only one degree of freedom, these axes will be different. In order to get one rotation centre the point will be calculated that has the minimum sum of squared distances to the axes. During the measurements of the orientation of the scapula, the clavicula was fixed, so that only the rotation of the AC-joint was measured.

2.3 Model simulations

2.3.1 Simulations

An abduction of the arm was simulated. Input were mean co-ordinates, rotations and forces as measured on ten living subjects. Only static postures were simulated. Seven postures were simulated, one every 30° of abduction. Three of the positions are depicted in Figure 9 (0°, 90° and 180°).

Model simulations were executed for several reasons. One reason is the comparison with the earlier measurements of Veeger et al.(1991). The following output parameters will be compared: orientation of the bones, muscle forces and muscle moments.

Another reason is to calculate the relative muscle length in the different postures. If the muscle length is known, the sarcomere lengths can be calculated and the position of these sarcomeres in the force-length relation. Further reasons are the comparison of rotation centres calculated with screw axes or positioned in the centre of the articular surface, and the influence of the movements on the ligament lengths.

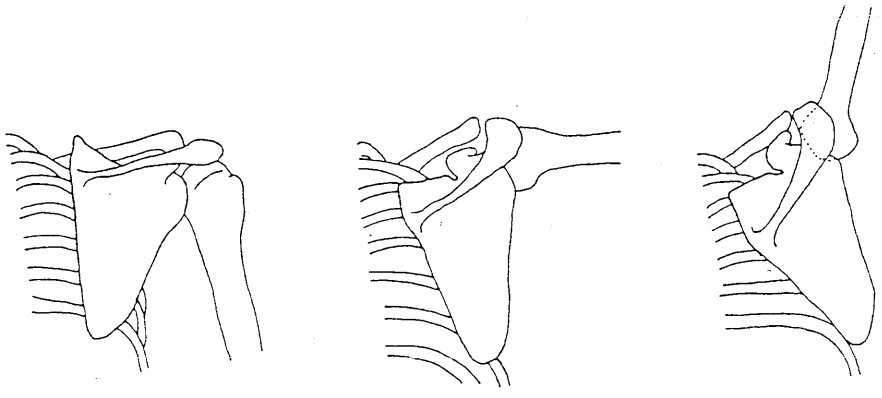

Figure 9.
Three postures during an abduction of the humerus.

2.3.2 The parameter file

The complete parameter file is given in Appendix A. For this parameter file the following parameters had to be measured and calculated:

- The centres of gravity of each body segment. This was calculated with the help of a table from Clauser et al.(1969). In the table the percentage of segment length from the distal end was given.
- Positions of rotation centres. For the SC- and AC-joint these rotation centres were

calculated with the help of screw axes, as explained before. For the glenohumeral joint the centre of a ball through the articular surface on the humeral head, fitted to the glenoid, was taken as rotation centre. As rotation centre in the elbow, which is roughly approximated in the model, the point of intersection between the line through the epicondyles medialis and lateralis and the middle line of a cylinder through the humerus shaft was taken.

- The position of the centre of the humeral head. Because muscle activity no longer keeps the humeral head in position, the glenohumeral head dislocates because of the weight of the arm. All position nodes that are attached to the humerus will be translated in the model over the distance between the actual rotation centre and the centre of the humeral head.
- Positions of palpable bony landmarks.
- Mathematical descriptions of bony contours: spheres, a cylinder and an ellipsoid. These are needed for the curved muscles and for the shape of the scapulothoracic gliding plane.
- Two points on the medial border of the scapula, at 2 cm distance from the ellipsoid surface of the thorax. The projections of the two points are to follow the ellipsoid SURFACE elements that form the scapulothoracic gliding plane.
- Attachment sites of ligaments and muscles.
- The masses of the various segments. For the clavicula and scapula the mass of half of the muscles that are attached to this bone is added to the mass of the bone itself. For the hand, forearm and upper arm the volume of these segments was measured by submersion and multiplied with the specific gravity of this segment as noted in tables of Clauser et al.(1969). The magnitude of the gravitational force was calculated by multiplying the mass with 10 ms^{-2}.
- Rotational inertia. With an equation of Hinrichs (1985) moments of inertia about a transversal and about a longitudinal axis are calculated. Input of the equation are anthropometric data like wrist circumference and fore-arm length in the case of the fore-arm.
- Physiological cross-sections. These are the cross-sections of the muscle parts at optimum sarcomere length.

2.3.3 The input file

For each movement that is simulated a separate input file is constructed. If one wants to simulate an abduction of the arm, different positions during this abduction have to be given.

Bony landmarks of ten living subjects were measured with the palpator in seven postures during abduction and anteflexion (Van der Helm and Pronk, 1995). From the bony landmarks orientations of the bones were calculated in Euler angles with respect to the virtual reference position. The virtual reference position is a position in which the clavicula and the scapula are

positioned in the frontal plane. With the Euler angles the positions of these bony landmarks of the cadaver are calculated. As input variables for the model the following co-ordinates are needed: the y- and z-co-ordinates of AC and the z-co-ordinate of TS. Further the Euler angles of the humerus are given and the direction of gravity, since the thorax moves with respect to the gravitational field.

For comparison with the earlier measurements (Van der Helm, 1991) the same input data were used as before. The input files for an abduction and an anteflexion are given in Appendix B.

2.3.4 Actual sarcomere length

Output of the model at a given posture is, among others, muscle length. Fibre length is the muscle length minus the tendon length, which is assumed to be a fixed length in every muscle part. From the fibre length the actual sarcomere length in a simulated position can be calculated. With the actual sarcomere length and a force-length curve, the maximal force output of the muscle part in that position can be calculated. For a force-length relation the curve that is depicted in Figure 10 is used. The equation of the force-length curve that is given below is an accumulation of lines as shown in Figure 11.

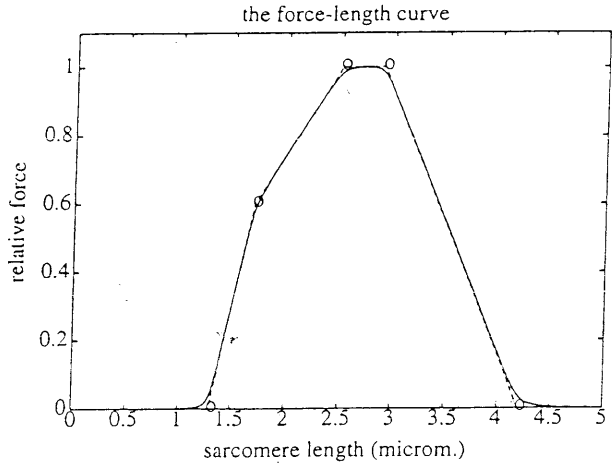

Figure 10.

The force-length curve. The dashed line is the multangular curve and represents the sliding filament theory. The solid line represents the equation below.

$$y = \tfrac{1}{2}t\,[x-c+\sqrt{(x-c)^2 + a^2/t^2}\,]$$

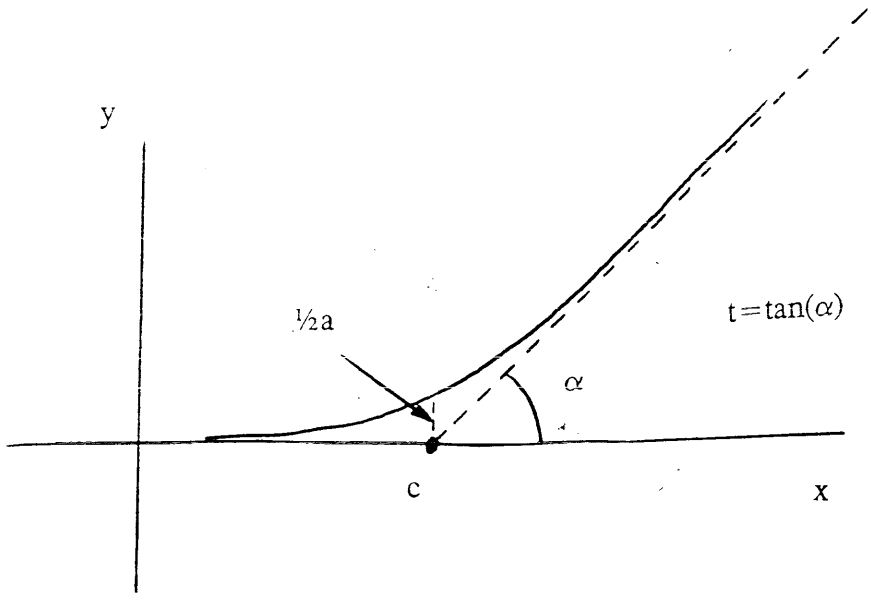

Figure 11.
The parameters of the curve that constitute the curve of the force-length relationship.

$$f(x) = \tfrac{1}{2}\,h_1\,(x-x_1+\sqrt{(x-x_1^2)+a^2/h_1^2}\,) +$$
$$+ \tfrac{1}{2}\,(h_2-h_1)\,(x-x_2+\sqrt{(x-x_2)^2+a^2/(h_2-h_1)^2}\,) +$$
$$+ \tfrac{1}{2}\,(h_3-h_2)\,(x-x_3+\sqrt{(x-x_3)^2+a^2/(h_3-h_2)^2}\,) +$$
$$+ \tfrac{1}{2}\,(h_4-h_3)\,(x-x_4+\sqrt{(x-x_4)^2+a^2/(h_4-h_3)^2}\,) +$$
$$+ \tfrac{1}{2}\,(h_5-h_4)\,(x-x_5+\sqrt{(x-x_5)^2+a^2/(h_5-h_4)^2}\,)$$

The equation of the force-length curve.
h1=1.5; h2=0.5; h3=0; h4=-1/1.3; h5=0
a=0.05
x1=1.3; x2=1.7; x3=2.5; x4=2.9; x5=4.2

Chapter 3: Results

3.1 Cadaver morphology

3.1.1 Positions

Table 1 shows the positions of all measured palpable bony landmarks, as depicted in Figure 5. Positions are expressed in the global co-ordinate system with the origin at IJ. The presented positions are those of the cadaver posture during the measurements. For the rotation and translation of the bones from the local co-ordinate systems to the global co-ordinate system, there was a maximum error of 1.86 mm and a mean error of 0.87 mm (thorax: 0.79 mm; scapula: 0.76 mm; clavicula: 0.58 mm; humerus: 1.01 mm) for the position of a screw. In Table 2 rotation matrices are given for all bones from the virtual reference position, in which the clavicula and scapula are positioned in the frontal plane, to the measured cadaver posture.

In Table C1, which is included in Appendix C because of its length, the positions of all origos and insertions of all measured muscle parts are presented. The muscle parts are numbered in the order that is given in Table 3. For some muscles there cannot be given an order. For both heads of the m. biceps, the two muscle parts attach, via a long tendon on the same position. For the m. coracobrachialis, m. teres minor and m. triceps, the attachment sites are not in one line.

In Table 4 positions of origos and insertions of all modelled ligaments are given.

Table 1: Positions of all measured palpable bony landmarks (in cm)

	X	Y	Z
IJ	0	0	0
PX	-0.6967	3.2172	-13.2803
C7	-1.1766	-12.3360	5.4601
T1	-1.1659	-13.6205	3.6695
T8	-0.5488	-15.6937	-17.0930
AC	15.7441	-8.6785	2.6627
AA	17.1703	-12.2083	0.7663
TS	5.9828	-16.2357	-1.1261
AI	8.6178	-16.6030	-12.5780
EL	20.7075	-9.2330	-30.2128
EM	14.5530	-12.0881	-30.7685
PSU	21.0454	-5.5916	-55.7187
PSR	17.1285	-1.8292	-55.0334
MC2	17.4195	-2.5092	-65.3630
MC2D	18.7956	0.1231	-64.1448
OL	17.8213	-12.6868	-30.2135

Table 2: Rotation matrices of the bones from anatomical position to the measured position.

thorax	0.9893	0.1393	0.0425
	-0.1253	0.9629	-0.2389
	-0.0742	0.2310	0.9701
clavicula	0.8712	-0.4579	-0.1768
	-0.4516	-0.8889	0.0770
	0.1924	-0.0127	0.9812
scapula	0.6714	0.6843	-0.2843
	0.7031	-0.7095	-0.0472
	0.2340	0.1683	0.9576
humerus	0.8907	0.4464	-0.0861
	0.4524	-0.8890	0.0705
	0.0451	0.1018	0.9938

Table 3
All measured and modelled muscles, the number of muscle parts per muscle that are measured and the order in which these muscle parts are numbered.

muscle	# elements	order elements
m. trapezius, scap.	11	cranial - caudal
m. trapezius, clav.	2	cranial - caudal
m. levator scapulae	2	medial - lateral
m. pectoralis minor	4	cranial - caudal
m. rhomboideus	5	cranial - caudal
m. serratus anterior	12	caudal - cranial
m. deltoideus, scap.	11	medial - lateral
m. deltoideus, clav.	4	lateral - medial
m. coracobrachialis	3	
m. infraspinatus	6	caudal - cranial
m. teres minor	3	
m. teres major	4	caudal - cranial
m. supraspinatus	4	caudal - cranial
m. subscapularis	11	cranial - caudal
m. biceps, caput longum	2	no order
m. biceps, caput breve	2	no order
m. triceps	4	
m. latissimus dorsi	6	cranial - caudal
m. pectoralis major, thor.	6	caudal - cranial
m. pectoralis major, clav.	2	medial - lateral

Table 4
Attachment sites of all origos and insertions of the ligaments (in cm).

Origo			Insertion		
X	Y	Z	X	Y	Z
lig. sternoclaviculare					
0.5852	-0.9163	-0.2021	1.6020	-2.8476	0.6707
-0.1716	-1.7581	-0.0429	1.6020	-2.8476	0.6707
lig. costoclaviculare					
4.7498	-2.8460	-0.1824	4.8140	-2.9251	-0.5033
3.6436	-1.9890	-0.7599	3.6785	-2.3953	-0.8285
3.1293	-2.1234	-1.2515	2.6487	-2.8512	-1.5952
lig. conoideum					
11.43	-8.678	1.479	10.83	-8.886	0.1418
10.09	-7.748	1.416	11.04	-8.031	0.07128
lig. trapezoideum					
12.62	-7.079	1.444	12.13	-6.942	0.7937
11.78	-8.124	1.359	11.24	-7.666	0.5789
12.69	-7.789	1.416	11.63	-7.705	0.9464
12.29	-8.612	1.431	10.99	-8.351	0.5484
lig. glenohumerale					
15.5880	-10.3107	-2.3838	17.2248	-9.5038	-3.4231
14.2563	-10.2333	-0.5642	17.6667	-8.1295	0.2190
13.0673	-6.5310	0.6207	17.2754	-6.0267	-0.1210
13.5980	-7.4995	-0.1984	14.6267	-6.5826	-2.0614
14.0018	-7.8071	-2.5541	15.1689	-8.0418	-4.2841
14.0018	-7.8071	-2.5541	16.2808	-9.4810	-4.9662

3.1.2 Muscle length, fibre length and sarcomere length

In Table C2, which is included in Appendix C because of its length, all measured and calculated lengths are presented. The first column gives mean sarcomere lengths of three fibre bundles per muscle part. Sarcomere lengths between 1.7 and 4.2 μm were measured, which is exactly the range in which a sarcomere can generate force, according to the sliding filament theory and the filament lengths of Walker & Schrodt (1974). Within a muscle part quite similar values were found, with an average deviation of 0.2 to 0.3 μm. A deviation of more than .5 μm of average in that muscle part is an exception. Larger differences existed between muscles. In some muscles the sarcomere length increased in adjoining muscle parts. This was especially the case in muscles with large attachment sites, for example in the m. deltoideus, as can be seen in Figure 12. Going from posterior, via lateral, towards anterior, sarcomere length increases.

The second column of Table C2 gives the fibre bundle lengths of the three fibre bundles per muscle part. The third column gives the mean sarcomere length per muscle part. The fourth column gives the tendon length. Tendon length is not measured, but calculated by subtracting the fibre length from the measured muscle length. Fibre length is the mean length of the three fibre bundles.

In the next last column muscle lengths as measured on the cadaver are given. In the last column muscle lengths are given as calculated by the shoulder model in the same position. The shoulder model calculates the shortest distance between the origo and insertion, either over a bony contour or not. It can be noticed that both values are not identical. Differences can amount up to 2 cm, while for m. latissimus dorsi and m. teres major even larger differences exist.

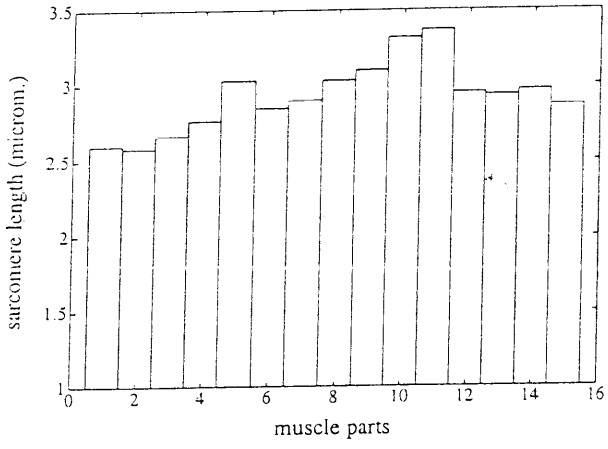

Figure 12

Sarcomere length of the muscle parts of the m. deltoideus (in μm). The first bar is the most posterior part. Going from posterior, via lateral, towards anterior, sarcomere length increases. The last four parts are the clavicular parts of the m. deltoideus.

3.1.3 Physiological cross-sections

Physiological cross-sections are given in Table C3. The first column gives the physiological cross-section (PCSA) at optimum sarcomere length, which is used in the shoulder model. The second column gives the PCSA at the measured sarcomere length. It can be seen that without this correction for sarcomere length an overestimation of PCSA exists. In the third column the cross-section area of the total muscle is given, as measured with the U-shape and the slide.

3.2 Model simulations

An abduction and anteflexion with steps of 30° are simulated. Orientations of the thorax, clavicula, scapula and humerus of a living subject are used as input. Data of the abduction are worked out completely. Data of the anteflexion are only occasionally given for comparison.

3.2.1 Model parameters

Positions of the segment mass centres are given in Table 5.

Rotation centres are given in Table 6. Those of the acromioclavicular joint and the sternoclavicular joint have been calculated from screw axes. The rotation centres are positioned inside the clavicula. For comparison also the centroids of the articular surfaces are given.

Table 5

Segment moment inertia about a transversal axis (I_t) and about a longitudinal axis (I_l) in kg*cm^2, mass of the body segments (in kg) and the positions of the mass centres (in cm).

body segment	I_t	I_l	mass	X	Y	Z
thorax				0	-6.799	-13.93
clavicula			0.156	8.435	-5.025	1.224
scapula	0.001	0.003	0.704	11.87	-11.74	-2.532
humerus	1.32	0.199	2.052	17.44	-8.738	-13.31
fore-arm	0.612	0.091	1.093	18.69	-12.21	-43.84
hand	0.064	0.019	0.525	21.45	-11.78	-61.09

Table 6

Rotation centres of all joints, expressed in the global co-ordinate system (in cm).

rotation centre	X	Y	Z
sternoclavicular joint	2.25	-2.453	-0.797
centroid surface SC	1.90	-1.432	-0.823
acromioclavicular joint	13.5	-8.283	1.687
centroid surface AC	14.95	-8.542	2.031
glenohumeral joint	16.37	-8.114	-1.791
elbow joint	17.63	-10.66	-30.49
radiocarpal joint	20.68	-12.17	-56.17

In Table 7 the parameters of the spheres, ellipsoid and cylinder that represent the bony contours are given. The first three numbers are the co-ordinates of the centres. The last three numbers are the x-, y- and z-distance from the centre to the surface of the bony contours. The parameters of the ellipsoid are depicted in Figure 2. The ellipsoid is not only used as bony contour for the curve of muscles, but also serves as SURFACE element for the scapulothoracic gliding plane.

Table 7, Bony contours.

Mx, My and Mz are the co-ordinates of the centre (in cm). R is the radius. Ax, Ay and Az are the distances from centre to surface of the ellipsoid (in cm). [dx dy dz] is the direction of the axis of the cylinder. sx, sy and sz are the co-ordinates of an arbitrary point on the longitudinal axis of the cylinder (in cm).

	Mx	My	Mz				R
BALL 1	16.5	-7.852	-1.999				2.723
BALL 2	16.37	-8.114	-1.791				2.443
	sx	sy	sz	dx	dy	dz	
CYLINDER	15.63	0.012	0.0	-0.001	0.396	0.918	0.897
	Mx	My	Mz	Ax	Ay	Az	
ELLIPSOID	0	-6.799	-13.93	13.91	8.544	19.82	

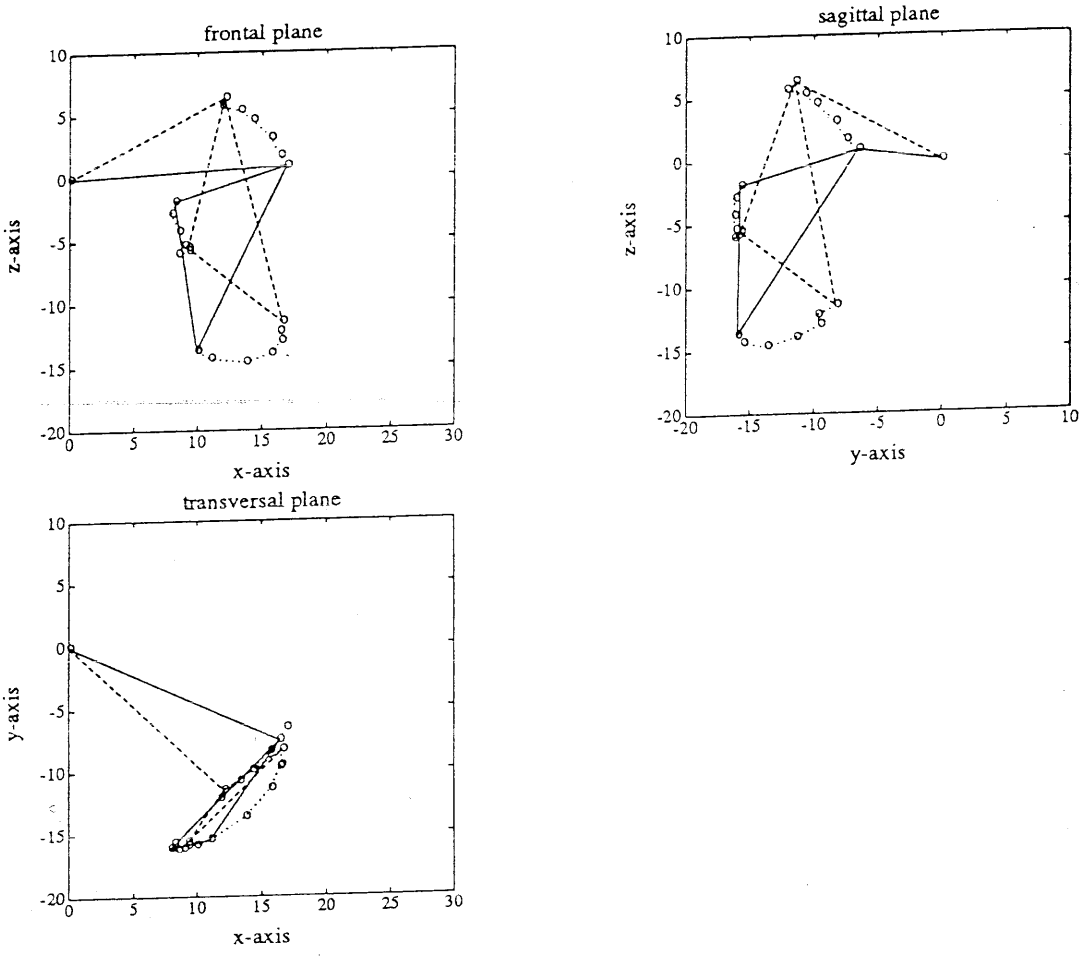

Figure 13.

Dorsal, lateral and cranial view of the clavicula and scapula in 7 positions during abduction. The solid line represents the clavicula and scapula at position 1 (0° abduction). The dashed line represents the clavicula and scapula at position 7 (180° abduction). Four dotted lines connect the seven positions of the palpable bony landmarks, respectively IJ, AC, TS and AI.

3.2.2 Rotations

Figure 13 shows the clavicula and scapula in 7 positions during abduction. The solid line represents the clavicula and scapula at position 1 (0° abduction). The dashed line represents the clavicula and scapula at position 7 (180° abduction). Four dotted lines connect the seven positions of the palpable bony landmarks, respectively IJ, AC, TS and AI.

3.2.3 Muscle length, joint and muscle moment and muscle force

Muscle lengths during the abduction are given in Figure D1.

Joint moments in the SC-joint, AC-joint and GH-joint about three global axes are presented in Figure D2. Joint moments about the y-axis, which is the axis about which the abduction takes place, are larger than joint moments about the x- and z-axes. Besides that the m. serratus has a favourable moment arm about the y-axis, the m. serratus anterior is also active, together with the m. rhomboideus, in order to keep the scapula in the right position. The right position is a position in which a large reaction force can be generated by the passive SURFACE element angulus inferior. About the GH-joint the m. deltoideus exerts most of the moment.

Muscle moments are given in Figure D3. Per joint only the muscle moments about the y-axis are shown and only of the muscles that contribute to the abduction.

Muscle forces are given in Figure D4. Muscles that do not contribute to an abduction are not shown. These muscles are: m. pectoralis minor, m. teres major and minor, m. triceps and m. latissimus dorsi.

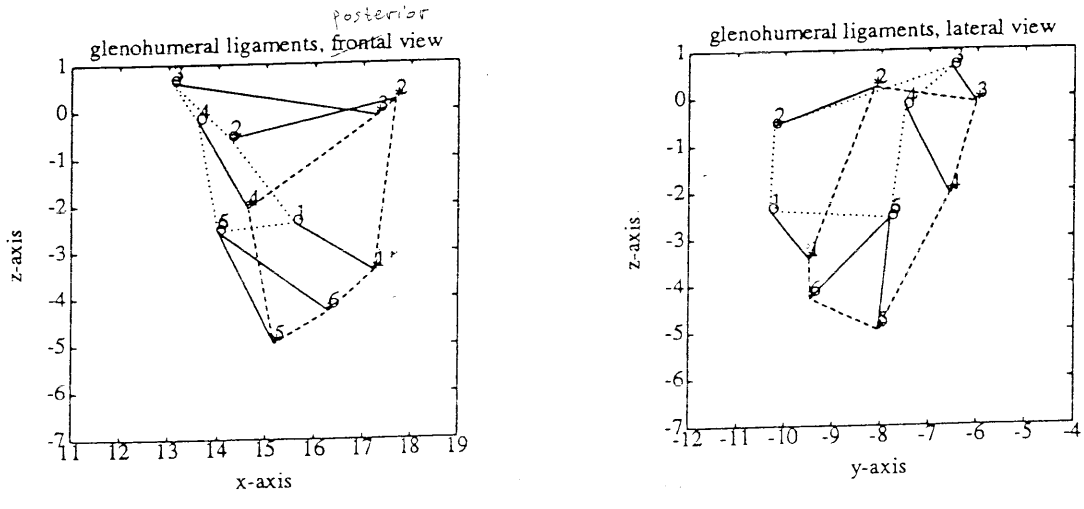

Figure 14.

The glenohumeral ligaments. The axes are in cm. For explanation see the text.

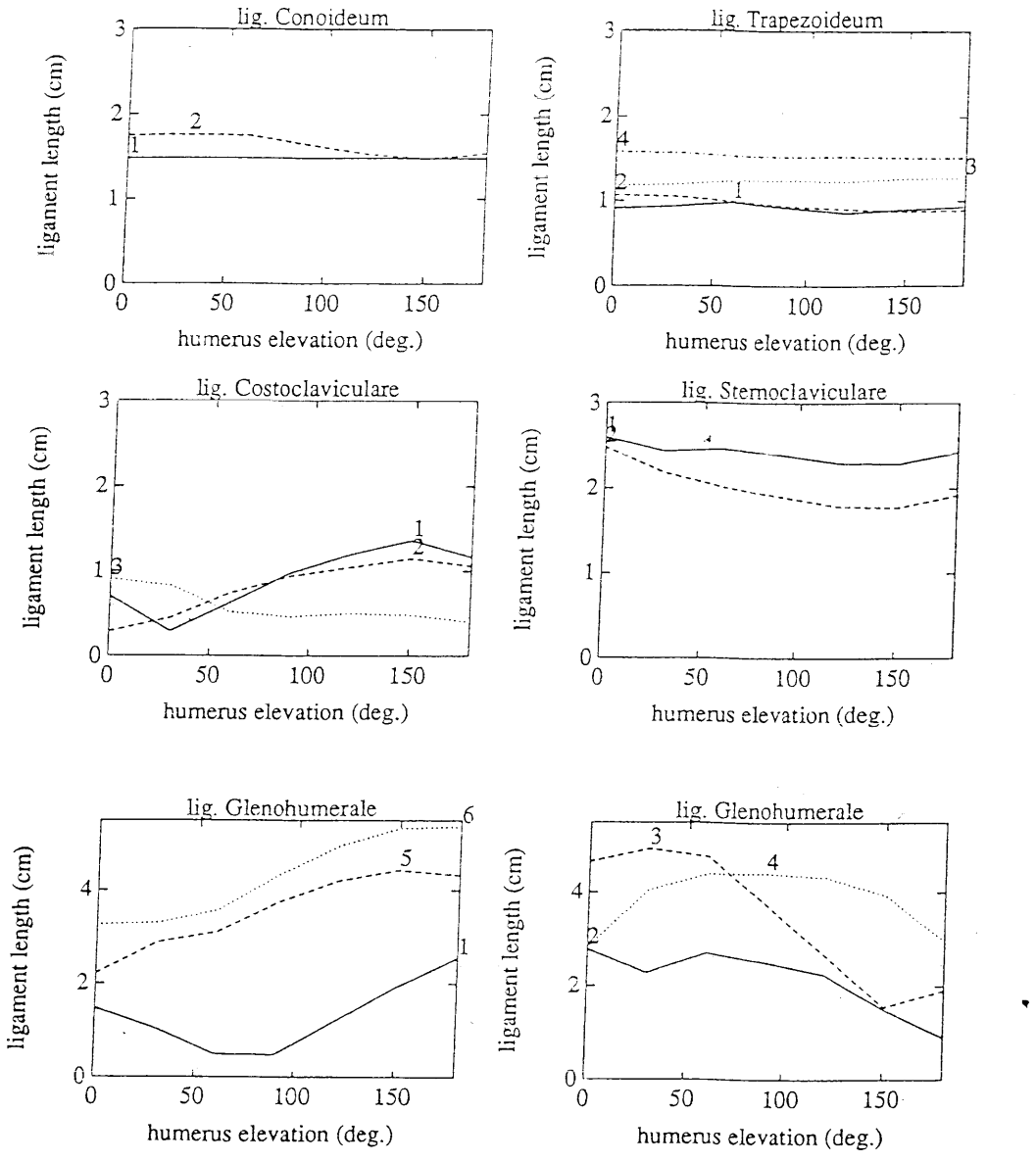

Figure 15.
Ligament lengths (in cm).

3.2.4 Ligament length

Ligament lengths of all ligaments depicted in Figure 4, are calculated with the shoulder model (Figure 15). Some ligaments, the lig. conoideum and lig. trapezoideum for example, do not change in length very much. Other ligaments, like the lig. costoclaviculare and lig. glenohumerale, do change considerably. Figure 14 depicts the glenohumeral ligaments viewed from posterior and viewed from lateral. The solid lines are straight line representations of the ligaments. The

dotted lines connect the attachment sites of the origo at the scapula, around the glenoid. The dashed lines connect the attachment sites of the insertion at the humeral head. It can be seen that the ligaments 1, 5 and 6 are the caudal ligaments and the ligaments 2, 3 and 4 the cranial ones. These are shown in different figures in Figure 15 because of their clearly different behaviour. The caudal glenohumeral ligaments lengthen during an abduction, while the cranial ligaments "shorten" during the abduction.

In reality ligaments cannot lengthen more than about 5%. The maximal length in the figure can be set at 105%. A ligament does not get shorter than 100%, due to its elasticity features. At lengths shorter than 100% the ligament is at slack length and will curve and fold. No force can be exerted at slack length.

3.3 Force-length relationship

The maximal force output of a muscle depends on its length. Maximal force output is the force that a muscle can exert at that length with maximal activation. At a sarcomere length of 2.7 μm, which is the optimum sarcomere length according to Walker and Schrodt (1974), a muscle part can exert the largest maximum force.

For every muscle part the maximal force output is calculated and depicted in Figure D5, which is included in Appendix D because of the many pictures. For every position during the abduction, the maximal force output is set out against sarcomere length. Also the force-length curve is depicted for clarity. The graphs for the different parts of a muscle are plotted below each other for comparison. During the abduction, sarcomeres lengthen or shorten, causing the maximum force output to change.

For most muscle parts it can be seen that the complete movement takes place within the range in which force can be exerted. Some muscle parts can only exert force in a few positions. In all other positions the muscle part is too long or too short to exert any active force. The m. Deltoideus (Figure 16) is a good example of this phenomenon. At the start of the abduction (positions 1 and 2), the sarcomeres are near optimum length. But at position 5 the muscle parts 3 to 11, which are the lateral muscle parts, are too short to exert force.

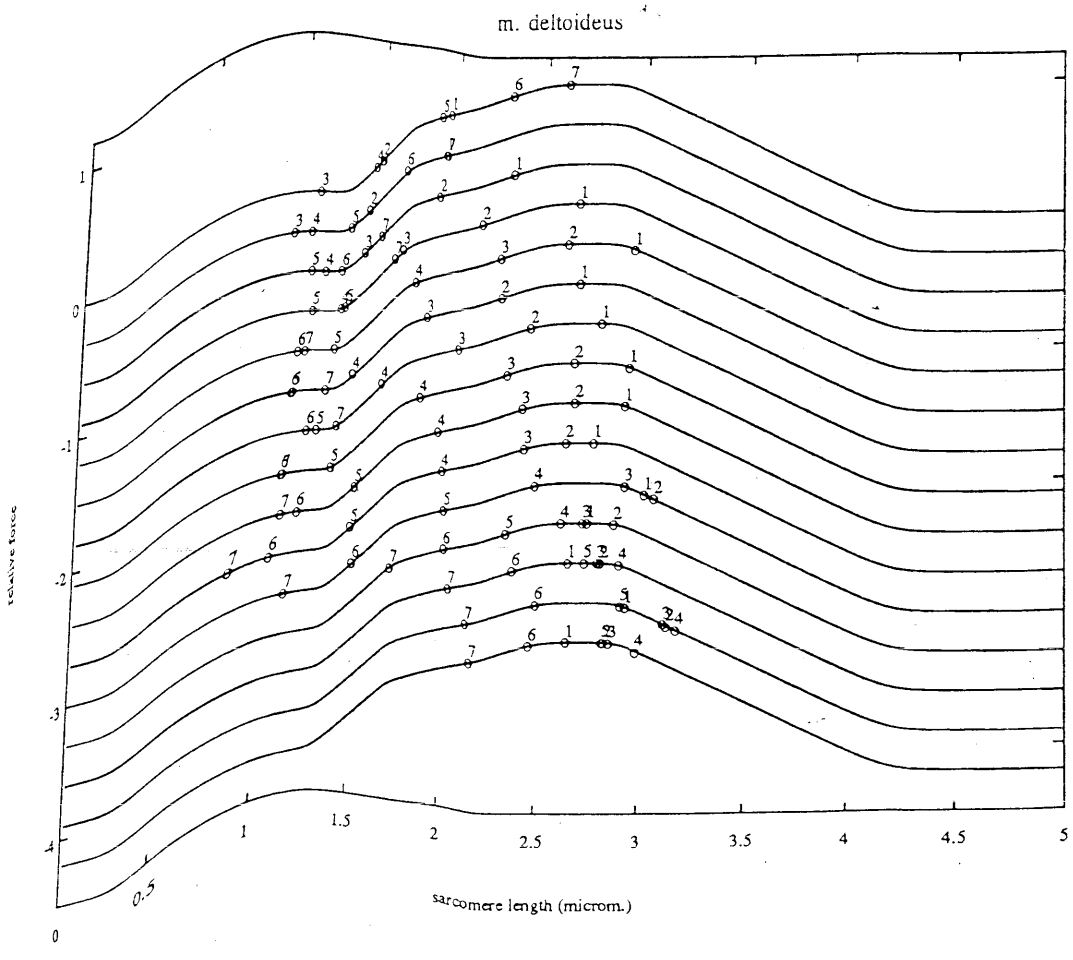

Figure 16. *Maximal force output of the m. deltoideus plotted as force-length curves. The different muscle parts within the m. deltoideus are plotted above each other.* The numbers refer to the seven abduction positions.

Chapter 4: Discussion

4.1 Muscle parameters

4.1.1 Sarcomere length

Laser diffraction is a very accurate method for measuring sarcomere lengths. The resolution is about 0.05 μm. Laser diffraction is very accurate for perfectly embalmed muscle tissue. If a muscle fibre is not very well embalmed, lengths of some sarcomeres cannot be perceived. If there is a large sarcomere length distribution, a measurement error can occur if too little samples are observed. In this study a lot of sarcomere lengths were measured in every muscle fibre bundle and averaged afterwards. So, although some muscle fibres were not embalmed perfectly, the mean sarcomere length is assumed to be determined accurately.

For some muscle parts very small sarcomere lengths of 1.3 and 1.4 μm were found. In the same muscle parts sarcomere lengths of 1.8 μm and longer were found. No sarcomere length between 1.4 μm and 1.8 μm was measured. The sarcomere lengths of 1.3 and 1.4 μm are assumed to be artefacts. Probably some muscle fibres are broken during the rigor mortis because too much force was applied to them. The lengths of 1.8 μm and more are assumed to be representative for the muscle part and used for further calculations.

Not all sarcomeres in a muscle bundle were equally long. Mostly between 0.2 or 0.3 μm deviation from the average sarcomere length in a fibre bundle was observed, which is, in the case of a sarcomere around optimum length, about 10%. This sarcomere length distribution can be a distribution within or a distribution between muscle fibres. In the first case the length of the sarcomere that can exert the least force, according to the force-length relationship, determines the force that can maximally be exerted. In a muscle fibre above optimum length, this is the shortest sarcomere, while in a muscle fibre shorter than optimum length, this is the longest sarcomere. If the distribution of sarcomere length only exists between muscle fibres, sarcomere length can be averaged. For simplicity, sarcomere lengths in a muscle bundle are averaged, which does not mean that there is thought to be no sarcomere length distribution within a muscle fibre.

Because of shrinking due to the embalming process (Huxley and Hawson, 1954; Page and Huxley, 1963), the measured sarcomere length is shorter than the initial sarcomere length, before the embalming process. This is of no influence for the further calculations of the force that a muscle part maximally can exert, since the number of sarcomeres in a fibre is calculated first, by dividing the fibre length (which is also subject to shrinking) by the sarcomere length. The number of sarcomeres is identical before and after the embalming process. From the number of sarcomeres in a fibre, optimum fibre length is calculated by multiplying with the optimum sarcomere length of 2.7 μm, as determined by Walker and Schrodt (1974).

4.1.2 Muscle length

In Table C2, which is included in Table C2 because of its length, the measured muscle length is given and the muscle length in the same posture as calculated with the model. The model calculates the shortest distance between origo and insertion. For some muscles this is the shortest distance around a curved surface. One would expect that the measured muscle length and the calculated distance between origo and insertion were identical. But this is not the case. Differences of up to 2 cm were often found. Even larger differences were found for the m. latissimus dorsi and m. teres major. Within a muscle the measured length of the muscle parts were not randomly longer or shorter than the calculated distance between origo and insertion. If one muscle part was longer, all other muscle parts in the muscle were longer. For the m. trapezius, going from cranial to caudal, the difference between measured and calculated length first decreases and than increases, but the reverse. For the cranial parts the calculated distance is longer, while for the distal muscle parts the measured length is longer. These two observations point to a common cause. It is not likely that it is caused by random measurement errors, because then the deviation within a muscle would be as large as between muscles. Several possible causes are considered.

First, on photographs that were taken during measurements, it could be seen that some muscle parts were not straight. These muscle parts had sometimes even big crinkles. These muscle parts were: the two cranial parts of the m. latissimus dorsi, the teres major and the two caudal parts of the m. pectoralis major. There can be two reasons for the larger length. The muscle can be below slack length, which means that the muscle is hanging loose around the bones. The muscle is around its shortest length and cannot be pulled tight in that posture. The second reason is that muscles might be pulled so hard after the fixation process that muscle fibres are broken. With the help of a microscope it could be seen that, for the cranial part of the m. latissimus dorsi there were some broken fibres, but most of them were intact.

Second, after inspection of the contralateral shoulder of the cadaver the scapula appeared much more movable than was thought initially. If the cadaver, which was embalmed in a horizontal position was positioned straight up, the total shoulder, i.e. the clavicula, scapula and humerus, descended about two centimetres. The question is raised then whether muscles change in length because of the descending of the scapula. Since the muscle tissue is embalmed it is assumed that, although it might stretch while the cadaver maintains this position, the muscle tissue will shorten elastically to its original length when the muscle is cut loose from the cadaver. So these muscle lengths actually belong to a cadaver posture with an elevated shoulder. From this point of view it can be expected that muscle parts running from the thorax towards other bones of the shoulder are longer or shorter than the calculated distance at the descended position. This can very well be seen at the m. trapezius (see Table C2, in Appendix C). The cranial parts are about 2 cm shorter, in the middle the difference is not much and the caudal parts are about 3 cm longer.

Third, for muscles that are curved around a bony contour, the line of pull is positioned

directly against the bony contour. In reality the muscle has a certain thickness. The line of pull is in the middle of the muscle. The outside curve of the measured muscle is longer than the inside curve of the calculated distance. This is for example the case for the m. deltoideus. Especially the anterior parts, which are curved the most, are longer than calculated by the model.

Since the differences between measured muscle length and the distance calculated by the model can be explained so well, there is little reason to think that the differences are caused by measurement artefacts. Muscle parts actually have this length. Besides, the measured sarcomere length and the measured fibre length are in proportion to the measured total muscle length. Also the tendon length is calculated by subtracting fibre length from muscle length. If the total muscle length is assumed to be not correct, also the fibre length and/or tendon length cannot be correct. For further calculations, the measured muscle lengths are assumed to be correct and will be used subsequently.

4.1.3 Tendon length

For some muscle parts the tendon length was negative. This means that the measured fibre length is longer than the measured muscle length. This is for example the case for the m. serratus anterior. The difference was never more than 0.2 cm and is assigned to measurement error. For a muscle fibre of 6 cm, which is the shortest muscle fibre, this is only 3%. It is assumed that, for those muscle parts, there is (almost) no tendon and that fibres are attached directly to the bone. In Table C2, in Appendix C, a tendon length of 0 cm is filled in for these muscle parts.

4.2 Changes of the model

4.2.1 The input file

In earlier experiments, besides rotations of thorax and humerus, the y- and z-co-ordinate of AC and the x-co-ordinate of TS were the input variables. With ACy and ACz and the constraint of the lig. conoideum the position of the clavicula is determined. The rotation of the scapula about the acromioclavicular joint is determined by the x-co-ordinate of TS. These variables were chosen on the basis of one cadaver. But when these input variables were used for the parameters of this cadaver they did not represent the desired movement very well. The clavicular orientation was about the same for the earlier experiments and this experiment, since ACy and ACz were given. The only constraint is the lig. conoideum.

For the scapula, though, there was only one input variable TSx. Constraints of the scapula are the SURFACE elements on the medial border of the scapula. The orientation of the scapula appeared quite sensitive for this input variable TSx. Especially the positions 1 and 2, namely 0° and 30° abduction, deviated considerably from the earlier experiments and from recorded data. The scapula was rotated medially, causing TS to be even more cranial than the clavicula, as can be seen in Figure 17. Therefore it was chosen to use the z-co-ordinate of TS as input variable. This resulted in a much better representation of an abduction, not only for positions 1 and 2, but also for the other positions.

4.2.2 Rotation centres

There is not much difference between a movement with rotation centres on the articular surface or calculated with screw axes. The difference at the angulus inferior, which should be the largest since its distance to the rotation centre is the largest, is only about 2 mm. So, for simplicity, positioning the rotation centre at the optical centroid of the articular surface is reasonable.

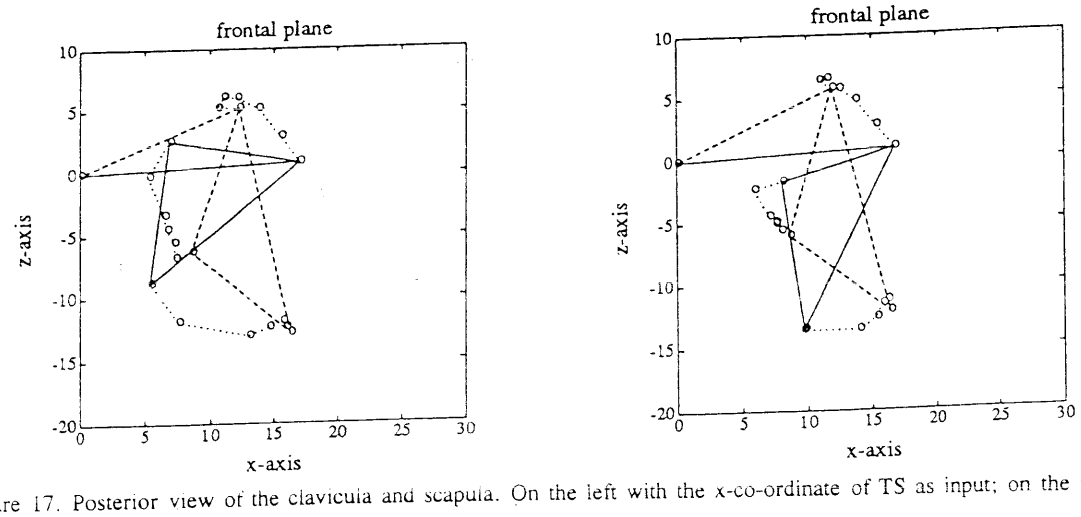

Figure 17. Posterior view of the clavicula and scapula. On the left with the x-co-ordinate of TS as input; on the right with the z-co-ordinate of TS as input.

4.2.3 The dividing of muscle elements

In earlier research (Veeger et al., 1991; Van der Helm, 1991) the density of muscle lines of action attaching to the bone at the origo or insertion is described with a t-criterion. This is the density of lines of action in a "flat" plane which suggests that the whole muscle is equally thick. This is however not the case. By measuring the PCSA of each muscle part, a distribution of cross-section can be calculated. This PCSA distribution is shown in Figure 18B. The x-axis is the t-value of the total muscle and expresses the distance between the points as given in Figure 18A. The y-axis gives the accumulative PCSA of the muscle parts. The solid line gives the PCSA distribution as measured and calculated in this study. The dashed line is the equal distribution line as used in the earlier experiments, which suggest that the muscle parts are equally thick. If a part of the solid line is steeper than the dashed line, this means that that part of the muscle is thicker than average. If the solid line is less steep, that part of the muscle is thinner. The first half of the m. serratus anterior, for example, which is the caudal half, is thicker than average. In the middle the m. serratus anterior is thinner than average and the last cranial part is thicker again.

This means that the caudal parts of the m. serratus anterior can exert more force than calculated in the earlier experiments. The magnitude of the deviation is not very large, about 1 cm^2, which means that 1 cm^2 cross-section is appointed to other muscle parts. For the m. trapezius the deviation is even smaller. Although the method for calculating the PCSA described in this study is more precise, the method used in the earlier experiments is a reasonable approximation.

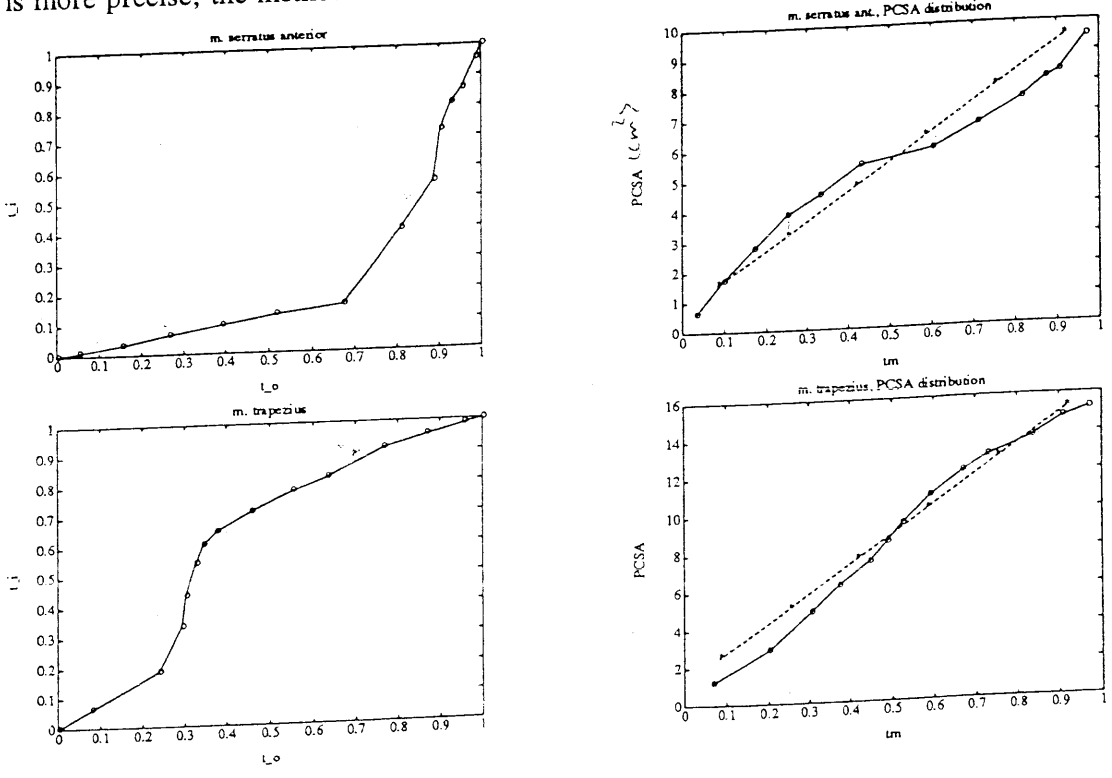

Figure 18A (left) and 18B (right).
T-values and PCSA-distributions of muscles with large attachment sites. For an exact explanation see the text.

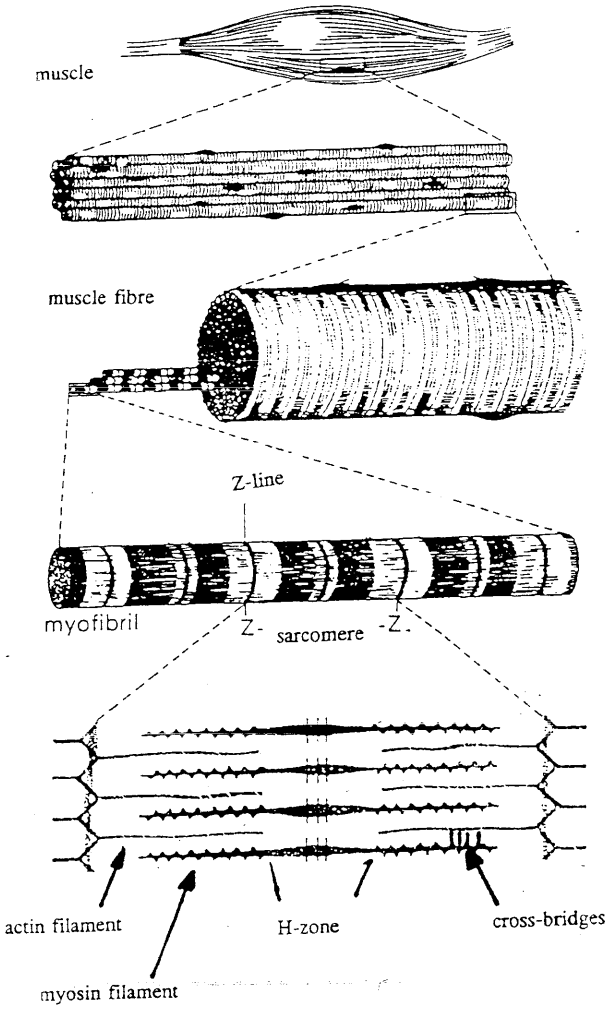

Figure 19.
From muscle to sarcomere.

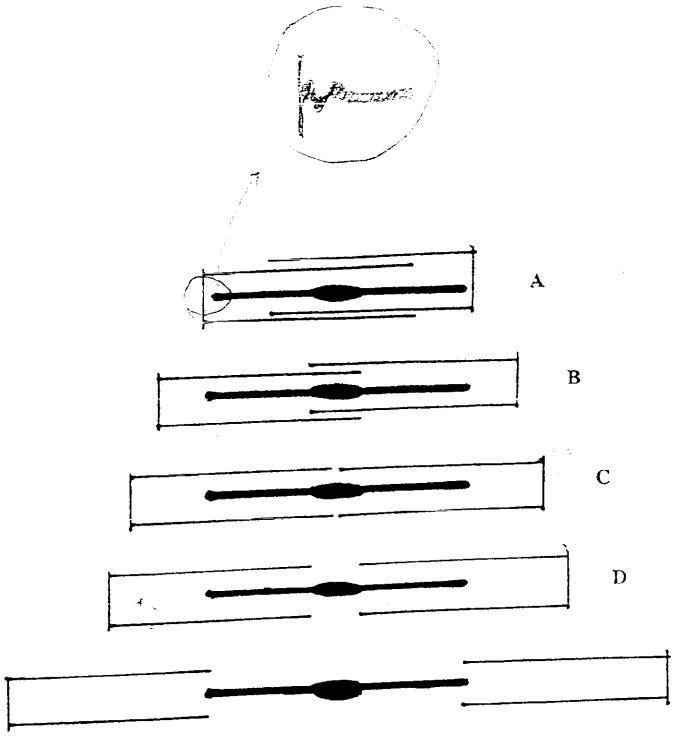

Figure 20.
A sarcomere at its smallest length (A),
at optimum length (B, C, D) and at its longest length.

4.3 Force-length relation

4.3.1 The sliding filament theory

For determining the force that a muscle part maximally can exert, the force-length relationship has to be known. Huxley and Niedergerke (1954) presented the sliding filament theory. With the sliding filament theory the amount of force that can maximally be exerted at a certain length can be predicted.

In a cross-striated skeletal muscle a light I-band and a dark A-band can be distinguished. Huxley and Niedergerke (1954) measured I- and A-band widths during isometric muscle contrac-

tion and during muscle shortening. During isometric muscle contraction both band widths remained the same, while during muscle shortening the I-band width got smaller and the A-band width remained constant. They explained this phenomenon with the sliding filament theory.

The smallest functional part of a muscle, a sarcomere, consists of two kinds of protein filaments, the myosin filaments and actin filaments (see Figure 19). The myosin filaments are thicker and form the A-band, which is darker. The actin and myosin filaments can slide along each other. By doing this the sarcomere, and thus the muscle, can lengthen and shorten. Since the thin actin filaments slide between the thick myosin filaments the light I-band gets smaller while the dark A-band remains at the same length. Huxley and Niedergerke (1954) measured isometric force at different sarcomere lengths and concluded that the amount of force that could maximally be exerted was proportional to the amount of overlap between the actin and myosin filament for the descending limb. For the ascending limb, the amount of force is inversely proportional to the amount of overlap between opposing actin filaments.

Huxley (1957) suggested that on the myosin filaments are myosin heads which can attach to the actin filament. This connection is called a cross-bridge. A cross-bridge can exert a certain amount of force. The total force of a sarcomere is determined by the number of bonded cross-bridges in parallel. The number of cross-bridges available for bonding depends on the amount of overlap between the actin and myosin filament. At optimum length (Figure 20 B, C and D), there is maximum overlap and all cross-bridges can be attached. At a shorter length, overlap of opposing actin filaments takes place (Figure 20 A). If there is an overlap of opposing actin filaments, less cross-bridges can be bonded, which causes the force to be lower at lengths below optimum length. At lengths longer than optimum sarcomere length, actin filaments are withdrawn from the myosin filaments. Part of the myosin heads are unable to reach the actin filament and only part of the cross-bridges can be attached (Figure 20 E), also resulting in a lower force.

Other researchers also measured isometric force at different fibre lengths (Gordon et al. 1966; Bagni et al. 1986) and found the same polygonal shaped curve as Huxley and Niedergerke (1954). The polygonal shaped curve is depicted in Figure 10 with the dashed line and will henceforth be referred to as the multangular curve.

With the force-length relationship, the force that a sarcomere maximally can exert can be calculated if sarcomere length is known.

4.3.2 Sarcomere length distribution

Unfortunately it is not as simple as described above. The multangular curve was not found by all researchers. Bobbert et al. (1990) measured a wider curve than predictions based on the sliding filament theory. The slopes of the force-length curve were less steep than the slopes of the multangular curve, found by Huxley and Niedergerke (1954). The ascending limb could be

accounted for by using a better estimation for actin length for the calculations. However, the change of the descending limb was explained by a distribution of sarcomere length between muscle fibres within a muscle. This implies that measuring sarcomere length in one muscle fibre is not enough. Sarcomere lengths in more muscle fibres need to be known to construct a force-length relationship of a complete muscle.

This effect is depicted in Figure 20. The three dotted lines represent sarcomere force-length curves of different fibres, relative to sarcomere length in the middle fibre. If force in the middle fibre is maximal, the force in two other fibres is sub-maximal. If the force of the three fibres is added, the dashed line is obtained. If there would be no sarcomere length distribution between fibres, the force of the three fibres is represented by the solid, which is obtained by adding three times the middle curve.

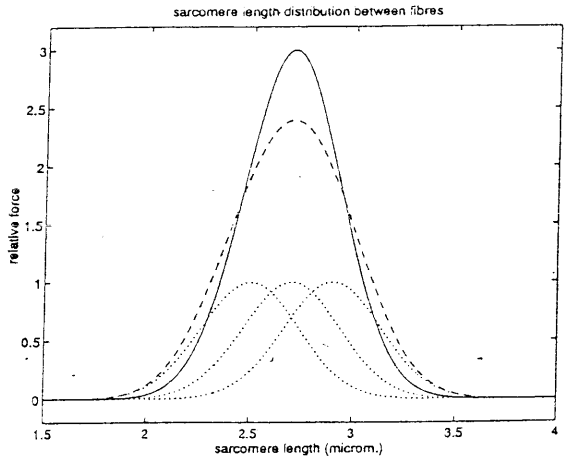

Figure 20.

The force of three muscle fibres if there is (the dashed line) and if there is no (the solid line) sarcomere length distribution between muscle fibres. The dotted lines represent the force of the separate muscle fibres, plotted against sarcomere length of the middle muscle fibre.

A wider curve can also be caused by a sarcomere length distribution within a muscle fibre. If one sarcomere reaches optimum length, other sarcomeres in series, in the same muscle fibre, are longer or shorter and can exert less force. Since the force in a muscle fibre is as strong as the weakest sarcomere, the maximum force of the whole fibre is as small as the force of the sarcomere that can exert the least force.

Edman & Reggiani (1984a, 1987) measured isometric force of very short muscle fibres (0.5 mm). They found no plateau and the descending limb of the force-length relationship had a symmetrical sigmoid shape (see Figure 21). They explained this with a distribution of myosin filament length, misalignment of filaments within a sarcomere or non-parallelism of z-lines

(sarcomere length differences within a sarcomere). There is no linear relationship between the force produced by the interaction between one set of myosin and actin filaments and the total force in the sarcomere. With a computer model they simulated the force of 12 sarcomeres in series with a length distribution of 3%. They found a curve with an almost flat plateau. The force-length relationship found, though, is still consistent with the sliding filament theory as posed by Huxley and Niedergerke (1954). Force of one sarcomere is proportional to the number of cross-bridges that are bonded in parallel.

From these experiments it can be concluded that the sliding filament theory still holds, but this relationship counts for the interaction between one myosin and one actin filament. For one sarcomere the force-length curve is a little more smooth. If the curve is to be extrapolated to the total muscle, the force-length curve gets even smoother, due to sarcomere length distribution within the fibre and between fibres.

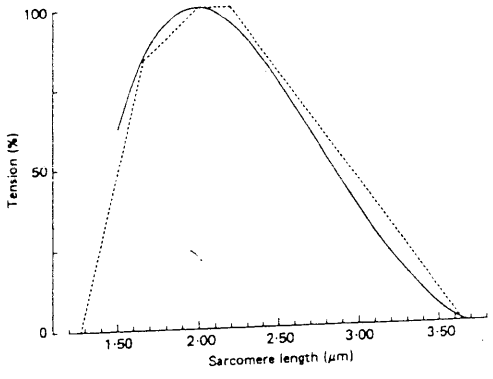

Figure 21.
The symmetrical sigmoid shaped curve as found by Edman and Reggiani (1987) (the solid line) and the multangular curve as found by Gordon et al. (1966) (the dashed line). The solid line of Edman and Reggiani (1987) is a computer simulation of a fibre with 12 sarcomeres in series with a maximal length distribution of 3%.

4.3.3 Sarcomere length redistribution

The starting point of the theories described above is that during an isometric contraction of a muscle fibre, not only fibre length remains constant, but also the sarcomere lengths remain constant. In reality this is not the case. During an isometric contraction of a fibre, the sarcomeres in the fibre keep lengthening and shortening. So actually, it is not an isometric contraction. For muscle fibres below optimum length, the lengthening and shortening cause a reduction of force. The lengthening sarcomeres might be able to exert more force, due to the force-velocity relationship, but the shorter sarcomeres get weaker and weaker. Above optimum fibre length the lengthening and shortening causes an increase of force. If activation of a muscle fibre above optimum length for an "isometric contraction" starts, the force does not remain constant, but

slowly rises. The force starts at the level of the multangular force-length curve, but increases steadily. After 3 seconds, force is still increasing.

Granzier & Pollack (1990) found a descending limb that started to descend at a larger length. They had an explanation for this. Lengths of parts of the muscle fibre (0.8 mm) were recorded. They found that as stimulation of a fibre over optimum length started, sarcomeres in the middle of a muscle fibre lengthened, while sarcomeres at the fibre ends shortened. In the middle of the fibre the lengthening speed causes the higher force, while at the ends the sarcomeres are closer to optimum length (because they are shorter) and can also exert more force. So actually it was dynamic force and not isometric force. They reasoned that if one sarcomere could be held at constant length, the multangular curve of Huxley and Niedergerke (1954) would be found. A distinction can be made between isometric force (with constant sarcomere length) and "fixed fibre ends" or "length clamped" force (with shortening and lengthening sarcomeres).

Also Ter Keurs et al. (1981) measured a higher isometric force at larger sarcomere lengths. The descending limb of the force-length relationship starts to descend at a larger sarcomere length than expected. They mentioned no possible explanations.

Edman and Reggiani (1984b) mentioned the same phenomenon and named it "tension creep". Tension creep could be observed after maximal stimulation of length clamped fibre segments started or after shortening of the fibre segment. It only occurred on the descending limb. Once sarcomere length reached the plateau, no tension creep occurred, because tension does not increase any further if the sarcomere shortens below optimum length.

Tension creep could be eliminated by holding a small segment (0.5 - 0.7 mm) at constant length during the tetanus. Sarcomere length in the whole fibre was observed to remain constant. An almost multangular curve was found without plateau and with a sigmoid shaped descending limb, that started at the predicted length. This finding provides evidence that tension creep is not a feature of the contractile process at sarcomere level.

Edman and Reggiani (1987) reasoned that in short length clamped fibre segments (0.5 mm) no tension creep occurred, even not when there was a sarcomere length distribution, because myofibrils are intimately connected by passive structures. A weak sarcomere may be supported by an adjacent parallel stronger sarcomere. This will prevent stronger sarcomeres in series to shorten at the expense of weaker sarcomeres. Instability and intrinsic movement will be reduced. It is unfavourable if a muscle acts at the descending limb of the force-length relation. If a muscle contracts, the force increases and the shorter and stronger sarcomeres shorten at the cost of the longer and less strong sarcomeres, which lengthen and can produce even less force. Because of the passive structures that intimately connect adjacent muscle fibres, the effect of the instability is not as large as thought before.

From these experiments it can be learned that the theoretical multangular curve can be approximated quite well, during controlled circumstances. However, during normal daily life,

tension creep will probably not occur very often. A position has to be maintained quite a while before tension is raised significantly. So, for isometric contractions, the force-length curve that is used to calculate muscle force in the shoulder model, probably will not have to be adjusted. But the studies described above do make clear that for dynamic situations, the multangular force-length relationship, that describes the behaviour during a maximal isometric contraction, seems to be not enough. During and after lengthening or shortening, other phenomena appear.

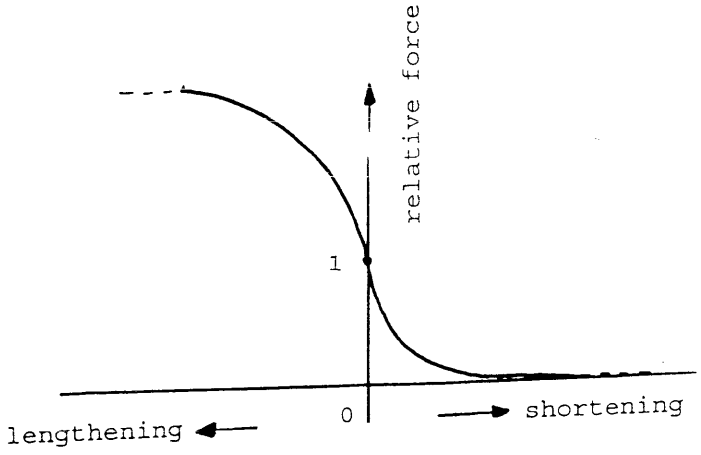

Figure 22.
The force-velocity relationship for a sarcomere. As the sarcomere lengthens, the force increases, while as the sarcomere shortens, force decreases.

4.3.4 Force-length curves during and after movement

Above it was concluded that isometric force-length curves could not very well be used for dynamic situations, as during shoulder movements. During dynamic situations the force is dependent on the velocity of contraction, according to the force-velocity relationship (Wilkie, 1950) as depicted in Figure 22. The dependency is caused by the fact that during shortening not all cross-bridges can be attached at the same time. The faster the filaments slide along each other, the more myosin heads have to release and attach to another site on the actin filament. During lengthening, not all myosin heads can release in time. Because the myosin heads are elastic, an elastic force is exerted during stretch. The faster the stretch, the less myosin heads are able to release in time, the higher the force.

Edman et al. (1978) studied force of length clamped fibre segments during stretch. They measured higher forces for all sarcomere lengths, proportional to the velocity of the stretch. Edman et al. (1982) did not only measure a higher force during stretch, but also after stretch. During maximal activation a length clamped fibre segment was stretched and than held at a

constant length. After the stretch the force slowly decreased until 3 seconds after the stretch. Than the force remained at a constant level, which was higher than the isometric force level at the same stretched length. Edman et al. (1982) named it "residual force enhancement after stretch". The residual force enhancement after stretch could not be the result of sarcomere length redistribution, since laser diffraction showed less length changes of sarcomeres than during an isometric contraction.

Because of the residual force enhancement after stretch, the descending limb of the force-length relationship starts to descend later and is less steep in the beginning. This is favourable because of the larger movement range than the multangular curve.

Edman et al. (1982) suggested that possibly this phenomenon is caused by a passive elastic component in parallel with the contractile element that is formed within the myofibrillar system during activation. This is an unsatisfying explanation. It does not describe what exactly happens and it does not explain all phenomena. It does, for example not explain why there is no residual force enhancement after a short (even a small incomplete) relaxation.

Morgan (1990, 1994) has a more reasonable explanation. As the fibre lengthens, the weakest sarcomere (which is the longest sarcomere, since it only occurs at the descending limb) "will lengthen more rapidly than the others and so become even weaker, and so stretch more rapidly. The lengthening of this one sarcomere will cause only a very small shortening of all the others, and so an imperceptible drop in tension. When this sarcomere reaches the yield point of its force-velocity curve, which it will do very quickly when the whole fibre is being lengthened, it will be unable to generate the required tension at any speed. Then it will lengthen almost infinitely quickly, limited only by very small inertial or passive viscous forces, until rising passive tension brings it to a stop." Morgan (1990, 1994) named the last phenomenon the "popping" of sarcomeres. The popped sarcomere exerts as much passive force as the non-popped active sarcomeres. Popped sarcomeres are longer than the others, which means that the other sarcomeres are shorter than if the fibre lengthening would have to be divided equally over all sarcomeres. The shorter sarcomeres cause a higher force, resulting in the residual force enhancement at the descending limb. With this explanation, also the observation that the residual force enhancement disappears after a relaxation, can be explained. During a relaxation the force decreases and, due to the passive force in the popped sarcomere, the sarcomere shortens until a length at which it can exert active force again. Computer simulations (Morgan,1990), which allow sarcomeres to pop, also find a residual force enhancement.

According to this theory, sarcomere length in a fibre is either smaller than mean sarcomere length in a fibre, or much longer than mean sarcomere length. The force that maximally can be exerted is the force that can be exerted maximally by the shorter sarcomeres, according to the multangular force-length curve. The force-length curve of one sarcomere can not be expanded to the force-length curve of a fibre. The force is right, but the sarcomere length is not. Edman et al. (1982)

measured sarcomere length using laser diffraction. The diameter of the laser beam was 1.5 mm, which means that the diffraction pattern on the screen is a mean diffraction pattern of about 600 sarcomeres. There might be popped sarcomeres between them. That would mean that the enhanced force does not belong to the sarcomere length that they measured, but to a shorter sarcomere length, which is according to the multangular force-length relationship.
This theory makes the problem of modelling muscle force only more complicated. The force-length relationship of one sarcomere (the multangular curve) does not count for the whole fibre. But, the same as for the tension creep during isometric force, it can be questioned whether the popping of sarcomeres also occurs during normal shoulder movements. Edman et al. (1982) produced a tetanus by a constant train of pulses. In reality, if force increases, force production might be taken over by another motor unit. Further research is necessary, before it is known whether the increased force enhancement after stretch also counts for a whole muscle-tendon complex.

Also during concentric contraction, when a muscle is shortening, the descending limb is not as steep as in the ~~square~~ multangular force-length curve. Edman et al. (1993) measured a depression of tetanic force after loaded shortening of a length clamped fibre segment (0.5 mm). The decrease of force was only found after loaded shortening. Without a load there was no decrease of force. The depression of force was ascribed to non-uniform behaviour along the fibre, which is the same as sarcomere length redistribution.

Meijer et al. (1995) determined isometric length-force curves during shortening from post-shortening force-length relationships. Isokinetic contractions with a constant speed and variable shortening ranges were performed. By jumping from one length-force relationship to force-length relationships with 1 mm decrements, the force-length curve during concentric contraction for a given initial muscle length can be constructed. The descending limb of the force-length curve appears to be almost horizontal, though lower than during isometric contraction.

Meijer et al. (1995) measured force after unloaded shortening. In that case, according to Edman (1993), it must be the "shortening-induced deactivation" or "movement effect", which is caused by a "transitory decrease in the calcium affinity of the troponin binding sites leading to a temporary deactivation of the contractile system". The movement effect is of short duration, active force being restored to normal within 1-2 s. Unfortunately Meijer et al. (1995) stopped stimulation about half a second after shortening. Meijer et al. (1995) ascribed the force reduction to intracellular processes, since no significant differences of muscle geometry existed. Individual sarcomere lengths were not measured.

Although the movement effect is of shorter duration than the depression of force after loaded shortening, the data of Meijer et al. (1995) can be very useful, since it is the phenomenon

itself that is important. Still, too little is known to construct a new force-length curve. The force reduction was measured after the shortening. Does the effect only occur after the shortening, or also during the shortening? It possibly also occurs during the shortening, but is the force depression constant during the total shortening range, or does the force depression increase during the shortening? Too many questions remain, to quantify a separate force-length curve for shortening muscles.

4.4 A curve for the shoulder model?

If a force-length relationship for the shoulder model is to be constructed, maybe a square relationship will not suffice, but until now, too little is known to quantify separate force-length relationships for isometric, concentric or eccentric contractions. For the purpose of the computer model of the shoulder, a multangular curve was constructed with rounded angles. It is clear that the multangular curve can be smoothed a little, because a muscle part not only contains sarcomeres in series but also parallel fibres. Due to fibre length distribution, the influence of muscle part shortening on the sarcomere length is different for the various parallel fibres (Huijing ,1995). Sarcomeres in one fibre will stretch more than sarcomeres in the next fibre. This causes the force-length relationship to be even more smooth.

There are other factors that are of greater influence on the maximal force of a muscle part, like the physiological cross-section. The exact shape of the force-length curve does not influence the maximal force output of a muscle part dramatically. Since the exact shape of the force-length curve needs to be explored further, the multangular curve can be used for the time being. Maybe in the future different curves will be necessary, because it is clear that there are phenomena that are not fully known and explained yet. Force-length relationships like in Figure 23 might be used then. A smooth curve (the solid line) could be used for isometric contractions, a wider curve, with a descending limb that starts to descend at a larger length (the dashed line) for an eccentric contraction, and a lower curve, with a less steep descending limb (the dotted line), for concentric contractions.

All researches described above were performed during maximal stimulation. Roszek et al. (1994) and Rack and Westbury (1969) submaximally stimulated a muscle at various lengths. For five submaximal stimulation frequencies a force-length relationship was made. It could be seen that the lower stimulation frequency was, the lower the force. Also it could be noted that the total curve shifted to the right as stimulation frequency decreased. This means that optimum length at submaximal activation is at a larger length than during maximal activation. Length-dependent calcium sensitivity seems to be a major factor determining the magnitude of the shift of optimal muscle length.

Huijing (1995) mentions four properties that influence muscle force, namely length-force

characteristics, force-velocity characteristics, degree of activation and fatiguability characteristics. He emphasizes that often these properties are modelled as being independent, but that this assumption is not correct. With modelling a muscle-tendon complex, the interdependency of the factors should be taken into account.

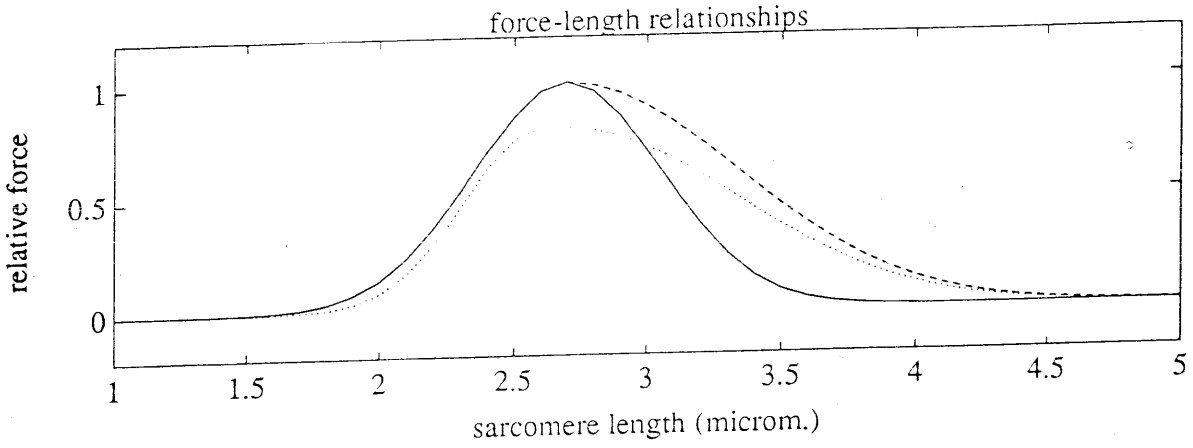

Figure 23

Maybe in the future, after further research about the exact shapes, a smooth curve (the solid line) could be used for isometric contractions, a wider curve, with a descending limb that starts to descend at a larger length (the dashed line) for an eccentric contraction, and a lower curve, with a less steep descending limb (the dotted line), for concentric contractions.

Herzog and Ter Keurs (1988) presented a method for measuring force of bi-articular muscles. By fixing one joint forces of all mono-articular muscles do not influence the joint moment. By rotating about the second joint and measuring maximal force in all positions, a moment-length curve can be measured. The question remains to what extent this curve can be generalized to other muscles. Probably different curves have to be obtained for every muscle. A second question is whether there is a joint that is spanned by only one bi-articular muscle. The method described might not be very useful for describing force-length relationships of all shoulder muscles, since there are few joints that are only crossed by one bi-articular muscle.

Winters and Kleweno (1993) used this method to obtain a force-length curve for the m. biceps. During an anteflexion of the humerus, muscle force of the m. biceps decreases for males and remains constant for females until 100° anteflexion. It was reasoned that for males, the m. biceps acts on the ascending limb of the force-length relationship during the anteflexion, while for females, the m. biceps acts on the plateau. Above 100° passive force of the bi-articular m. triceps heads increases, resulting in a reduction of net joint torque.

These findings do not agree with the findings of the present study. For the m. biceps, sarcomere lengths were measured of 3.5 μm at 0° anteflexion. During anteflexion, as the muscle

shortens, maximal force would first rise, according to the descending limb. Which theory is right? Further research is necessary. For the present study it can be noticed that measured muscle length does not agree with the model calculations. Possibly tendon tissue shrinks a lot during the embalming process. Does this shrinking also affect the measured sarcomere length? These questions cannot be answered without further research.

4.5 sarcomere length range during movement

Herring et al. (1984) evaluated four conflicting theories about the factors which determine at what muscle length optimum sarcomere length is to be found. These four theories were:

1. The excursion-maximum stretch hypothesis.
   At the joint angle at which muscle length is maximal, actin and myosin filaments barely overlap. Sarcomere length is 4.2 μm in the maximally stretched muscle.
2. The excursion-average stretch hypothesis.
   Optimum sarcomere length is at the mean of the smallest and largest muscle length. However, they found that maximal tension occurred at 0.5 μm longer than optimum length, so sarcomere length at the mean muscle length is $2.7 + 0.5 = 3.2$ μm.
3. The postural position hypothesis.
   Since the postural length is by definition the most frequent muscle length, optimum sarcomere length (the 3.2 μm) should occur at that length.
4. The active position hypothesis.
   The joint position at which the most often activation occurs, is the position at which sarcomere length should be optimal.

After evaluation on pig mandibular muscles, Herring et al. (1984) concluded that the active position hypothesis was the most successful hypothesis. Also the excursion-average stretch hypothesis could not be rejected, because the muscle length at which stimulation is the most frequent is very much near the mean muscle length. For shoulder movements the mean muscle length will not be that close to the most active position, since most activity occurs at lower abduction and anteflexion angles.

The four hypotheses start with the assumption that the muscle is homogeneously distributed, which means that muscle fibres are equally long and there is no sarcomere length distribution within or between muscle fibres. In reality a muscle is not homogeneous. Maybe attaining force-length curves for complete muscles is much easier. In that case it first has to be known whether the above described active position theory is really true and then electromyograph studies have to be done on all shoulder muscles during normal daily life movements. From these results, force-length curves of all shoulder muscles might be attained.

The hypotheses can be compared to the data found in this study. This can easily be done with the Figures 5D (in Appendix D). An abduction can be considered to be a complete move-

ment, position 1 being the one extreme and position 7 (totally abducted) the other. For the muscle parts in the middle of the m. deltoideus, the optimum length is not at the mean muscle length (which is position 4, halfway abducted), but at position 2, about 30° abducted. This result rejects the excursion-average stretch hypothesis. According to the active position hypothesis, this finding would imply that most electrical activity should occur at that position, which is quite likely, because a lot of manipulations (like typing, dish washing) are made around that position. The fact that this agrees with each other, is a confirmation that the measured sarcomere lengths in this study are quite likely to be measured rightly.

Lieber and Friden (1994) intraoperatively measured sarcomere length in a human m. extensor carpi radialis brevis, using laser diffraction. During flexion and extension of the wrist a sarcomere length range was measured from 2.44 to 3.33 μm. They reasoned that this range includes the plateau and the first half of the descending limb. They concluded that human skeletal muscles can function on the descending limb of their sarcomere length-tension relationship under physiological conditions. Thus muscle force changes during joint rotation are an important component of the motor control system.

Lieber and Friden (1994) also mentioned studies about human gait, during which muscles also act at the descending limb. Studies of swimming fish, mentioned by Lieber and Friden (1994), suggest that active physiological sarcomere lengths lie almost exclusively on the plateau of their length-tension relationships, resulting in maximum efficiency and muscle power output. They also mentioned research of frog jumping, during which sarcomere lengths well onto the descending limb of the length-tension curve occurred in normal joint configurations. From these findings they concluded that various muscle-joint systems operate with sarcomeres on different portions of the isometric length-tension curve. This could be a result of the different types of movements initiated by these muscles: oscillatory for the fish, propulsive for the frog and manipulative for the human wrist extensor muscle.

For the range of sarcomere length, Lieber and Friden (1994) used the multangular curve. But actually the descending limb during movement starts to descend later and is less steep. The question remains to what extent the muscles really act on the descending limb in these situations.

4.5.1 Maximal forces during abduction and anteflexion

In Figure D5, in Appendix D, it can be seen what forces muscle parts can exert, according to the constructed force-length curve of Figure 12.

It appears that, even for the m. latissimus dorsi, for which very short sarcomere lengths were

measured, during most of the trajectory, a force can be exerted. If sarcomere length at the measured cadaver position would have been around optimum length, no force could have been exerted at larger lengths in an abducted position.

In this study it was found that sarcomeres in the m. biceps are long while sarcomeres in the m. triceps are short. The m. biceps is a bi-articular muscle. Both the glenohumeral joint and the elbow influence its length. Since the elbow is extended and the arm cannot be retroflexed at the glenohumeral joint much further, this stretched sarcomere length can be explained very well. Sarcomere length of its antagonist, the m. triceps, is consequently very short.

Within muscles a sarcomere length distribution seems to exist between the different muscle parts, for example in the m. triceps. This could be very adequate to obtain a larger range of movement in which force can be exerted.

4.6 Cadaver reliability

No two human beings are the same. How should a representative parameter set of a human being be obtained? There is no standard abduction. One subject rotates his shoulder more than the other one, for example. An abduction measured on one subject might not be possible with the morphology of the cadaver.

Because one cannot measure muscle lengths of a living person, measurements are done on cadavers. The cadaver should be representative, which means that it should be a cadaver of a not too old, healthy, active man, who has not been ill for a long time before he died. This way as much motions as possible can be simulated.

Winters and Kleweno (1993) noticed a different optimum muscle length of the m. biceps for males and females. It is not known yet whether wether this difference of optimum muscle length is also present for other muscles, mono-articular muscles for example.

Most subjects that participate in experiments to test the shoulder model are male students. Anatomy of the cadaver should be comparable to these subjects. Maybe different cadavers should be measured for women, children, athletes or office men.

Chapter 5: Conclusions

- A complete set of parameters of the right shoulder of a cadaver is measured. All measured parameters are proportional to each other, which allows for modelling and calculations of shoulder movements. Also for analysis of shoulder movements and movement range of the shoulder in general, these data are very valuable.

- With the knowledge of muscle length, muscle fibre length and sarcomere length a more realistic muscle model could and was implemented in the shoulder model.

- Measured muscle lengths did not for all muscles agree with the calculated distance between origo and insertion. For most differences a reasonable explanation was found.

- With the measured muscle parameters and a simulated abduction by the shoulder model, it was looked at what maximal muscle forces could be exerted during the abduction. Almost all muscles acted within the range of the force-length relationship in which force could be exerted.

- The shape of the force-length curve was discussed. Deviating force-length curves were found in several studies. In all these studies circumstances were very much controlled. Further research is necessary to be able to quantify all phenomena during a shoulder movement, and to find out whether all phenomena can be generalized to shoulder movements. Until more is known, the multangular curve, based on the sliding filament theory (Huxley and Niedergerke, 1954) will be used. The shape of the force-length curve is not the only factor determining the maximal force of a muscle. Also the physiological cross-section and the force-velocity relationship are important.

5.1 Suggestions for further research:

- Filament lengths of muscle biopts of living subjects are to be measured, in order to check whether those are the same as those of the cadaver. From the filament lengths, a multangular force-length curve can be obtained.

- The exact shapes of force-length curves during isometric, eccentric and concentric contractions have to be measured. Also the relationship between force-length curves for sarcomeres, muscle fibres and a complete muscle-tendon has to be explored further.

- If elasticity features and maximal forces of all measured ligaments are known, a force-length relationship of ligaments can be constructed. With the ligament force-length relationship forward dynamic simulations can be executed.

- If muscle and joint geometry parameters of the elbow are known, also an elbow flexion can be simulated. Right now muscle and joint geometry parameters are being measured at the Anatomical Laboratory in Leiden.

References

Bagni M.A., Cecchi G., Colomo F. and Tesi C. (1986). The sarcomere length-tension relation in short length-clamped segments of frog single muscle fibres. J. of Physiology 377:91P.

Bobbert M.F., Ettema G.C. and Huijing P.A. (1990). The force-length relationship of a muscle-tendon complex: experimental results and model calculations. European Journal of Applied Physiology 61: 323-329.

Clauser C.E., McConville J.T. and Young J.M. (1969). Weight, volume and center of mass of segments of the human body. Wright-Patterson Air Force Base Ohio (AMRL-TR-69-70). 1969, 339-356.

Edman K.A.P., Elzinga G. and Noble M.I.M. (1982). Residual force enhancement after stretch of contracting frog single muscle fibres. J. of General Physiology 80: 769-784.

Edman K.A.P. and Reggiani C. (1984a). Absence of plateau of the sarcomere length-tension relation in frog muscle fibres. Acta Physiologica Scandinavica 122: 213-216.

Edman K.A.P. and Reggiani C. (1984b). Redistribution of sarcomere length during isometric contraction of frog muscle fibres and its relation to tension creep. J. of Physiology 351: 169-198.

Edman K.A.P. and Reggiani C. (1987). The sarcomere length-tension relation determined in short segments of intact muscle fibres of the frog. J. of Physiology 385: 709-732.

Edman K.A.P., Caputo C. and Lou F. (1993). Depression of tetanic force induced by loaded shortening of frog muscle fibres. J. of Physiology 466: 535-552.

Gordon A.M., Huxley A.F. and Julian F.J. (1966). Length-tension relation in a muscle. J. of Physiology 184: 170-192.

Granzier H.L.M. and Pollack G.H. (1990). The descending limb of the force-sarcomere length relation of the frog revisited. J. of Physiology (1990), 421: 595-615.

Herring S.W., Grimm A.F., Grimm B.R. (1984). Regulation of sarcomere number in skeletal muscle: a comparison of hypotheses. Muscle & Nerve 7: 161-173.

Herzog W. and Ter Keurs H.E.D.J. (1988). A method for the determination of the force-length relation of selected in-vivo human skeletal muscles. Pflügers Archiv 411: 637-641.

Hinrichs R.N. (1985). Regression equations to predict segmental moments of inertia from anthropometric measurements: an extension of the data of Chandler et al. (1975). J. of Biomechanics 18: 621-624.

Huijing P.A. (1995). Parameter interdependence and success of skeletal muscle modelling. Human Movement Science 14: 443-486.

Huxley A.F. and Niedergerke R. (1954). Structural changes in muscle during contraction; interference microscopy of living muscle fibres. Nature 173: 971-973.

Huxley H.E. (1957). The double array of filaments in cross-striated muscle. J. of Biophysical and Biochemical Cytology 3: 631:648.

Lieber R.L., Loren G.J., Friden J. (1994). In vivo measurement of human wrist extensor muscle sarcomere length changes. J. of Neurophysiology 71(3): 874-881.

Martin R. and Saller K. (1957). Lehrbuch der Anthropologie, Fischer, Stuttgart.

Meijer K., Grootenboer H.J., Koopman H.F.J.M. and Huijing P.A.J.B.M. (1995). The isometric length-force relationship during concentric contractions of the rat medial gastrocnemius muscle. Integrated Biomedical Engineering for Restoration of Human Function, 19-20 October, 1995.

Morgan D.L. (1990). Modeling of lengthening muscle: the role of inter-sarcomere dynamics. Chapter three in: Multiple muscle systems: biomechanics and movement organization (Edited by: Winters J.M. and Woo S.L-J.), pp 46-56. Springer, New-York.

Morgan D.L. (1994). An explanation for residual increased tension in striated muscle after stretch during contraction. Experimental Physiology 79: 831-838.

Pronk G.M. (1991). The shoulder girdle. Doctoral thesis, Delft University of Technology, I.S.B.N.90-370-0053-3.

Pronk G.M. and Van der Helm F.C. (1991). The palpator: an instrument for measuring the positions of bones in three dimensions. J. of Medical Engineering & Technology 15(1): 15-20.

Rack P.M.H. and Westbury D.R. (1969). The effects of length and stimulus rate on tension in the isometric cat soleus muscle. J. of Physiology 204: 443-460.

Roszek B., Baan G.C. and Huijing P.A. (1994). Decreasing stimulation frequency-dependent length-force characteristics of rat muscle. J. of Applied Physiology 77(5): 2115-2124.

Ter Keurs H.E.D.J., Luff A.R. and Luff S.E. (1981). The relationship of force to sarcomere length and filament lengths of rat extensor digitorum longus muscle. J. of Physiology 317:24P.

Van der Helm F.C.T. (1991). The shoulder mechanism, a dynamic approach. Doctoral thesis, Delft University of Technology, I.S.B.N.90-370-0055-X.

Van der Helm F.C.T., Veenbaas R. (1991). Modelling the mechanical effect of muscles with large attachment sites: application to the shoulder mechanism. J. of Biomechanics 24(12): 1151-1163.

Van der Helm F.C.T., Veeger H.E.J., Pronk G.H., Van der Woude L.H.V., Rozendal R.H. (1992). Geometric parameters for musculoskeletal modelling of the shoulder system. J. of Biomechanics 25(2): 1429-1434.

Van der Helm F.C.T. (1994). Analysis of the kinematic and dynamic behavior of the shoulder mechanism. J. of Biomechanics 27(5): 527-550.

Van der Helm F.C.T. (1994). A finite element musculoskeletal model of the shoulder mechanism. J. of Biomechanics 27(5): 551-569.

Van der Helm F.C. and Pronk G.M. (1995). Three-dimensional recording and description of motions of the shoulder mechanism. J. of Biomechanical Engineering 117(1): 27-40.

Veeger H.E.J., Van der Helm F.C.T., Van der Woude L.H.V, Pronk G.M., Rozendal R.H. (1991). Inertia and muscle contraction parameters for musculoskeletal modelling of the shoulder mechanism. J. of Biomech. 24(7): 615-629.

Walker S.M. and Schrodt G.R. (1974). I segment lengths and thin filament periods in skeletal muscle fibres of the rhesus monkey and the human. Anatomical Record, 178: 63-82.

Wilkie D.R. (1950). The relation between force and velocity in human muscle. J. of Physiology 110: 249-280.

Winters J.M. and Kleweno D.G. (1993). Effect of initial upper-limb alignment on muscle contributions to isometric strength curves. J. of Biomechanics 26(2): 143-153.

Appendix B: The input files and euler angles for abduction and anteflexion.

ACz and ACy are the z- and y-co-ordinate of the acromioclavicular joint in cm. TSx and TSz are the x- and z-co-ordinate of the trigonum spinae in cm. AIx and AIz are the x- and z-co-ordinate of the angulus inferior in cm. ACz, ACy and TSz are the co-ordinates that are actually used.
ph is the pole angle of the humerus in rad; eh is the elevation angle of the humerus in rad; ah is the axial rotation of the humerus in rad; kfx, kfy and kfz are the x-, y- and z-directions of the external force in rad.

abduction:

ACz	ACy	TSx	TSz	AIx	AIz
0.9473	-6.5802	7.8786	-1.7141	9.9009	-13.8891
2.7231	-9.3383	5.9659	-2.2841	9.4805	-14.0280
4.7779	-10.6369	6.9585	-4.4372	13.9227	-13.8182
5.6942	-11.5144	7.4784	-5.0524	15.4694	-12.7856
6.5123	-11.9378	7.8773	-4.8923	16.4049	-11.5485
6.3512	-12.5959	7.9820	-5.6271	17.0191	-11.2018
5.7320	-12.0504	8.4644	-6.0280	17.2586	-12.0534

ph	eh	ah	kfx	kfy	kfz
0.6877	-0.1955	-0.1868	0	0	-1
-0.1626	-0.5425	-0.6150	-0.0142	0.0047	-0.999
-0.1065	-1.0278	-0.8641	-0.0257	-0.0101	-0.9996
-0.0362	-1.5601	-0.9753	-0.0243	-0.0199	-0.9995
0.0516	-2.0187	-0.9262	-0.0406	-0.1306	-0.9906
0.2895	-2.5108	-0.9623	-0.0325	-0.1849	-0.9822
0.8502	-2.8251	-0.7059	-0.0499	-0.1573	-0.9863

anteflexion:

ACz	ACy	TSx	TSz	AIx	AIz
2.6760	-8.6660	5.9590	-1.0690	8.6830	-12.6900
0.8755	-6.6206	6.5131	-1.9026	8.5865	-14.0690
1.6656	-7.5909	6.2627	-2.8519	9.8113	-14.5996
3.1426	-8.4407	6.6853	-4.2481	11.7623	-14.9725
4.5404	-9.9301	7.1930	-5.3911	13.3096	-14.1827
5.3027	-10.8103	7.7305	-5.8536	14.9479	-13.0733
5.6959	-12.1748	7.3074	-6.0685	15.7324	-12.1856
6.3264	-11.5031	7.9876	-5.5439	16.8656	-11.3394

ph	eh	ah	kfx	kfy	kfz
0.0162	0.0278	-0.0186	0	0	-1
0.5917	-0.1885	-0.2190	0	0	-1
1.3686	-0.5080	-0.5854	-0.0003	0.0267	-0.9996
1.4008	-0.9920	-0.6022	-0.0215	-0.0584	-0.9981
1.3706	-1.5355	-0.5722	-0.0517	-0.0508	-0.9974
1.2920	-1.9828	-0.5124	-0.0687	-0.0800	-0.9944
1.2182	-2.4856	-0.7513	-0.0896	-0.1346	-0.9868
0.9403	-2.8411	-0.6674	-0.0054	-0.1514	-0.9885

Appendix C

Table C1. Positions of origos and insertions of all modelled muscle parts in the global co-ordinate system (in cm). The order of the muscle parts is given in Table 3.

	Origo			Insertion		
	X	Y	Z	X	Y	Z
m. trapezius (scapular part)						
1	-1.8904	-11.2763	5.3785	14.9943	-11.2320	2.1376
2	-1.8890	-11.4008	5.0862	13.7056	-12.9513	1.8133
3	-1.5481	-11.6880	4.2946	11.6866	-13.8968	1.1798
4	-1.5203	-12.0471	3.7619	10.5146	-14.3565	0.8749
5	-1.4931	-12.4189	2.6528	9.6328	-14.0479	0.8735
6	-1.7264	-13.5464	0.0240	10.7836	-14.7089	0.4617
7	-1.5555	-14.6363	-3.3357	9.6328	-14.0479	0.8735
8	-1.0707	-15.1100	-6.2337	10.0464	-14.7600	0.4819
9	-0.7985	-15.2673	-11.0358	8.0615	-14.7187	0.2544
10	-0.4623	-15.4907	-14.7352	8.7510	-14.9916	0.1651
11	-0.0797	-14.9085	-17.8932	9.4482	-15.0027	-0.1575
m. trapezius (clavicular part)						
1	-2.0275	-11.0706	12.9772	11.0890	-7.2724	2.6412
2	-2.0679	-10.5027	7.2103	13.4498	-8.4792	2.7459
m. levator scapulae						
1	3.3216	-6.0184	14.8053	5.7675	-14.7590	0.0382
2	2.3209	-6.2825	12.5541	5.9216	-13.8047	1.2786
m. pectoralis minor						
1	5.2394	1.2778	-6.0785	11.8653	-5.6065	-0.2066
2	6.0317	2.0711	-9.3504	11.8653	-5.6065	-0.2066
3	9.7596	1.0814	-9.4911	12.2797	-5.2336	-0.7740
4	9.0032	1.5395	-11.4038	12.8109	-5.0028	-1.5095
m. rhomboideus						
1	-1.9280	-10.6627	6.3098	5.9951	-15.0321	-1.5981
2	-1.8523	-11.3814	5.0964	6.6717	-16.2233	-8.6566
3	-0.6490	-12.5183	3.2077	6.6721	-16.3374	-9.1878
4	-1.5564	-13.4013	0.7291	6.9441	-16.4000	-10.3684
5	-1.3305	-14.4514	-1.9454	7.1993	-16.2116	-11.5347
m. serratus anterior						
1	13.3596	-4.8814	-20.9784	7.4699	-16.5086	-12.0571
2	13.0221	-2.8009	-18.8449	7.5406	-16.1092	-12.0256
3	12.2995	-1.4578	-15.9176	7.8735	-15.6214	-12.0602
4	12.2434	-0.8921	-12.2213	7.9400	-15.4002	-11.5350
5	11.8141	-1.5652	-8.6058	7.7207	-15.3605	-10.9807
6	10.9746	-3.0547	-4.2826	7.9827	-15.4684	-10.5253
7	0.9647	1.0111	1.0597	6.7538	-15.5386	-6.1059
8	0.9928	1.0385	1.0864	6.2681	-15.2769	-3.2108
9	0.9631	1.0095	1.0582	5.7479	-14.3685	-0.2098
10	0.9247	0.9721	1.0218	6.0232	-13.2329	0.9804
11	0.9631	1.0095	1.0582	6.2498	-12.4420	1.3507
12	0.9247	0.9721	1.0218	6.9048	-10.8610	1.9912
m. deltoideus (scapular part)						
1	9.4684	-14.8917	-0.5938	18.4682	-9.3818	-12.8570
2	12.4423	-13.9445	0.6504	18.4354	-8.8027	-11.4201
3	15.6743	-12.5073	1.1467	18.4354	-8.8027	-11.4201
4	16.8045	-11.8412	0.2822	18.3433	-8.5794	-10.2688
5	17.7887	-10.1069	0.9357	18.2755	-8.1677	-9.6175
6	17.2357	-11.5633	1.3549	18.6297	-8.9985	-12.6555
7	17.6406	-11.0204	0.8921	18.6042	-9.1048	-14.9233
8	17.7691	-9.9746	1.4686	18.6297	-8.9985	-12.6555
9	17.7420	-9.3512	1.2981	18.3699	-7.9508	-13.6077
10	17.6354	-8.4395	1.2686	18.2577	-7.7531	-12.4748
11	16.9584	-7.3841	1.4149	18.0666	-7.4050	-11.1522

Table C1, continuation.

	Origo			Insertion		
	X	Y	Z	X	Y	Z
m. deltoideus (clavicular part)						
1	13.1735	-7.1266	2.2178	18.0666	-7.4050	-11.1522
2	11.0221	-6.4419	2.4778	17.8219	-7.4870	-13.8208
3	11.7164	-6.3099	2.1909	17.9425	-7.4318	-11.8671
4	11.5554	-6.2463	1.5782	17.8219	-7.4870	-13.8208
m. coracobrachialis						
1	14.0877	-5.2927	-0.9444	16.4611	-8.8362	-16.5218
2	13.6445	-5.3079	-1.6714	16.3390	-9.7459	-18.3031
3	13.7733	-4.7612	-0.9841	16.4287	-9.3859	-19.2460
m. infraspinatus						
1	11.6715	-12.6272	-4.4540	18.6553	-8.3201	-0.7757
2	7.2284	-16.9435	-10.2442	18.2532	-7.8173	-0.2216
3	8.5397	-16.1837	-8.0291	18.2532	-7.8173	-0.2216
4	7.9280	-15.9666	-5.7979	18.0313	-7.9007	0.0926
5	7.4454	-14.7615	-2.6400	18.0313	-7.9007	0.0926
6	9.6984	-14.9459	-0.5077	18.4047	-7.9531	-0.5318
m. teres minor						
1	12.7792	-13.0276	-6.7477	19.1127	-7.8953	-2.4843
2	12.1281	-14.0941	-7.0786	19.2611	-7.6760	-1.9229
3	13.8582	-12.0536	-4.0956	19.1127	-7.8953	-2.4843
m. teres major						
1	10.5848	-14.3588	-11.0116	15.7273	-8.0832	-8.5045
2	9.3963	-15.1616	-11.9722	16.0988	-8.1194	-10.3697
3	10.3854	-15.6632	-9.4777	16.0016	-8.1496	-9.7721
4	11.1904	-14.2404	-9.9469	15.5616	-7.8543	-6.9451
m. supraspinatus						
1	10.8974	-12.4454	-0.0242	17.6841	-6.7197	-0.3548
2	11.1947	-13.4896	0.8748	17.6841	-6.7197	-0.3548
3	7.2031	-12.9122	1.1051	17.6841	-6.7197	-0.3548
4	8.6127	-10.7781	1.2976	17.6841	-6.7197	-0.3548
m. subscapularis						
1	10.9262	-12.1769	-1.7034	15.3153	-6.4822	-0.5466
2	8.2648	-12.3104	0.3642	15.4282	-6.1775	-0.8850
3	7.2365	-14.4474	-2.4352	15.3153	-6.4822	-0.5466
4	9.0112	-14.7856	-5.0507	15.3467	-5.7682	-1.4950
5	9.7204	-14.2263	-6.3095	15.7158	-5.6155	-1.2757
6	8.6998	-15.7568	-8.6726	15.3709	-5.4648	-1.9393
7	9.3425	-15.0225	-10.1783	15.0507	-5.7762	-2.0724
8	11.3908	-12.9011	-6.9038	15.0507	-5.7762	-2.0724
9	11.0814	-14.1235	-9.6232	14.8434	-6.3132	-2.4856
10	13.1875	-11.9956	-5.4618	15.1323	-7.1525	-3.7387
11	13.7269	-10.8867	-4.5412	15.1617	-7.7733	-4.2712

Table C1, continuation.

	Origo			Insertion		
	X	Y	Z	X	Y	Z
m. biceps, caput longum						
1	14.6956	-8.5567	-0.2158	17.6988	-9.1577	-35.9757
2	14.6956	-8.5567	-0.2158	17.6988	-9.1577	-35.9757
m. biceps, caput breve						
1	13.7946	-4.7684	-0.9974	17.6988	-9.1577	-35.9757
2	13.7946	-4.7684	-0.9974	17.6988	-9.1577	-35.9757
m. triceps, caput longum						
1	14.3191	-11.5205	-4.2065	17.0632	-12.4702	-31.6776
2	14.4811	-9.6574	-4.0742	18.2275	-11.8252	-32.5161
3	14.8925	-10.4851	-3.6625	18.3164	-11.8208	-32.1787
4	14.4811	-9.6574	-4.0742	18.5857	-11.4229	-35.1703
m. latissimus dorsi						
1	-0.4863	-15.3443	-12.5442	15.9401	-6.7855	-5.8336
2	-0.1396	-14.9621	-19.6172	16.0506	-6.8480	-6.4862
3	-0.2030	-14.0633	-25.0985	16.0506	-6.8480	-6.4862
4	0.8435	-13.0657	-31.0486	15.9401	-6.7855	-5.8336
5	6.8915	-10.7368	-30.8142	15.9401	-6.7855	-5.8336
6	9.5151	-9.5563	-29.7617	16.0506	-6.8480	-6.4862
m. pectoralis major (thoracal part)						
1	6.3409	2.5610	-15.7614	16.8804	-6.6790	-8.3321
2	3.0930	3.5846	-14.0508	16.9646	-6.7293	-8.8986
3	1.1166	3.3334	-12.2429	16.9918	-6.8021	-9.3971
4	1.6226	3.5329	-10.0782	16.9441	-6.6338	-8.4562
5	0.8495	1.7979	-4.1932	16.8798	-6.4897	-7.4597
6	1.1766	0.4842	-2.2733	16.9441	-6.6338	-8.4562
m. pectoralis major (clavicular part)						
1	6.3029	-1.6236	0.2330	17.2010	-7.0012	-10.8629
2	7.9598	-2.6360	0.6903	16.8798	-6.4897	-7.4597

Table C2. Sarcomere length (l_s), fibre bundle length (l_b), mean sarcomere length (Ml_s), tendon length (l_t), measured muscle length (l_m), modelled muscle length (l_m_m). Sarcomere length is given in μm, all other lengths are given in cm.

l_s			l_b			Ml_s	l_t	l_m	l_m_m
m. trapezius									
2.6	2.9	2.9	16.2	14.4	14.4	2.80	0.3	15.3	17.1
2.6	3.0	2.6	10.7	11.6	11.9	2.73	2.7	14.1	16.3
2.7	2.8	2.6	11.2	9.7	11.2	2.70	5.4	16.1	17.2
2.7	2.8	2.8	10.2	9.8	9.3	2.77	5.3	15.1	16.0
2.7	2.75	2.6	9.3	9.4	8.8	2.68	3.5	12.7	13.8
2.55	2.6	2.7	8.8	8.1	9.1	2.62	3.3	12.0	12.6
2.5	2.5	2.5	8.2	7.1	8.8	2.50	3.6	11.6	11.4
2.4	2.7	2.4	7.0	7.3	7.1	2.50	4.8	11.9	12.6
2.5	2.7	2.6	10.9	8.8	9.5	2.60	3.4	13.1	12.0
2.5	2.5	2.5	12.6	11.9	10.6	2.50	3.5	15.2	13.0
2.7	2.6	2.6	13.9	12.4	13.3	2.63	3.1	16.3	14.4
2.7	2.7	2.7	15.4	14.4	16.6	2.70	4.7	20.2	17.3
2.5	2.4	2.5	17.1	16.7	15.5	2.47	6.6	23.0	20.1
m. levator scap.									
2.5	2.5	2.4	14.0	13.9	15.4	2.47	1.9	16.3	17.3
2.6	2.5	2.7	13.0	12.3	12.3	2.60	1.8	14.3	14.0
m. pectoralis min.									
2.5	2.5	2.4	6.1	5.9	9.0	2.47	5.1	12.1	11.2
2.4	2.6	2.4	7.9	10.8	11.1	2.47	4.1	14.0	13.3
2.4	2.5	2.5	9.7	8.9	10.9	2.47	2.9	12.7	11.1
2.5	2.4	2.4	13.6	12.4	11.3	2.43	2.6	15.0	12.5
m. rhomboideus									
2.6	2.5	2.8	10.4	9.3	9.1	2.63	1.5	11.1	12.1
2.7	2.7	2.7	10.9	9.4	12.0	2.70	6.6	17.4	16.9
2.7	2.8	2.7	13.0	12.6	12.6	2.73	3.2	15.9	14.9
2.7	2.6	2.7	12.9	12.5	12.2	2.67	3.1	15.6	14.3
2.5	2.5	2.5	10.7	10.8	11.4	2.53	4.0	15.0	13.0

Table C2, continuation.

l_s			l_b			Ml_s	l_r	l_m	l_{m_m}
m. serratus ant.									
2.6	2.6	2.5	15.6	15.1	16.0	2.57	2.5	18.1	16.2
2.7	2.5	2.5	16.0	17.1	14.5	2.57	0.9	16.8	17.0
2.7	2.7	2.5	16.8	16.2	14.4	2.63	0.7	16.5	17.0
3.2	2.9	3.9	16.1	15.7	15.9	3.33	0	15.7	16.9
3.0	3.1	3.0	14.1	14.3	14.0	3.03	1.1	15.2	16.3
3.1	3.1	3.0	12.9	14.6	14.1	3.07	0	13.8	15.5
2.5	2.7	2.8	10.1	12.1	11.4	2.67	0.9	12.1	13.8
2.9	2.8	2.7	9.0	7.9	9.4	2.80	1.1	9.9	10.3
2.7	2.4	2.2	6.9	8.2	6.5	2.43	0.7	7.9	9.0
2.8	3.0	2.5	6.5	6.8	7.0	2.77	0.5	7.3	13.0
2.3	2.5	2.3	7.4	8.6	7.3	2.37	0	7.5	6.9
2.0	2.3	2.3	7.9	7.5	7.7	2.20	0	7.4	10.4
m. deltoideus									
2.6	2.6	2.6	10.3	10.9	11.4	2.60	8.0	18.9	16.2
2.55	2.6	2.6	8.2	10.5	8.5	2.58	7.6	16.7	14.4
2.8	2.35	2.85	9.6	7.0	8.1	2.67	6.2	14.4	13.4
2.75	2.85	2.7	7.6	6.4	6.5	2.77	4.5	11.3	11.2
3.3	2.9	2.9	8.3	6.9	6.9	3.03	3.5	10.9	10.8
2.85	2.8	2.9	7.9	8.6	7.8	2.85	6.7	14.8	14.3
2.7	3.1	2.9	7.8	8.4	8.1	2.90	8.2	16.3	16.0
3.0	3.0	3.1	8.1	7.7	8.1	3.03	6.5	14.5	14.2
3.1	3.1	3.1	8.5	8.6	8.1	3.10	7.1	15.5	15.2
3.25	3.4	3.3	9.4	9.0	9.2	3.32	6.4	15.6	14.4
3.5	3.1	3.5	8.8	9.2	9.6	3.37	4.8	14.0	13.5
2.85	3.0	3.0	8.8	9.7	8.9	2.95	6.2	15.3	14.4
2.9	3.0	2.9	10.9	10.9	8.8	2.93	8.8	19.0	17.7
3.0	2.9	3.0	8.1	10.0	9.1	2.97	6.7	15.8	15.4
2.8	2.9	2.9	9.9	11.5	10.2	2.87	7.3	17.8	16.7
m. coracobrach.									
2.5	2.6	2.8	6.8	5.8	6.7	2.63	9.2	15.6	16.1
2.6	2.5	2.6	7.4	5.9	6.2	2.57	10.4	16.9	17.4
2.5	2.4	2.6	6.3	6.7	7.2	2.50	11.3	18.0	19.0
m. infraspinatus									
2.8	2.7	2.7	4.5	9.3	5.4	2.73	3.8	10.2	9.5
2.6	2.8	2.5	6.5	7.2	7.3	2.63	10.7	17.7	18.1
2.7	2.7	2.7	6.0	8.2	6.1	2.70	8.4	15.2	15.6
2.7	3.0	2.8	7.3	8.0	6.5	2.83	7.1	14.4	14.6
2.7	3.0	3.0	8.4	6.4	7.7	2.90	5.0	12.5	13.2
2.6	2.8	2.7	8.4	6.4	7.8	2.70	3.5	11.0	11.4
m. teres minor									
2.3	2.4	2.4	4.5	5.1	3.6	2.37	4.9	9.4	9.2
2.5	2.4	2.5	5.1	4.8	5.2	2.47	5.1	10.1	10.9
2.4	2.6	3.0	5.0	4.9	5.1	2.67	1.8	6.8	6.9
m. teres major									
2.6	2.1	2.1	14.4	8.4	12.8	2.27	0.6	12.5	8.5
2.6	2.3	2.1	13.8	13.8	13.7	2.33	1.2	15.0	9.9
2.4	2.2	2.2	13.5	11.6	13.4	2.27	1.5	14.3	9.4
2.0	2.2	2.1	10.0	7.5	8.0	2.10	3.4	11.9	8.3
m. supraspinatus									
3.3	3.1	3.0	6.4	5.9	6.5	3.13	1.7	8.0	9.3
3.0	3.0	3.1	6.7	6.3	6.9	3.03	2.5	9.1	9.8
3.0	3.2	3.2	6.1	6.7	6.8	3.13	5.2	11.7	12.5
3.2	3.0	3.3	6.3	6.4	6.8	3.17	3.1	9.6	10.3

Table C2, continuation.

l_s			l_p			Ml_s	l_z	l_m	l_m m
m. subscapularis									
2.8	3.2	2.7	5.8	6.4	5.7	2.90	2.8	8.8	7.4
2.6	3.0	2.9	7.2	6.1	7.1	2.83	4.4	11.2	9.6
2.8	2.7	2.7	7.3	7.9	5.3	2.73	5.9	12.7	11.6
3.3	2.8	2.4	7.5	7.1	8.8	2.83	5.5	13.3	11.6
2.5	2.7	2.4	8.9	7.1	6.4	2.53	6.6	14.1	11.7
2.6	2.7	2.5	7.2	6.7	8.1	2.60	7.7	15.0	14.0
2.4	2.5	2.5	7.7	7.1	7.7	2.47	7.9	15.4	13.6
2.5	2.6	2.5	6.3	7.0	8.2	2.53	4.0	11.2	9.4
2.5	2.4	2.5	6.5	6.5	6.8	2.47	5.9	12.5	11.3
2.4	2.6	2.7	6.2	6.4	6.7	2.57	1.0	7.4	5.5
2.7	2.6	2.6	6.5	6.1	6.2	2.63	0	6.1	3.4
m. biceps									
3.2	3.2	3.2	13.1	16.4	16.2	3.20	13.3	28.5	38.5
3.1	3.2	3.1	15.9	15.1	14.2	3.13	13.4	28.5	38.5
3.4	3.5	3.6	15.5	15.6	14.4	3.50	16.3	31.5	34.3
3.5	3.5	3.6	15.5	15.6	14.0	3.53	16.5	31.5	34.3
m. triceps									
2.1	2.2	2.2	82	81	89	2.17	20.1	28.5	27.6
2.3	2.1	2.1	65	75	67	2.17	21.6	28.5	28.8
2.2	2.2	2.0		69	66	2.10	21.5	31.1	28.8
1.9	2.2	2.2	70	62	64	2.10	22.0	28.5	31.4
m. latissimus dor.									
2.5	2.4	2.5	229	186	228	2.47	9.0	30.4	20.3
2.1	2.4	2.4	265	240	225	2.30	8.3	32.6	23.2
2.4	2.3	2.3	261	252	251	2.33	10.5	36.0	26.6
2.3	2.2	2.5	275	274	281	2.33	12.0	39.7	30.7
2.6	2.4	2.0	264	276	270	2.33	7.2	34.2	27.1
2.0	2.0	2.0	255	253	248	2.00	6.9	32.1	24.4
m. pectoralis maj.									
2.3	2.4	2.4	181	156	159	2.37	3.6	20.1	15.9
2.5	2.4	2.4	153	161	180	2.43	4.3	20.8	18.0
2.3	2.5	2.3	165	164	159	2.37	5.3	21.6	19.0
2.6	2.4	3.1	203	169	178	2.70	2.8	21.1	18.5
3.1	3.1	2.9	182	158	165	3.03	2.6	19.4	18.3
3.0	2.7	3.0	164	129	174	2.90	3.6	19.2	18.4
3.0	3.1	3.0	150	141	168	3.03	1.7	17.0	16.5
2.9	2.8	2.8	131	109	103	2.83	1.4	12.8	12.7

Table C3. Physiological cross-sections of all muscle parts at optimum length (PCSA at l_0) in cm^2, physiological cross-section at the measured sarcomere length (PCSA) in cm^2, and measured cross-sections with the U-shape and the slide in cm^2.

Muscle	PCSA at l_0	PCSA	measured
m. trapezius	1.1826	1.2317	
	1.6831	1.7924	
	1.9850	2.1376	
	1.3787	1.4464	
	1.2218	1.3203	
	1.0090	1.1183	
	0.9721	1.1276	
	1.3819	1.6065	
	1.2286	1.3756	
	0.8068	0.9358	
	0.9155	1.0079	
	0.9744	1.0466	
	0.4739	0.5575	
total	15.2134	16.7042	17.05
m. levator scapulae	0.9633	1.1340	
	1.0433	1.1648	
total	2.0066	2.2988	1.96
m. pectoralis minor	0.4656	0.5498	
	1.0721	1.2593	
	1.0655	1.2529	
	0.4599	0.5475	
total	3.0631	3.6096	3.724
m. rhomboideus	0.5127	0.5663	
	0.9239	0.9924	
	1.4230	1.5104	
	0.8156	0.8872	
	0.6667	0.7630	
total	4.3419	4.7193	4.508
m. serratus anterior	0.6119	0.6918	
	1.0974	1.2413	
	1.0471	1.1520	
	1.0972	0.9687	
	0.6360	0.6081	
	0.9694	0.9171	
	0.4730	0.5141	
	0.7581	0.7863	
	0.7933	0.9508	
	0.6302	0.6651	
	0.2278	0.2788	
	1.1228	1.4883	
total	9.4643	10.2626	10.388

Table C3, continuation.

Muscle	PCSA at l_0	PCSA	measured
m. deltoideus	2.8888	3.2221	
	2.1090	2.3663	
	4.4564	4.8395	
	1.1711	1.2287	
	1.1982	1.1436	
	2.8486	2.9008	
	1.4862	1.4883	
	2.1476	2.0533	
	2.8614	2.6768	
	4.4518	3.8952	
	2.3928	2.0678	
	1.2817	1.2599	
	1.5958	1.5768	
	1.0453	1.0233	
	1.1177	1.1302	
total	33.0522	32.8726	29.7
m. coracobrachialis	2.0059	2.2134	
	1.4832	1.6743	
	1.1366	1.3186	
total	4.6257	5.2064	2.744
m. infraspinatus	2.7201	2.8972	
	2.7479	3.0325	
	1.9359	2.0792	
	2.0741	2.1223	
	3.0229	3.0434	
	1.8200	1.9630	
total	14.3209	15.1376	12.65
m. teres minor	1.2239	1.5003	
	1.9515	2.2937	
	1.7965	1.9686	
total	4.9718	5.7626	5.292
m. teres major	1.6536	2.1059	
	0.8497	1.0639	
	2.0042	2.5647	
	1.5779	2.1925	
total	6.0854	7.9271	8.232
m. supraspinatus	1.2045	1.1165	
	1.1274	1.0776	
	2.5830	2.3894	
	1.2999	1.1914	
total	6.2148	5.7750	5.684
m. subscapularis	0.4446	0.4453	
	0.7757	0.7995	
	2.6372	2.7965	
	2.7422	2.8803	
	1.1409	1.3081	
	1.4884	1.6659	
	1.6212	1.9075	
	0.6128	0.7019	
	2.2174	2.6074	
	0.4692	0.5306	
	0.1576	0.1735	
total	14.3071	15.8164	12.152

Table C3, continuation.

Muscle	PCSA at l_0	PCSA	measured
m. biceps	1.4239	1.2904	
	2.1063	1.9499	
	1.7607	1.4607	
	3.2749	2.6901	
total	8.5659	7.3911	5.880
m. triceps	2.2679	3.0358	
	3.0146	4.0494	
	2.8806	3.9847	
	3.3289	4.6355	
total	11.4920	15.7055	12.65
m. latissimus dorsi	0.5629	0.6608	
	0.8814	1.1203	
	1.2860	1.5984	
	0.9644	1.2013	
	0.8784	1.1056	
	1.0529	1.5267	
total	5.6260	7.2131	7.7
m. pectoralis major	1.2542	1.5395	
	1.1779	1.4057	
	1.6463	2.0199	
	1.5681	1.7025	
	1.3347	1.2768	
	1.9771	1.9698	
	1.7880	1.7112	
	1.1320	1.1570	
total	11.8782	12.7824	12.65

Appendix D

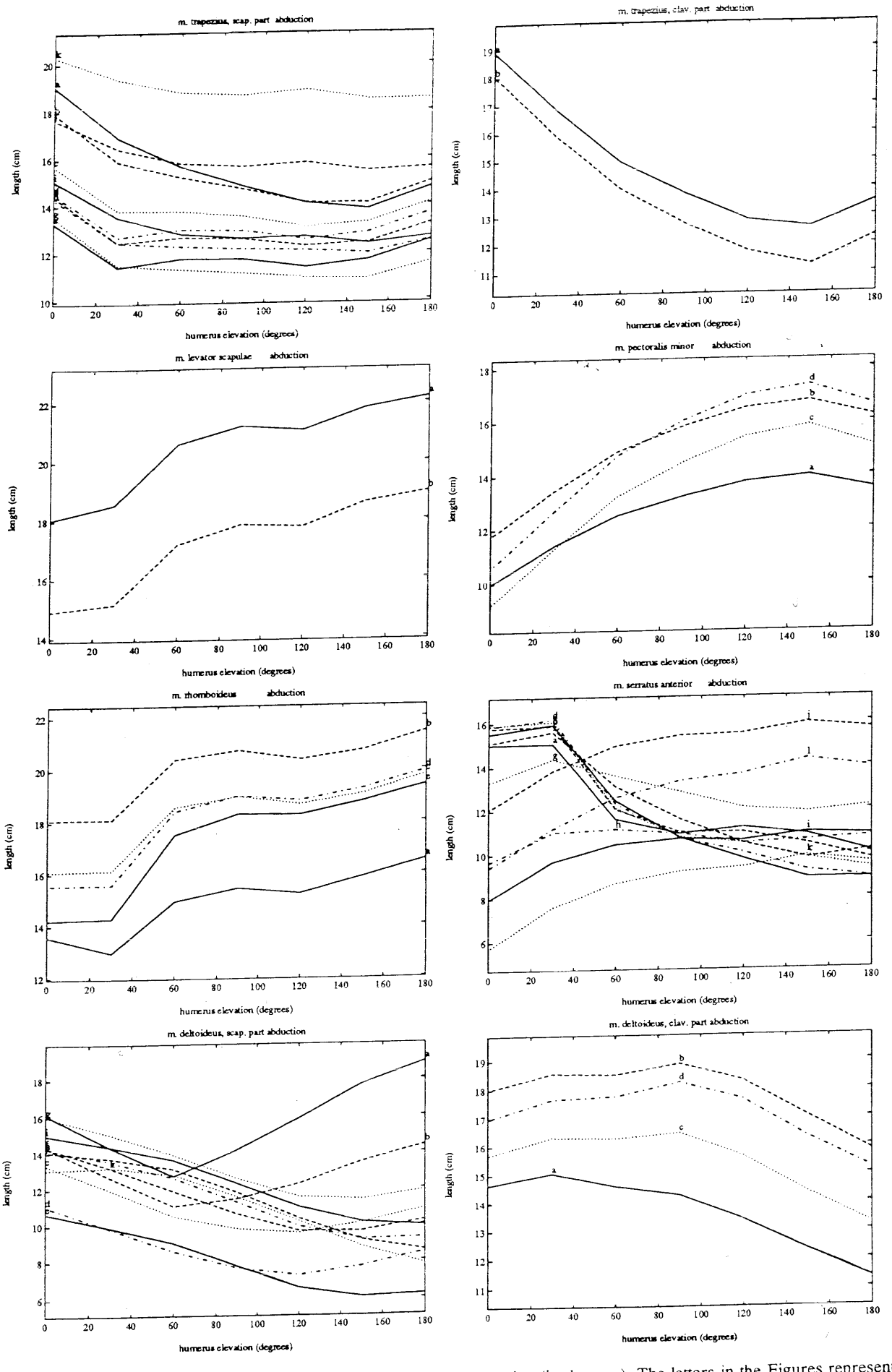

Figure D1: Muscle length of all muscle parts in cm during the abduction (in degrees). The letters in the Figures represent the muscle parts.

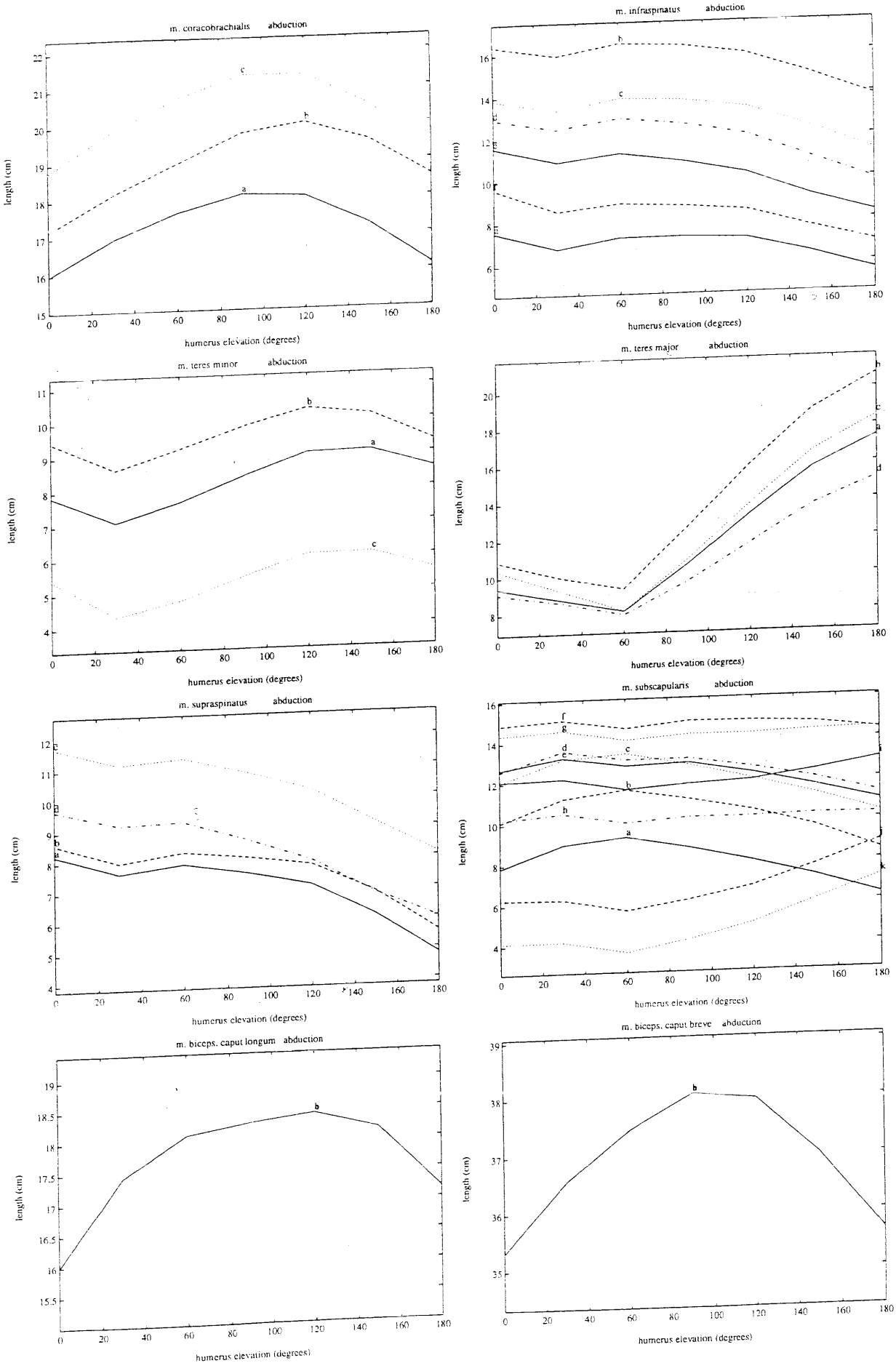

Figure D1, continuation.

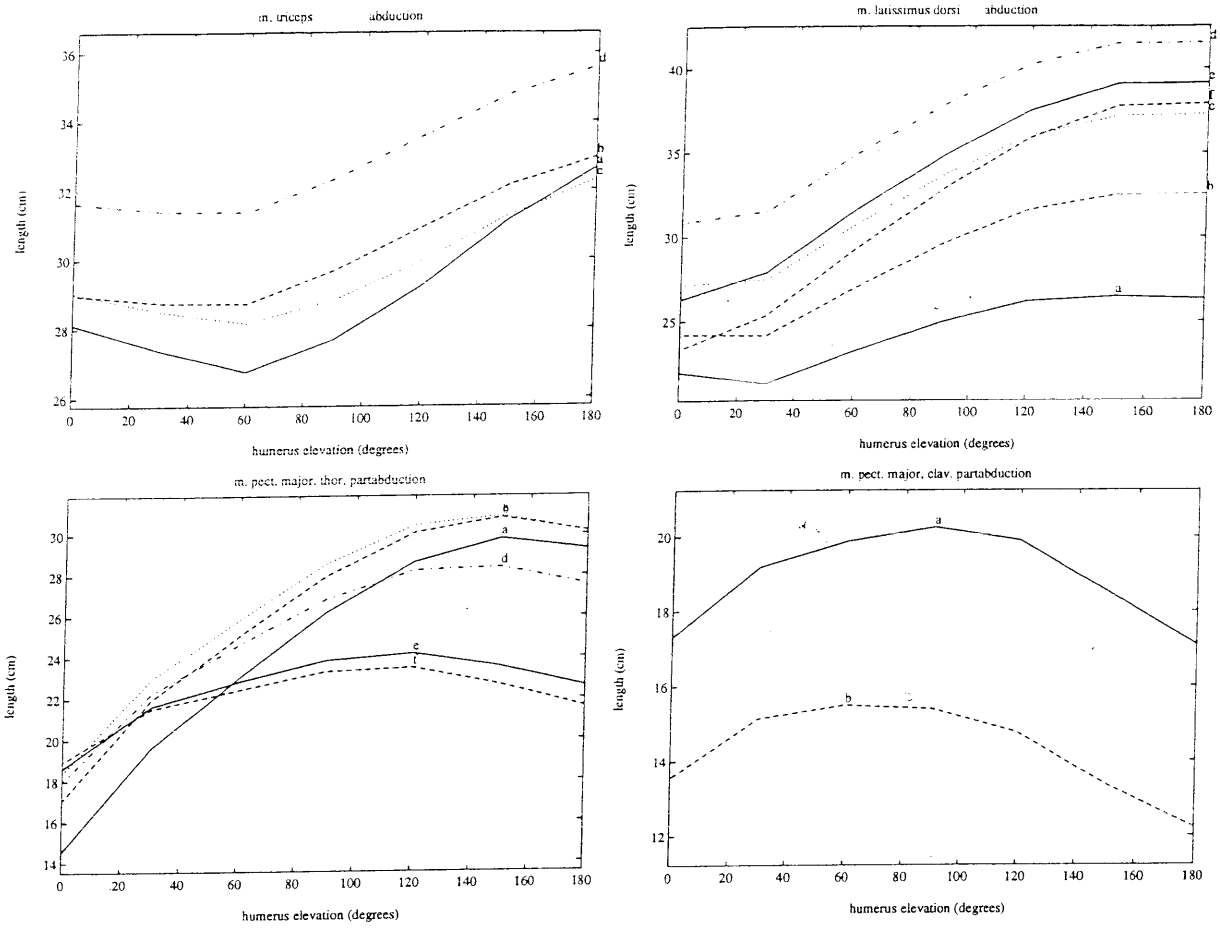

Figure D1, continuation.

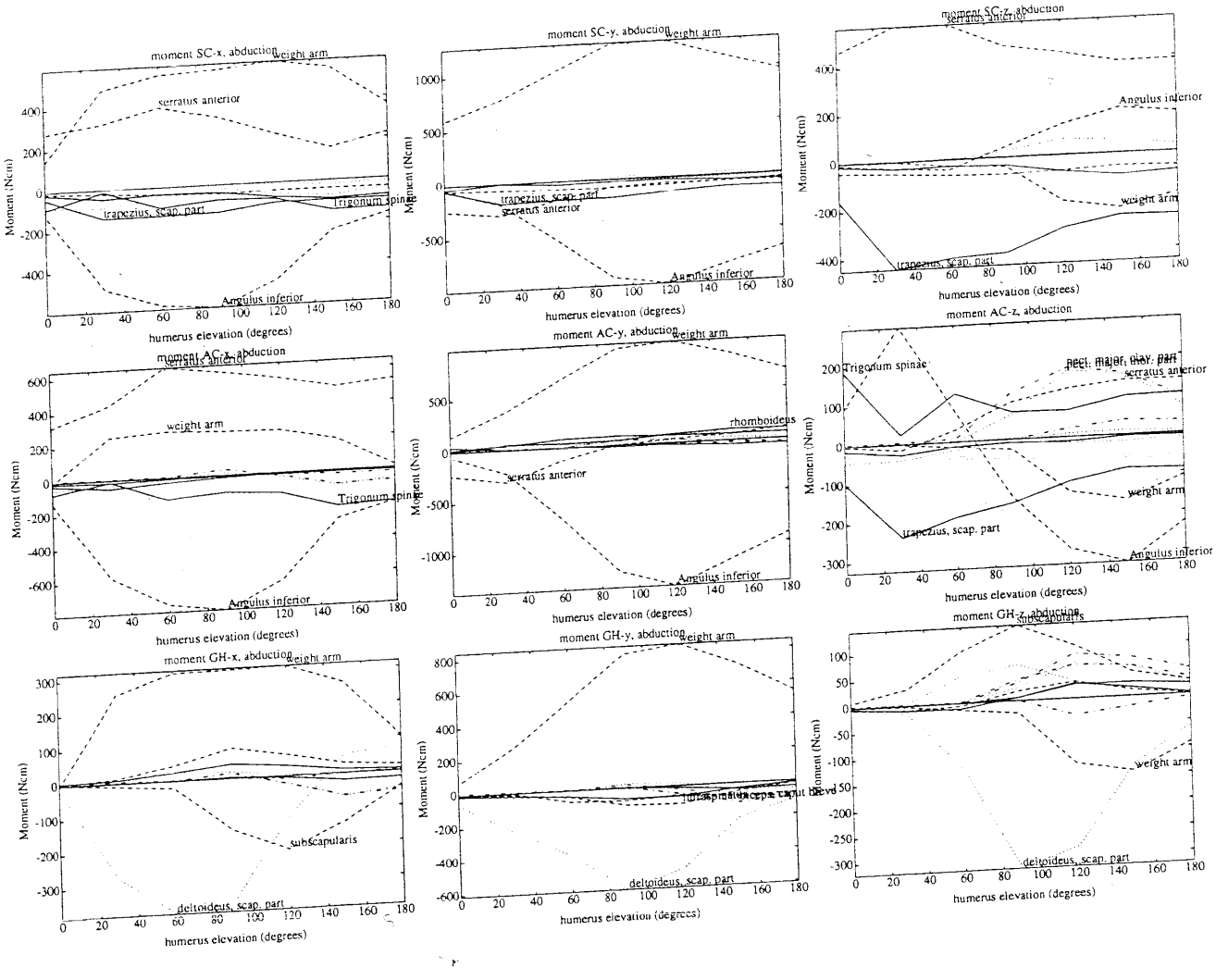

Figure D2.
All moments around the x-, y-, and z-axis of the sternoclavicular, the acromioclavicular and the glenohumeral joint. On the x-axis the humerus elevation (in degrees) and on the y-axis the moment (in Ncm). Muscle moment is the total muscle moment, the sum of all muscle parts.

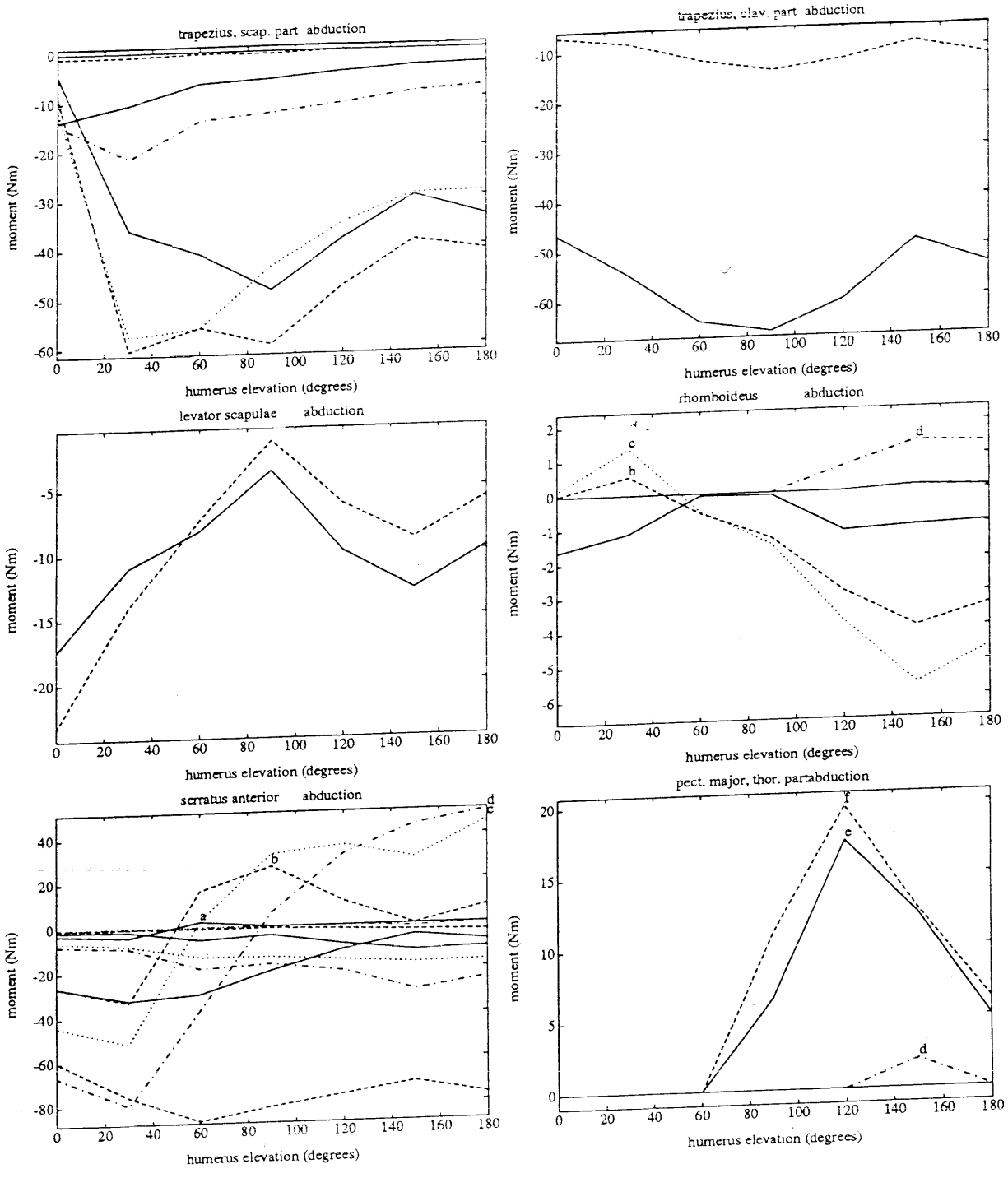

Figure D3.
Moment at the sternoclavicular joint of all muscle parts (in Nm) around the y-axis, which is the axis about which the abduction takes place.

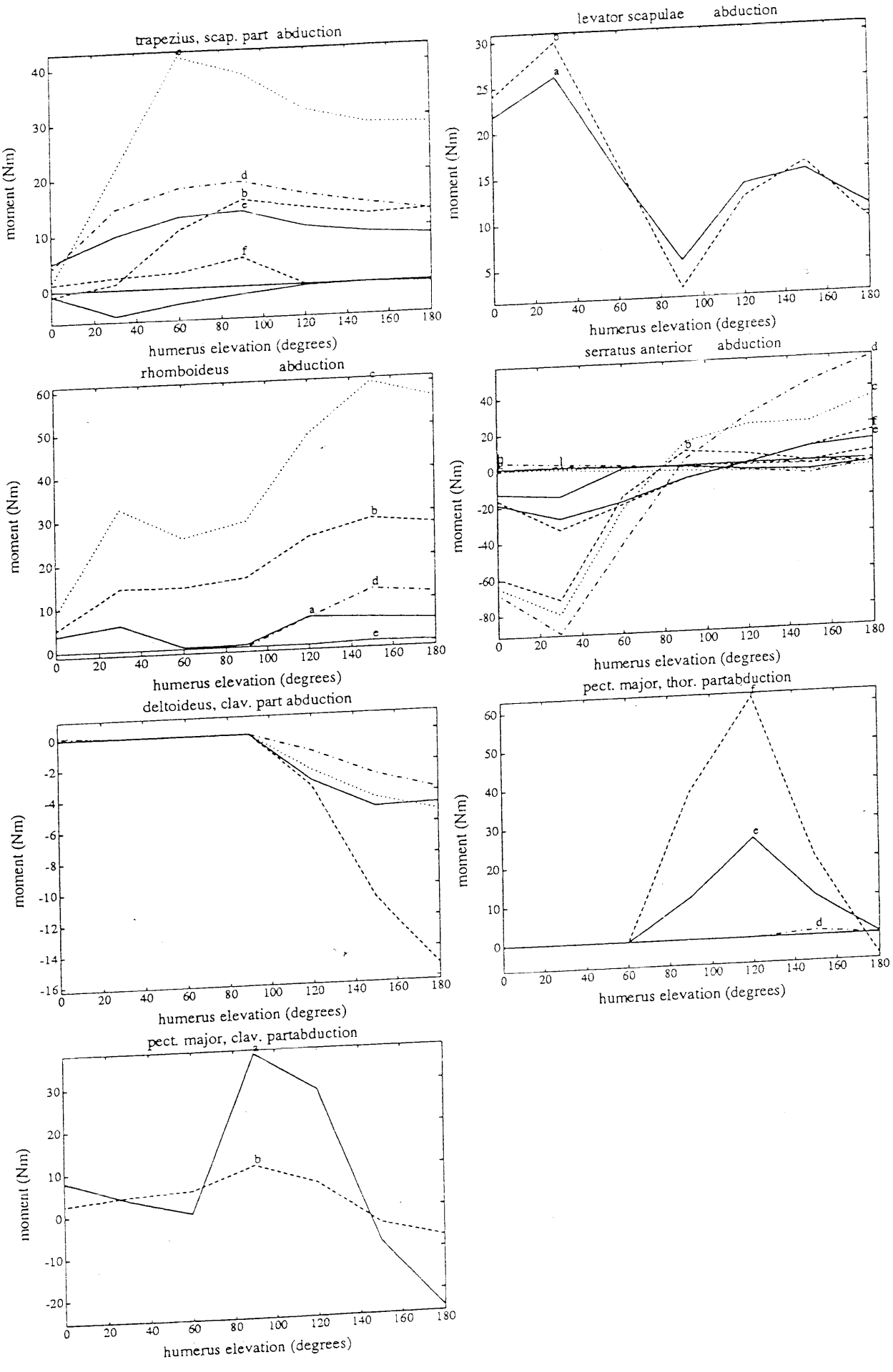

Figure D3, continuation.
Moment at the acromioclavicular joint of all muscle parts (in Nm) around the y-axis, which is the axis about which the

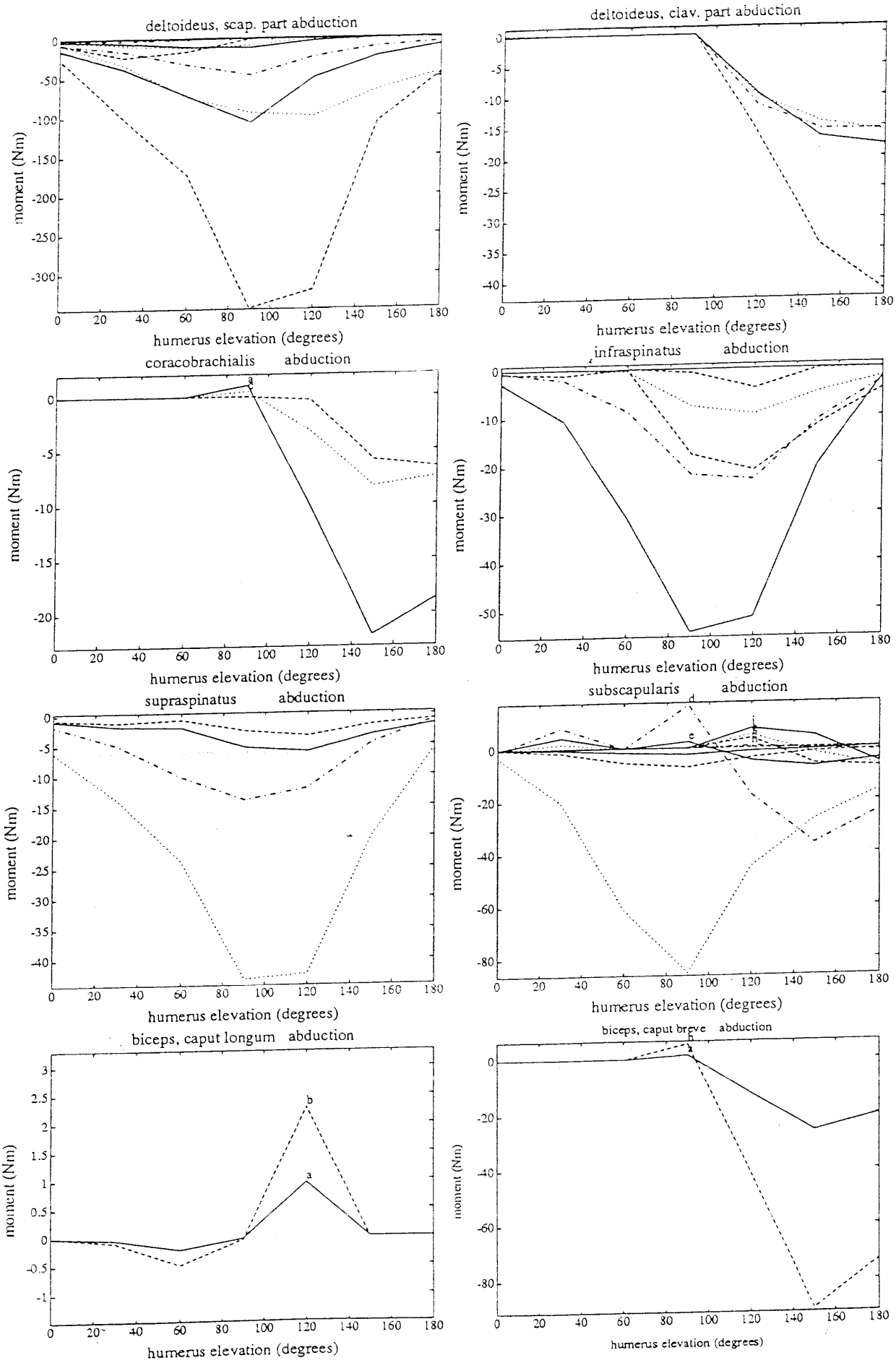

Figure D3, continuation.
Moment at the glenohumeral joint of all muscle parts (in Nm) around the y-axis, which is the axis about which the abduction takes place.

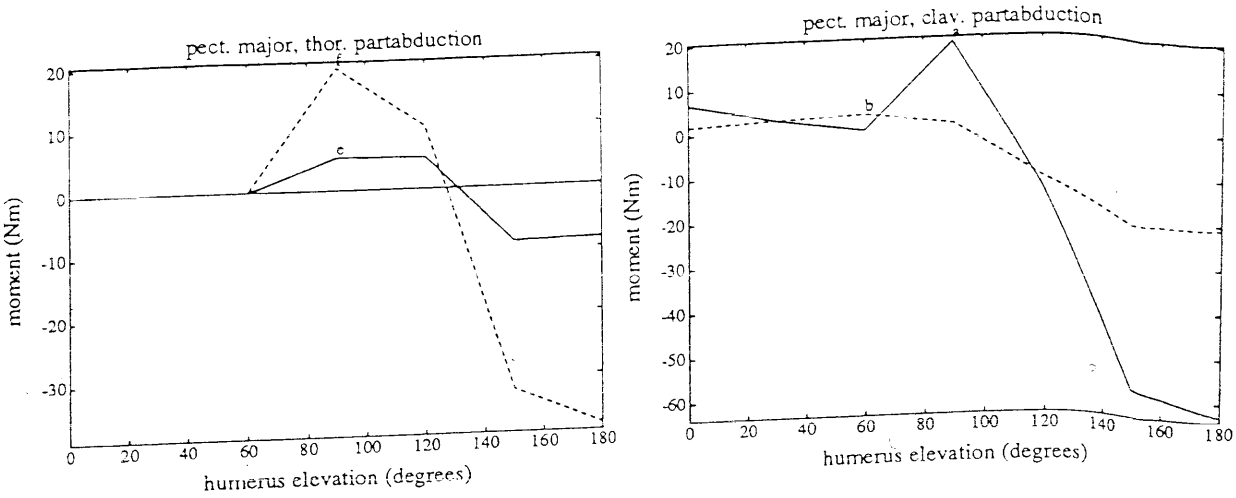

Figure D3, continuation.
Moment at the glenohumeral joint of all muscle parts (in Nm) around the y-axis, which is the axis about which the abduction takes place.

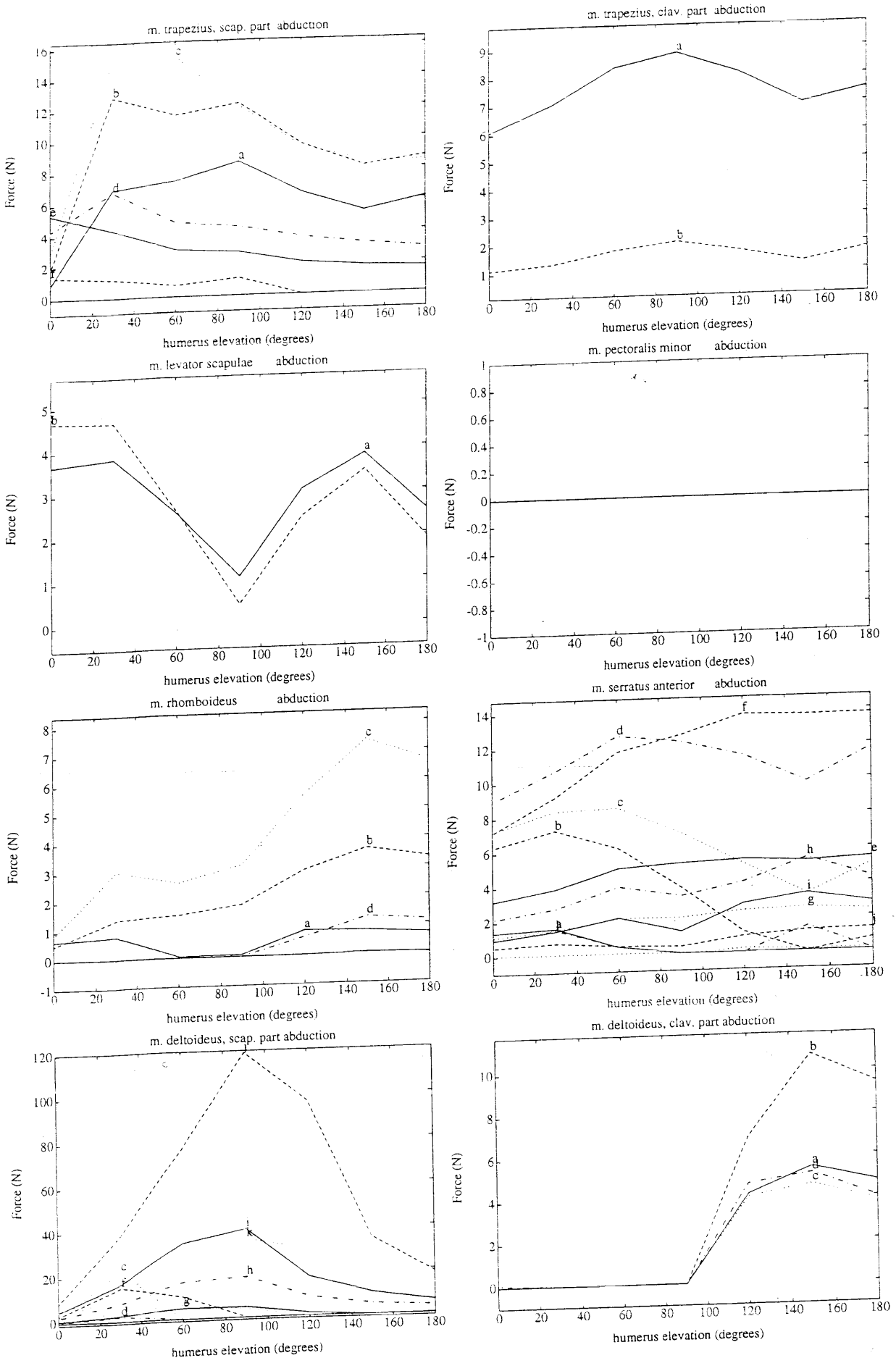

Figure D4.
Muscle force (in N) of all muscle parts. On the x-axis is the humerus elevation (in degrees).

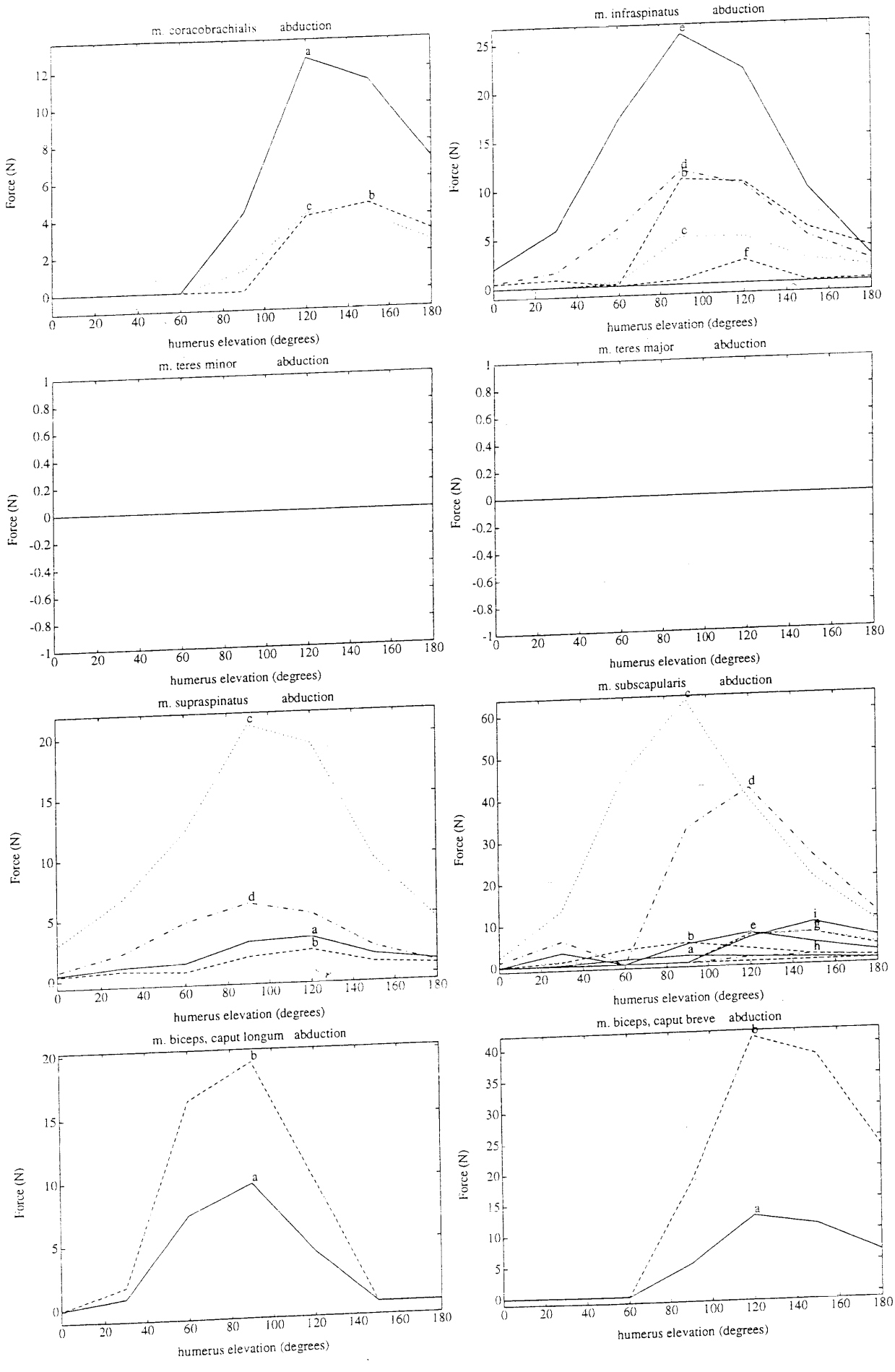

Figure D4, continuation.

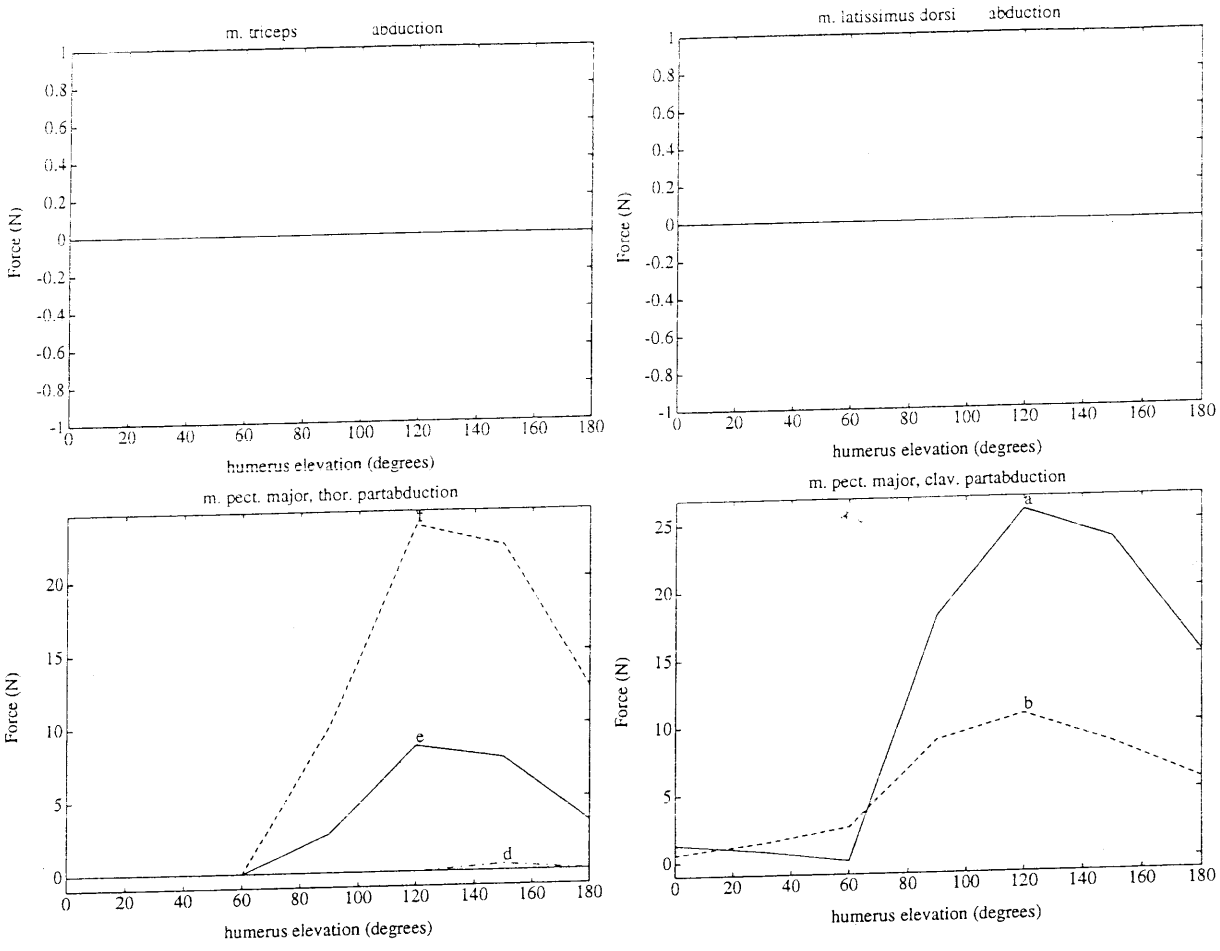

Figure D4, continuation.

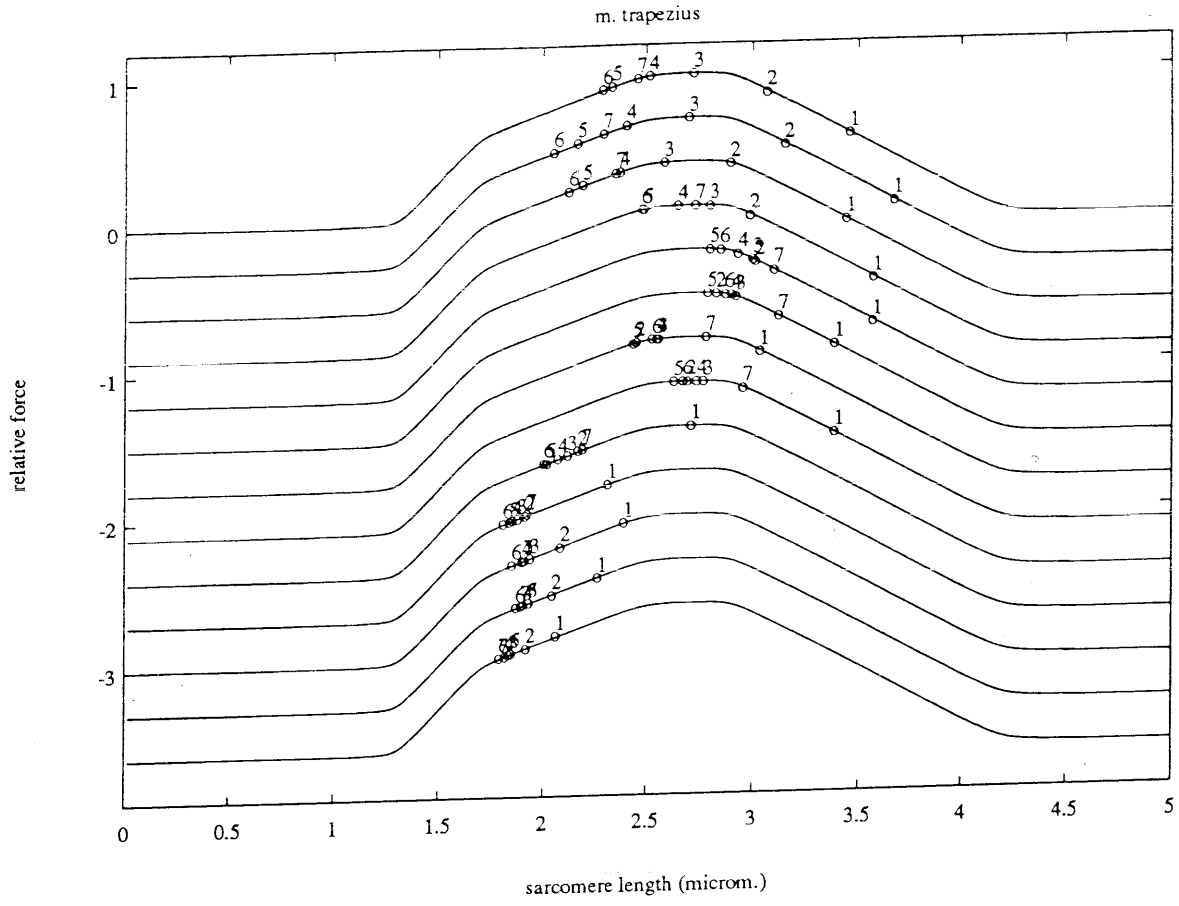

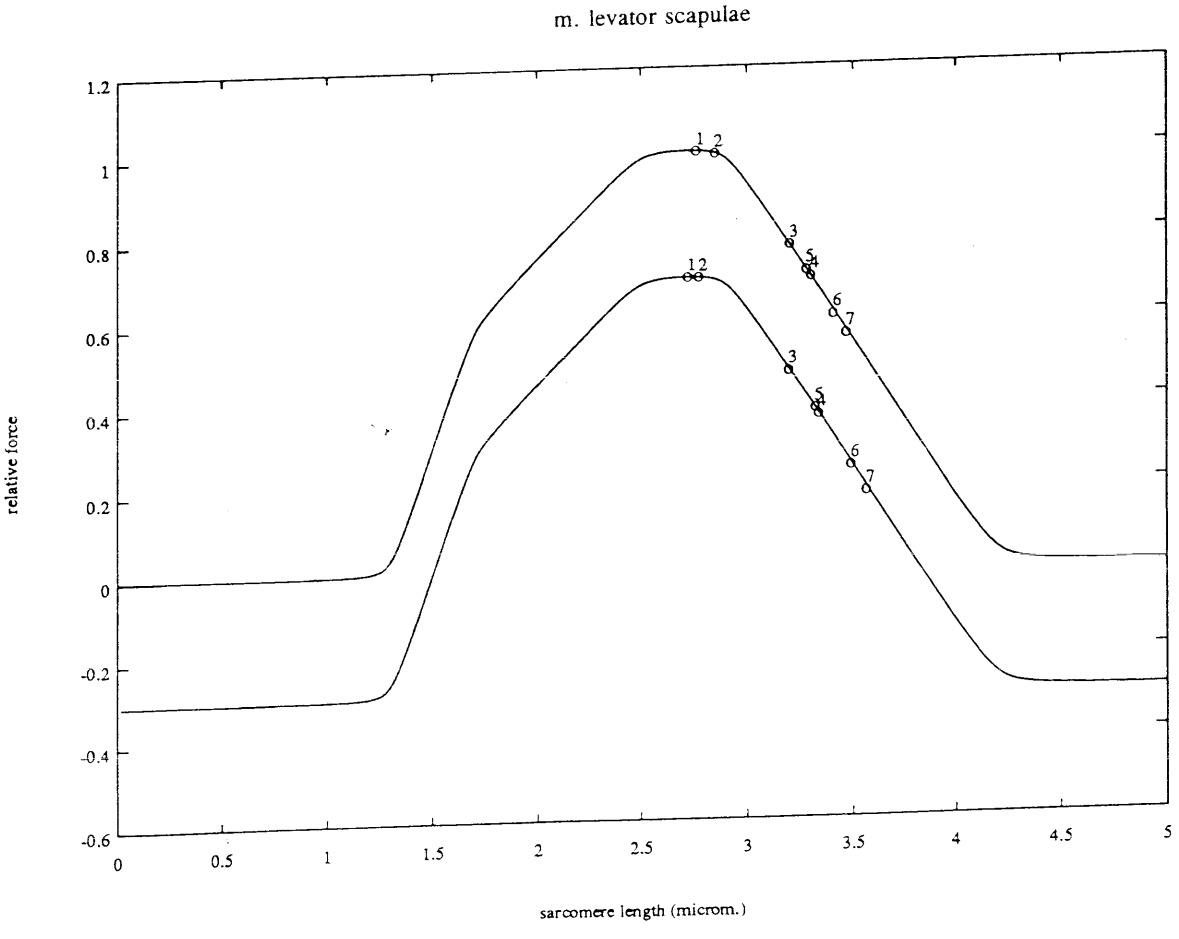

Figure D5. An abduction.
On the x-axis sarcomere length (in μm) and on the y-axis relative force. Each line represents the force-lengh relationship of one muscle part. The numbers represent the position during the abduction (position 1 is 0° abduction, position 7 is 180° abduction). The lines for each muscle part are plotted beneath each other. The scale on the y-axis only counts for the upper line.

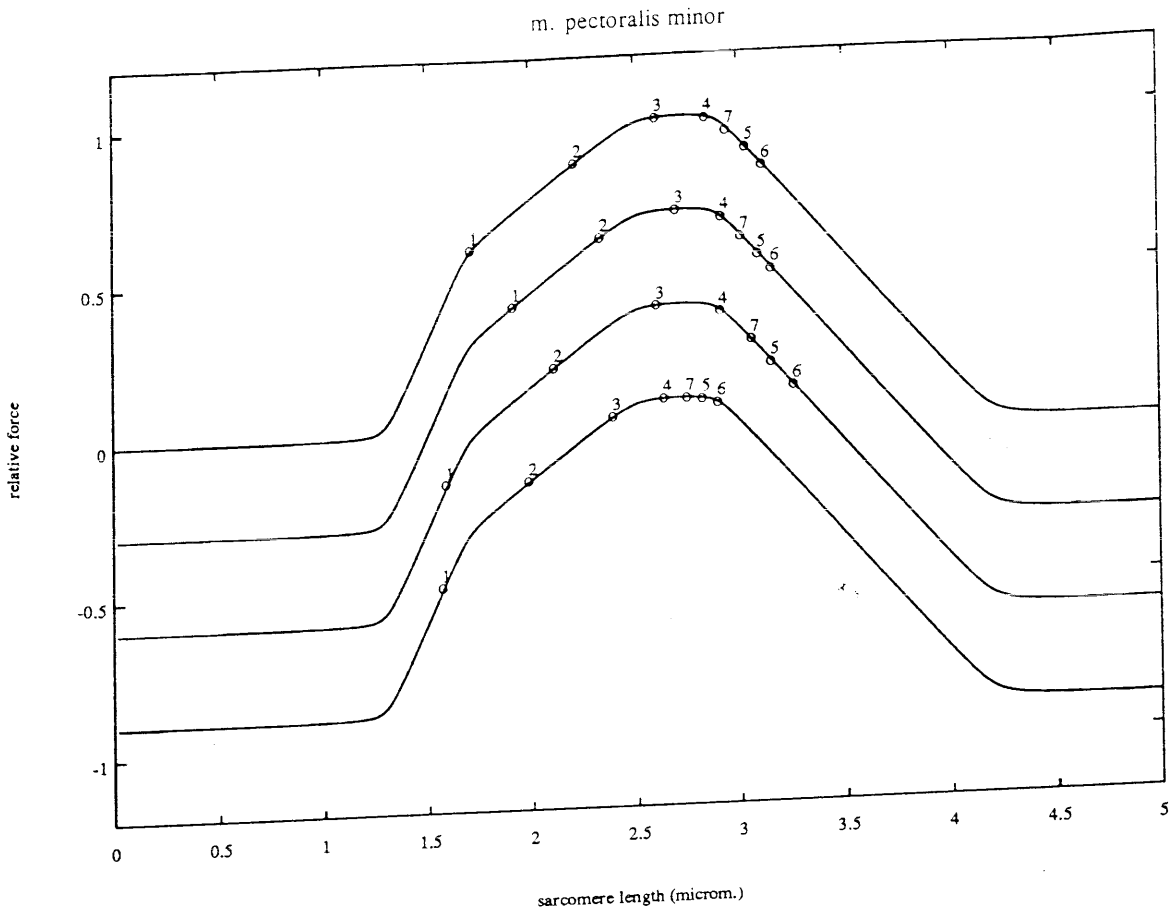

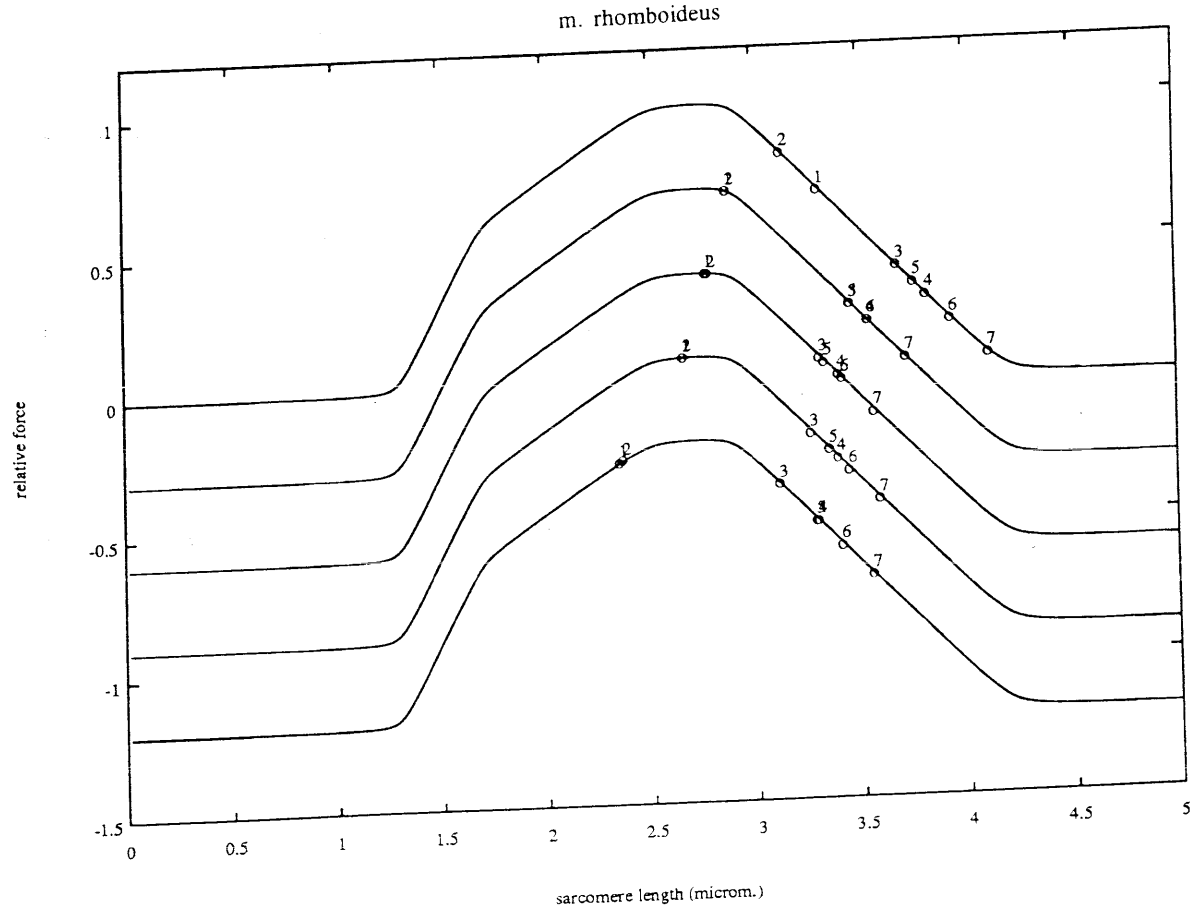

Figure D5, continuation. An abduction.

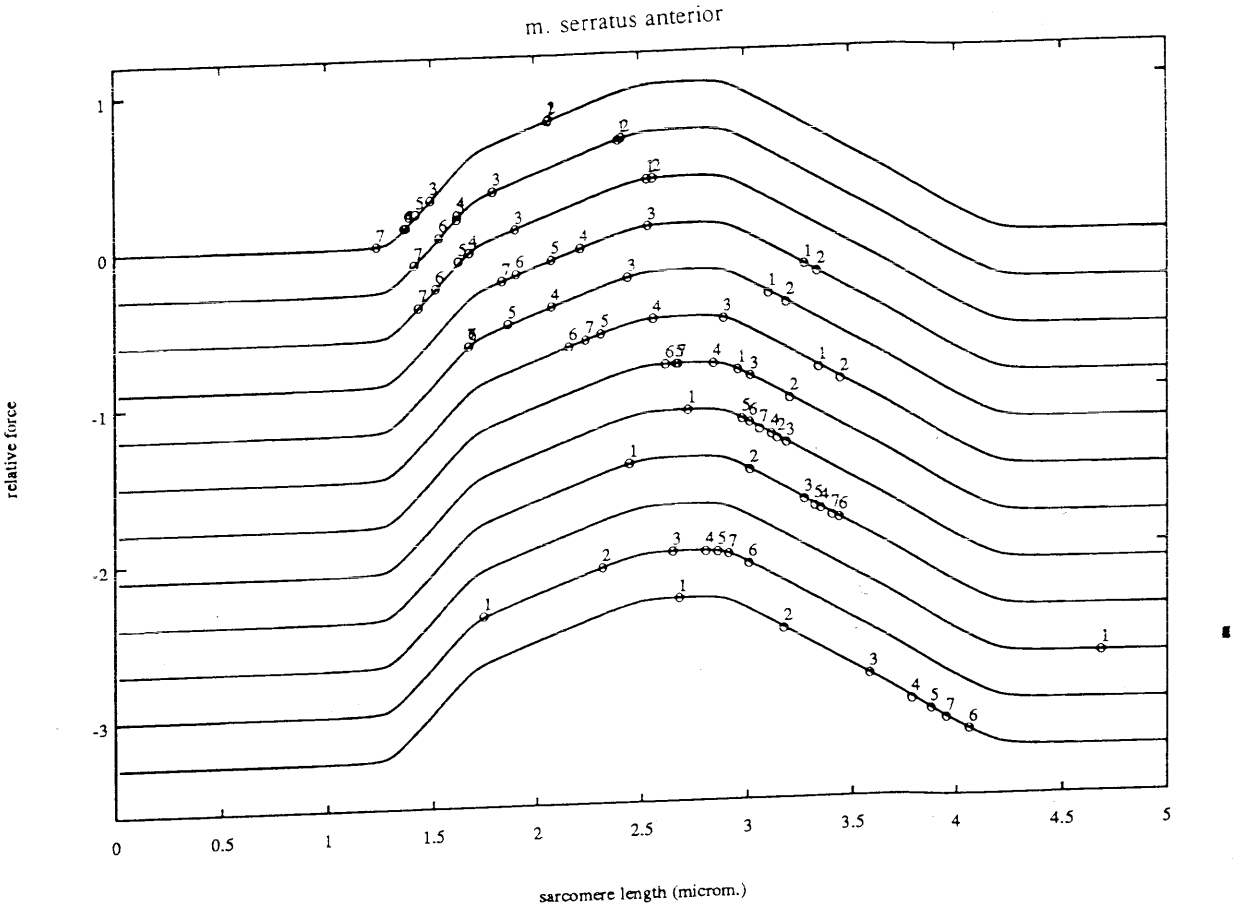

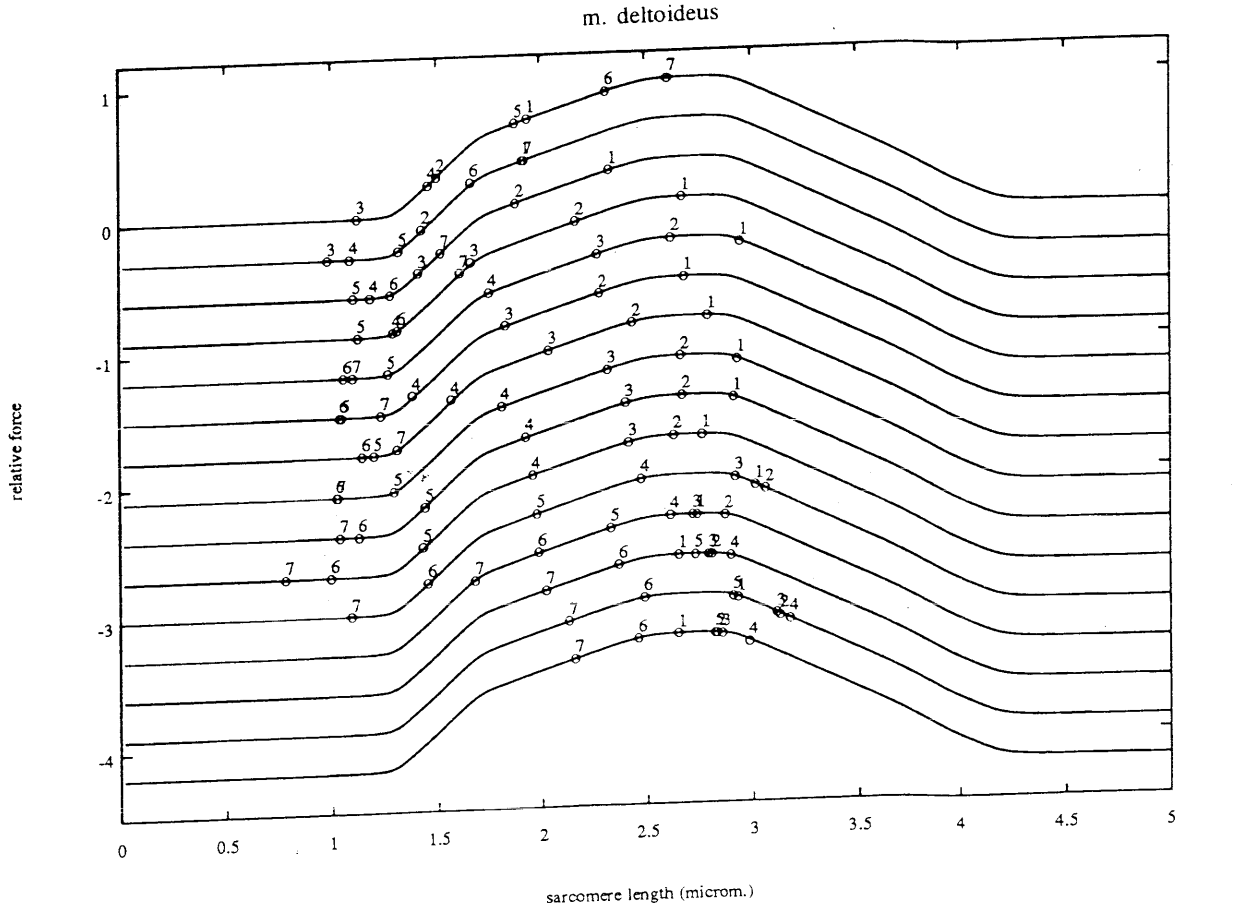

Figure D5, continuation. An abduction.

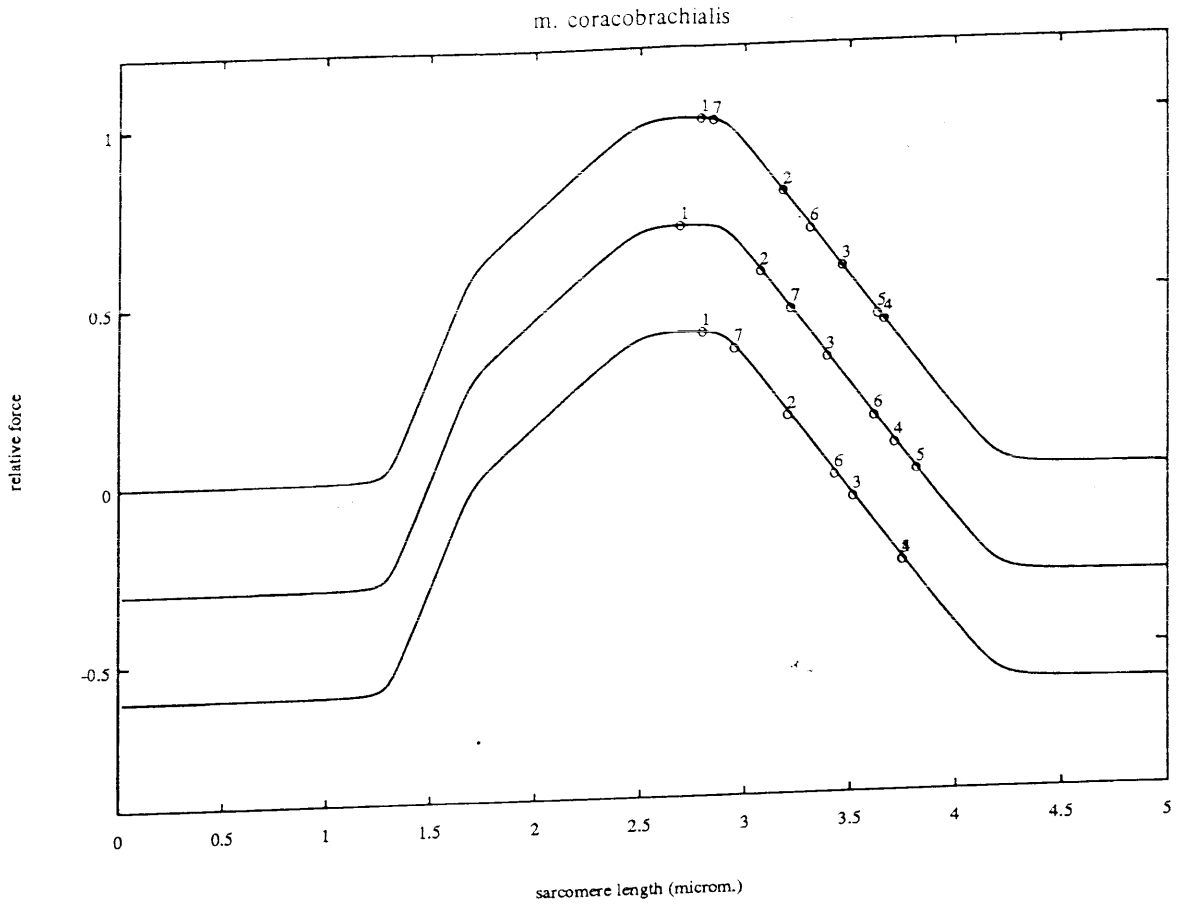

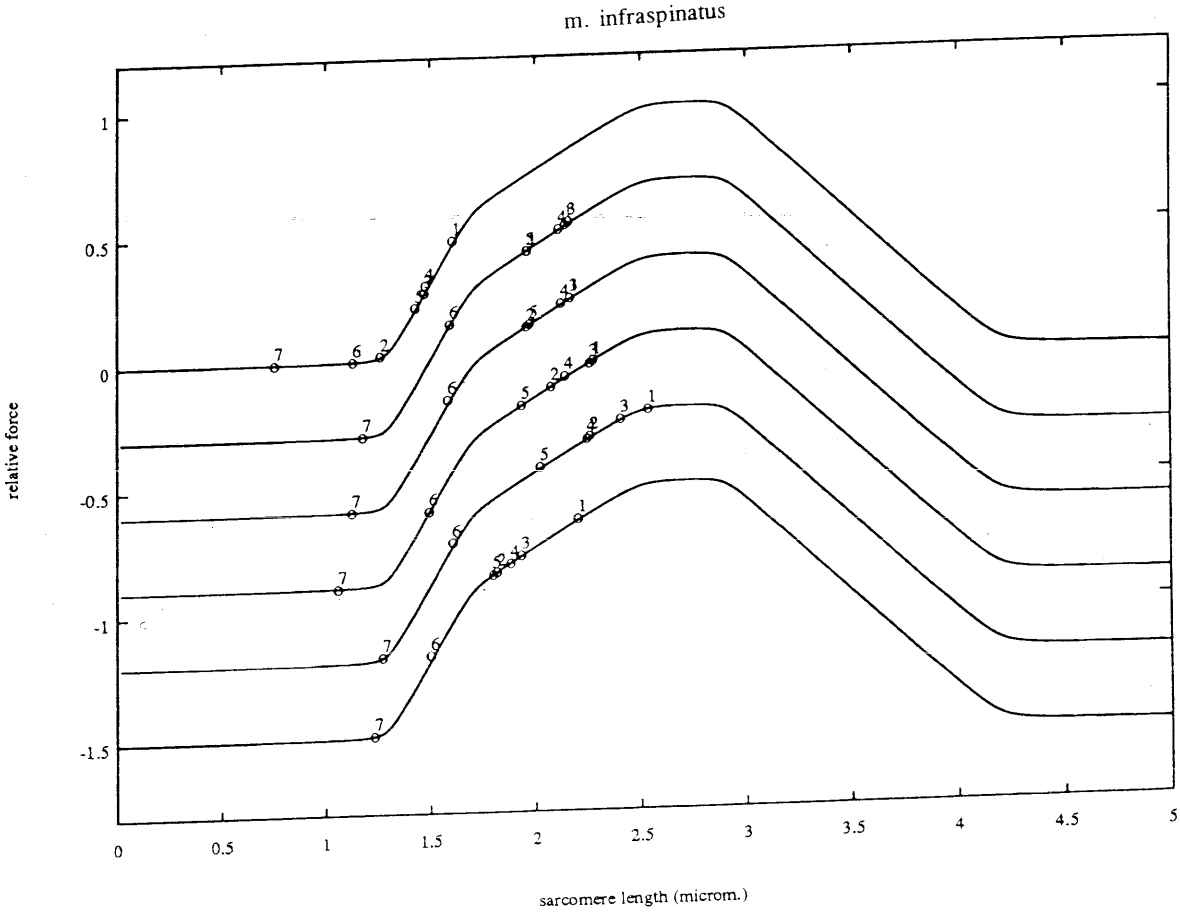

Figure D5, continuation. An abduction.

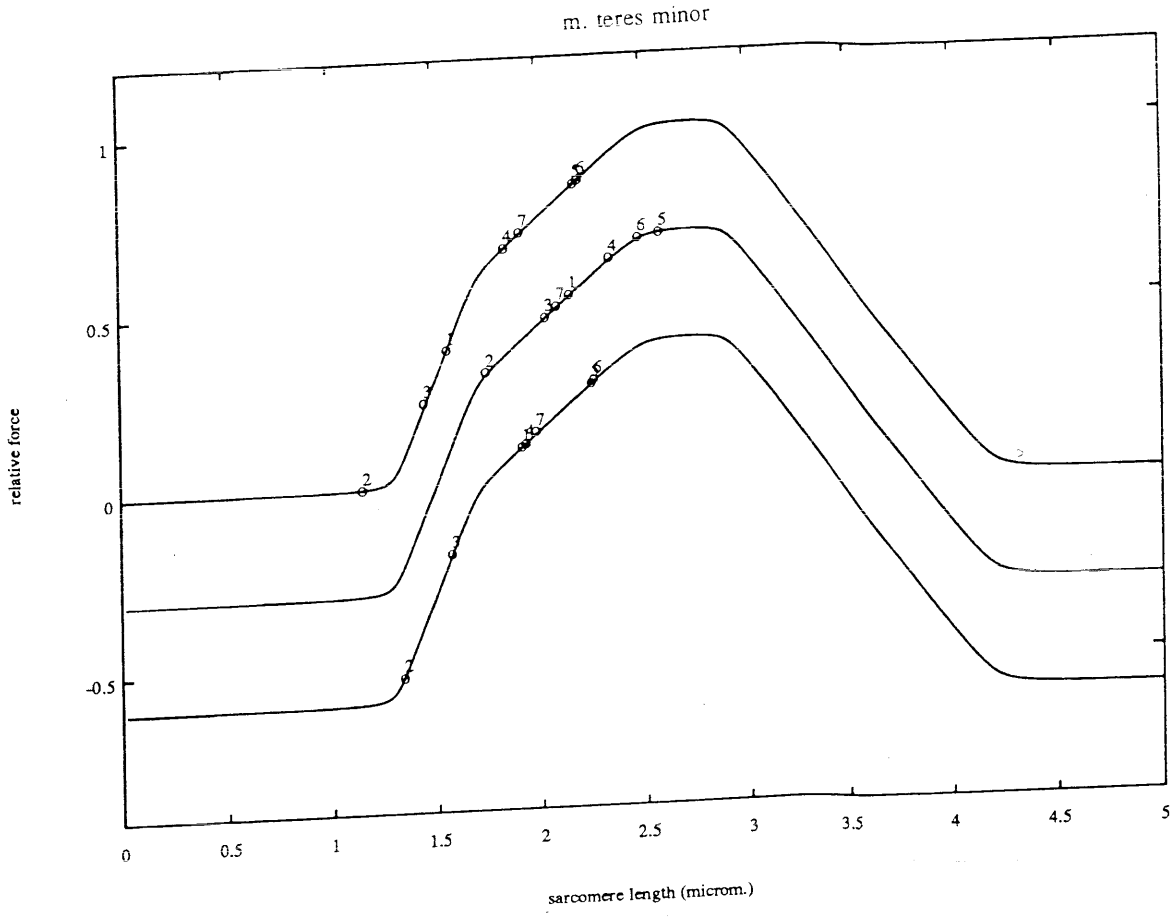

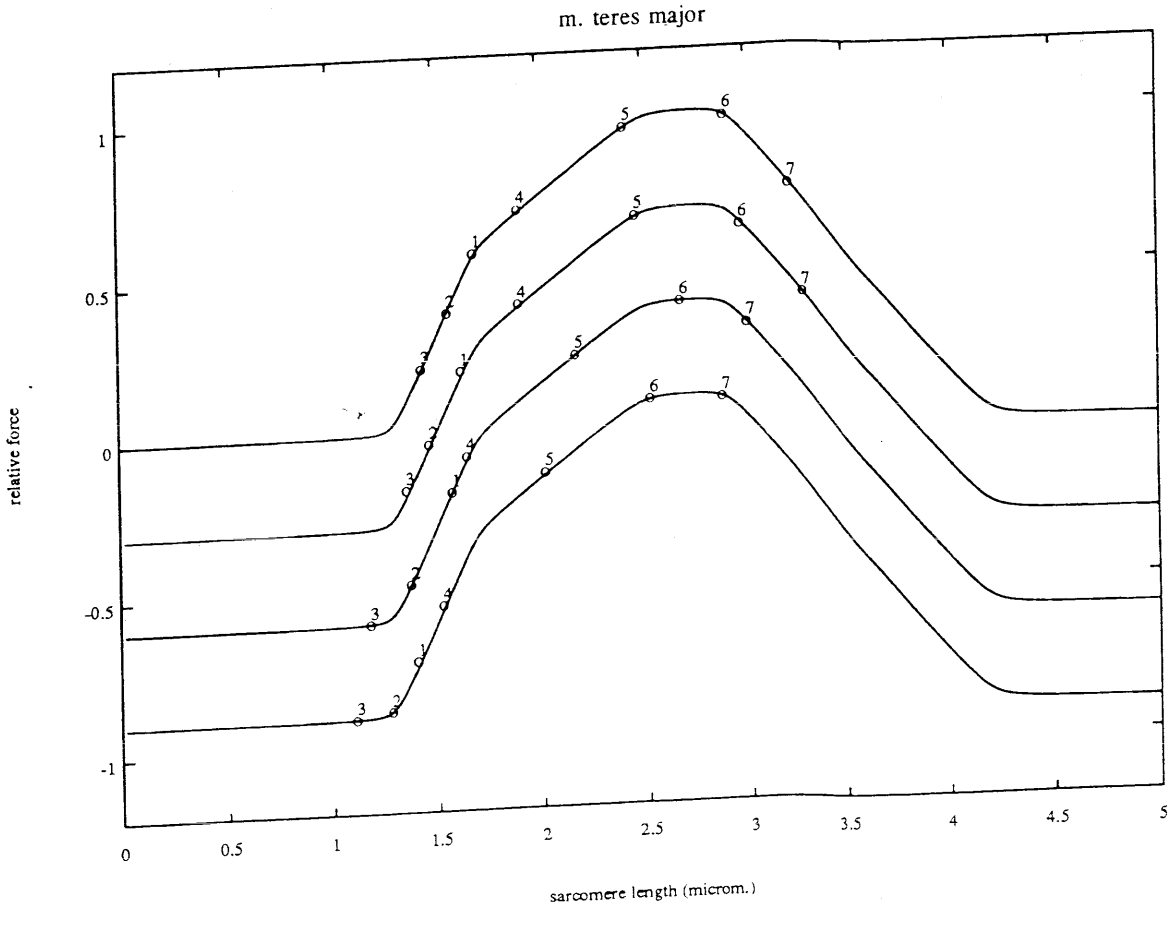

Figure D5, continuation. An abduction.

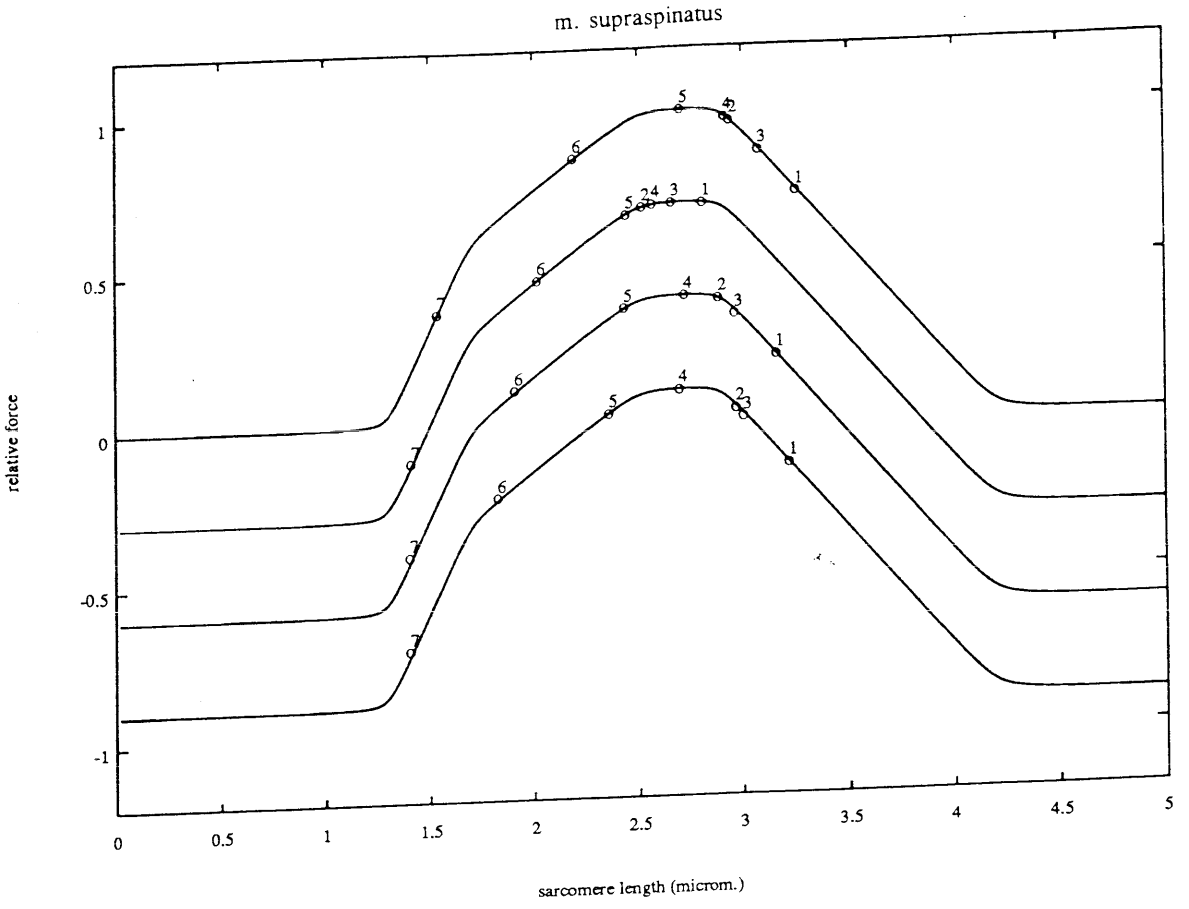

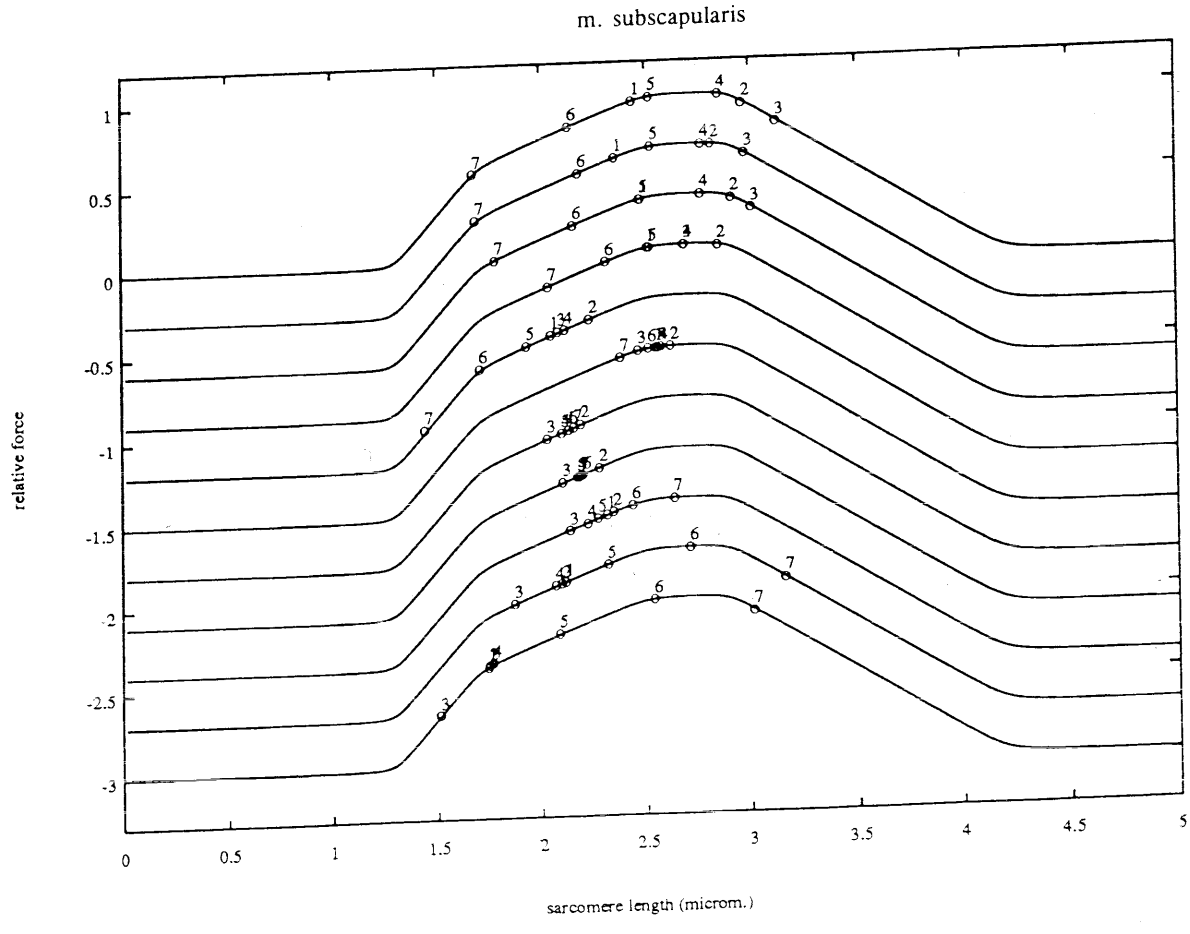

Figure D5, continuation. An abduction.

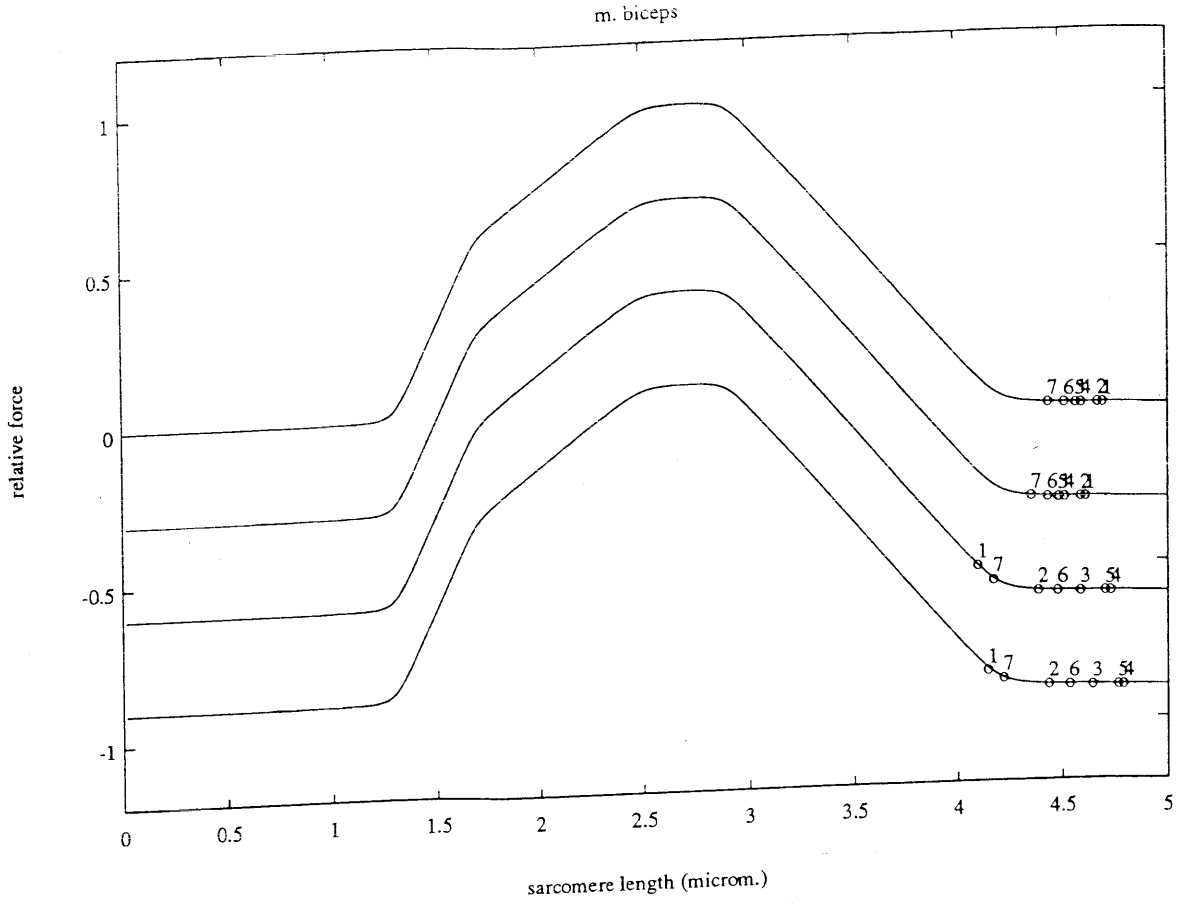

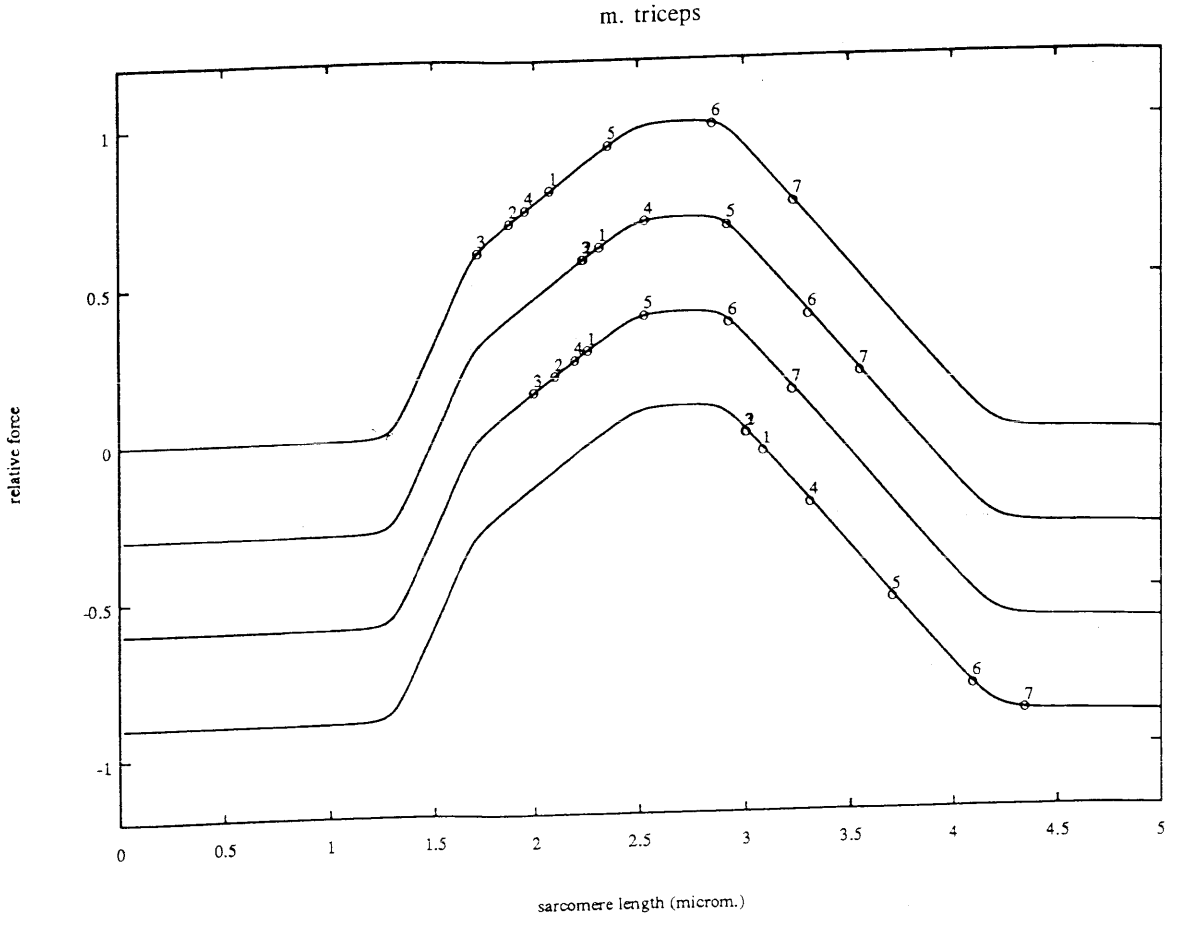

Figure D5, continuation. An abduction.

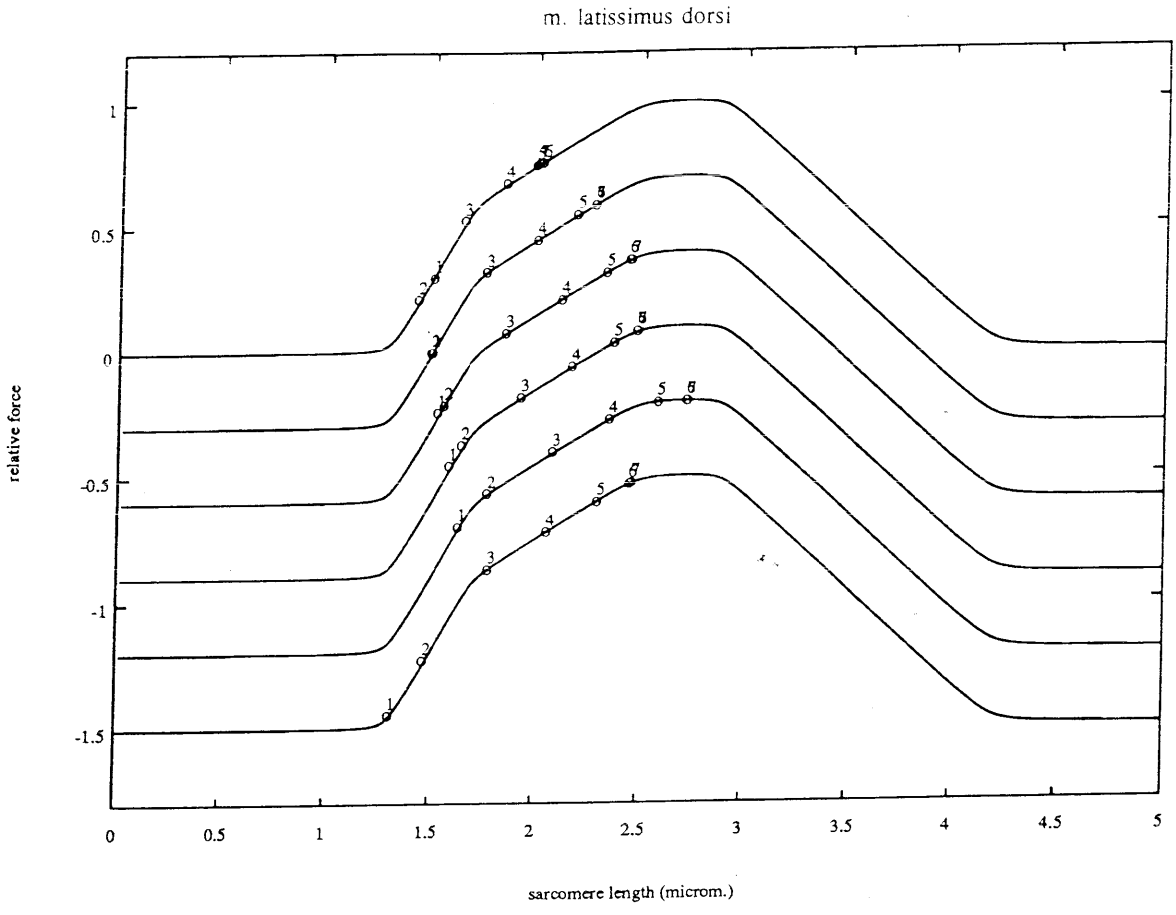

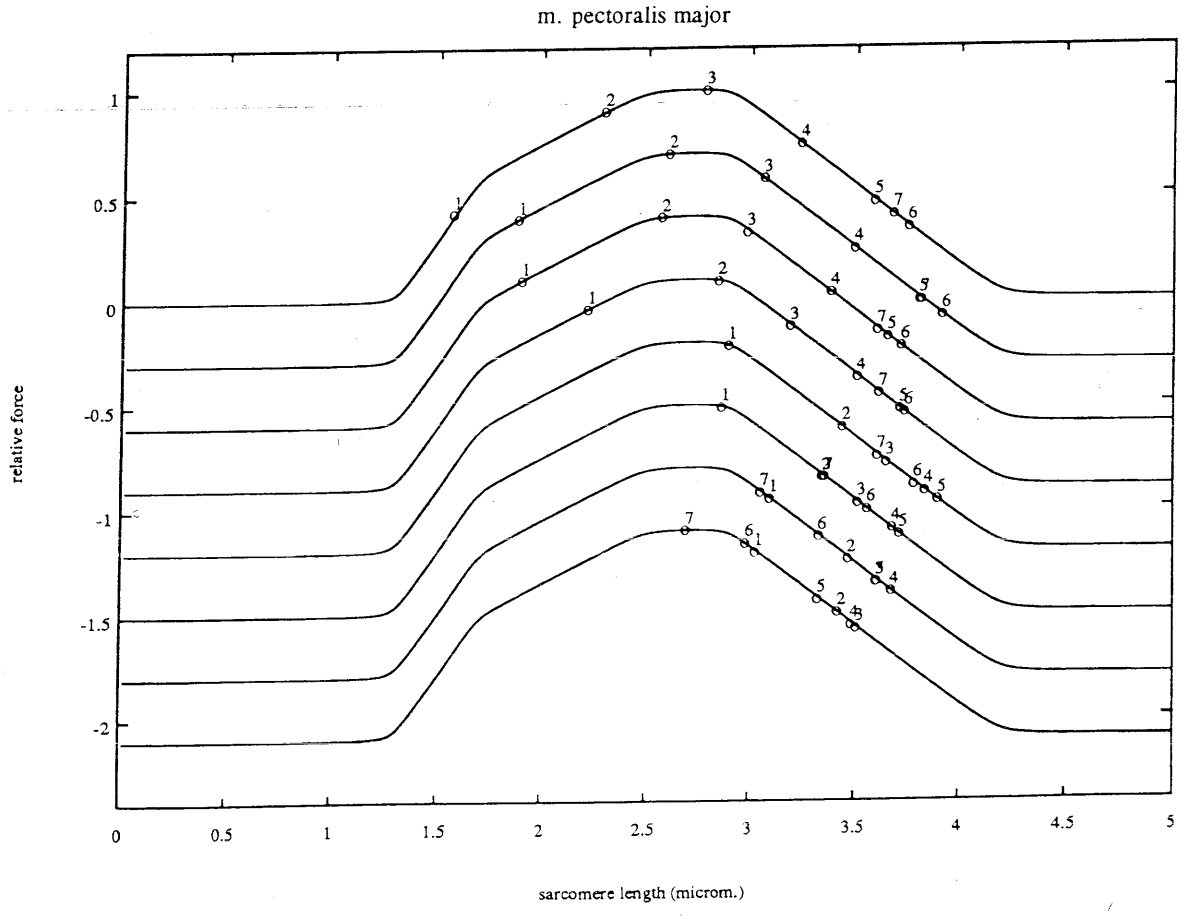

Figure D5, continuation. An abduction.

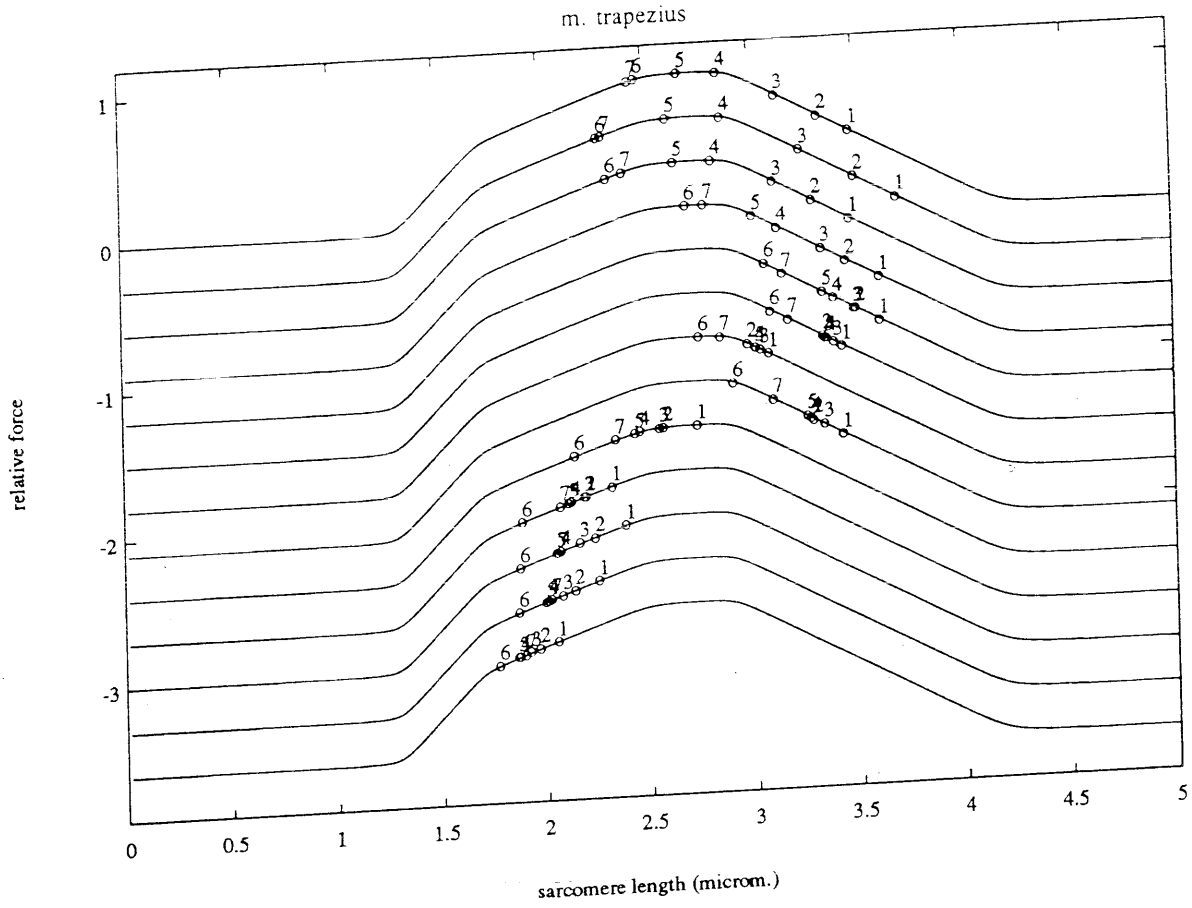

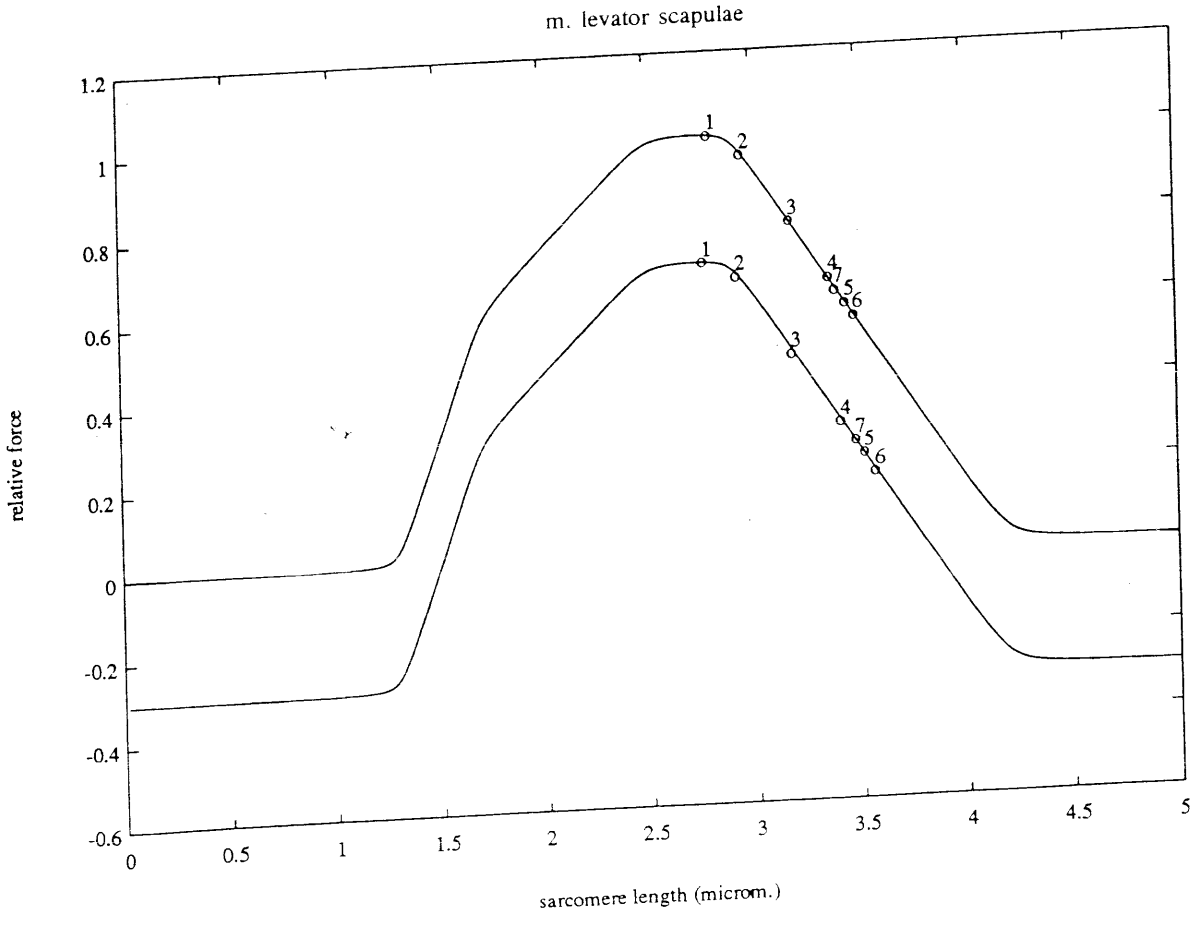

Figure D5. An anteflexion.
On the x-axis sarcomere length (in μm) and on the y-axis relative force. Each line represents the force-lengh relationship of one muscle part. The numbers represent the position during the anteflexion (position 1 is 0° anteflexion, position 7 is 180° anteflexion). The lines for each muscle part are plotted beneath each other. The scale on the y-axis only counts for the upper line.

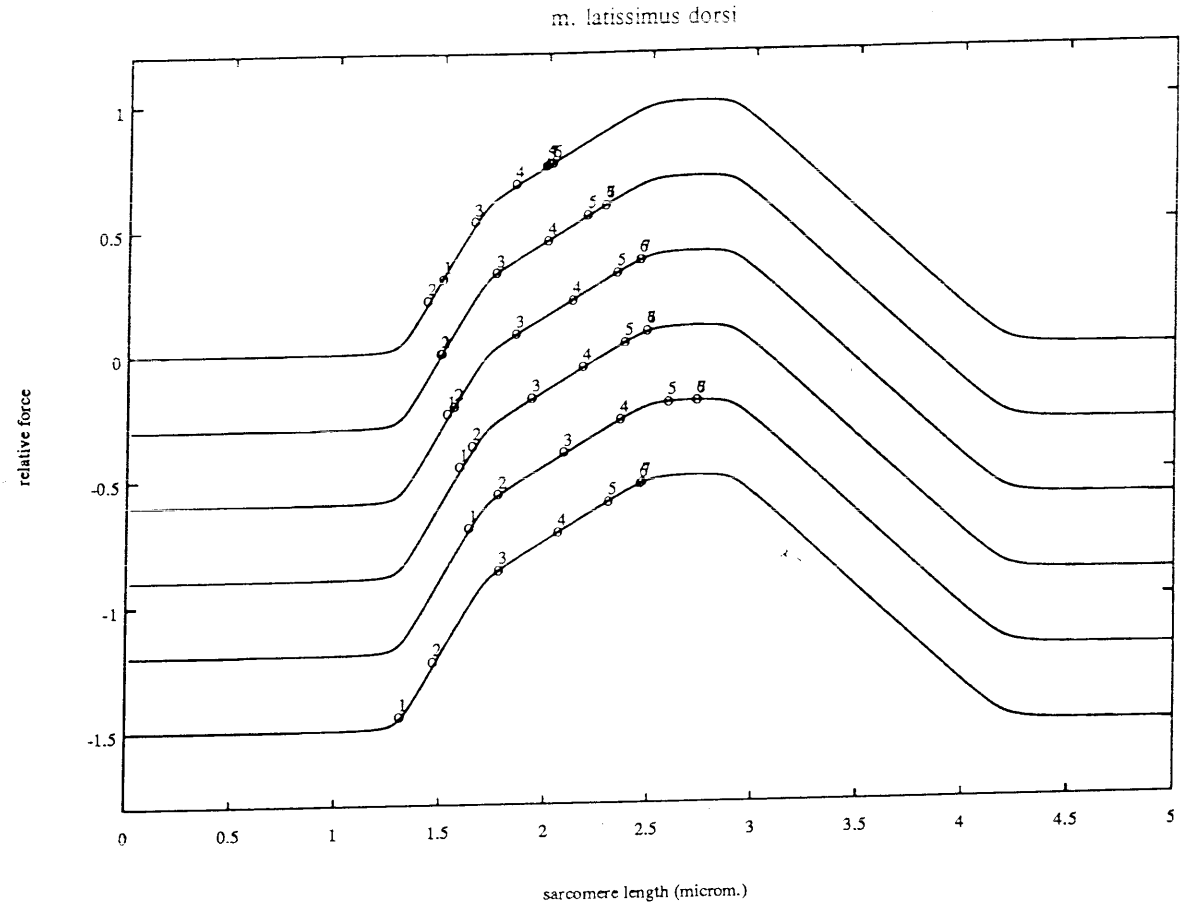

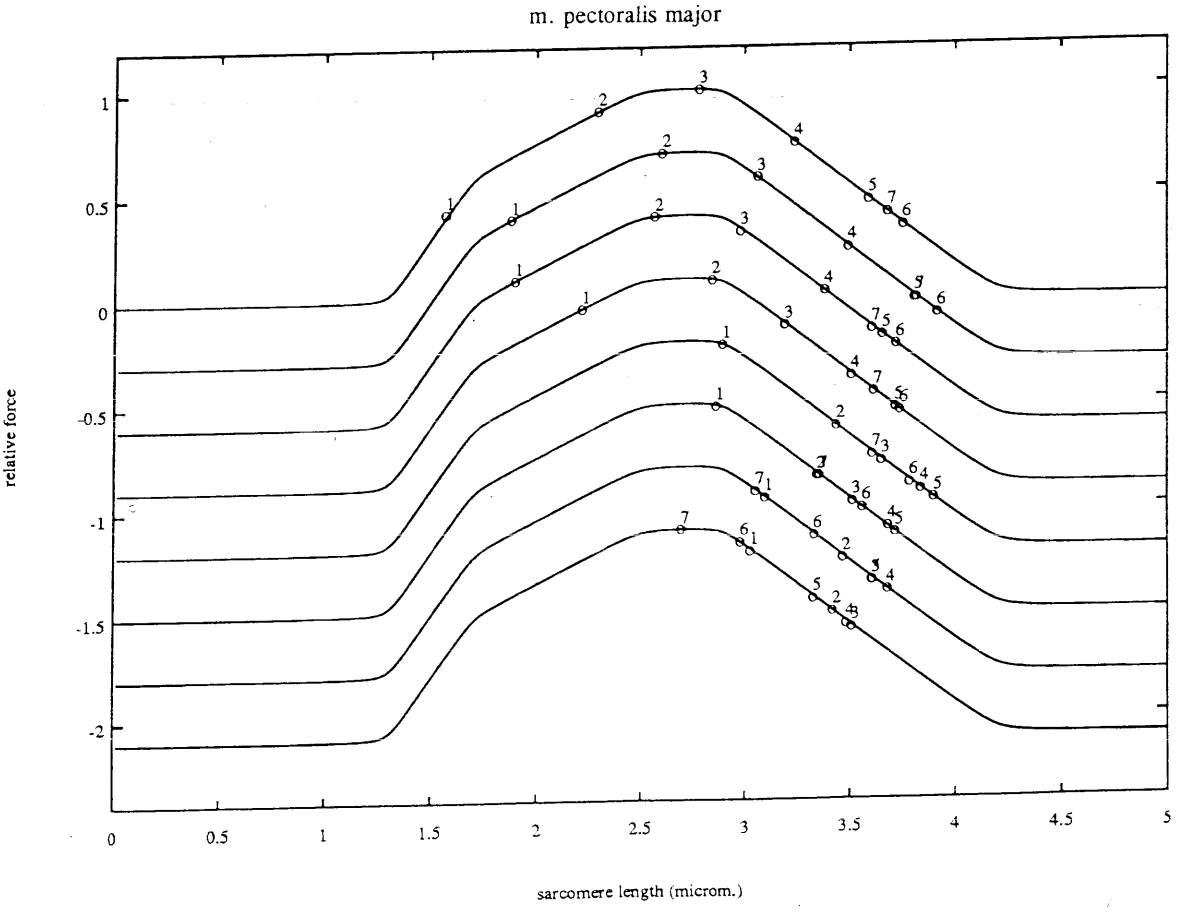

Figure D5, continuation. An abduction.

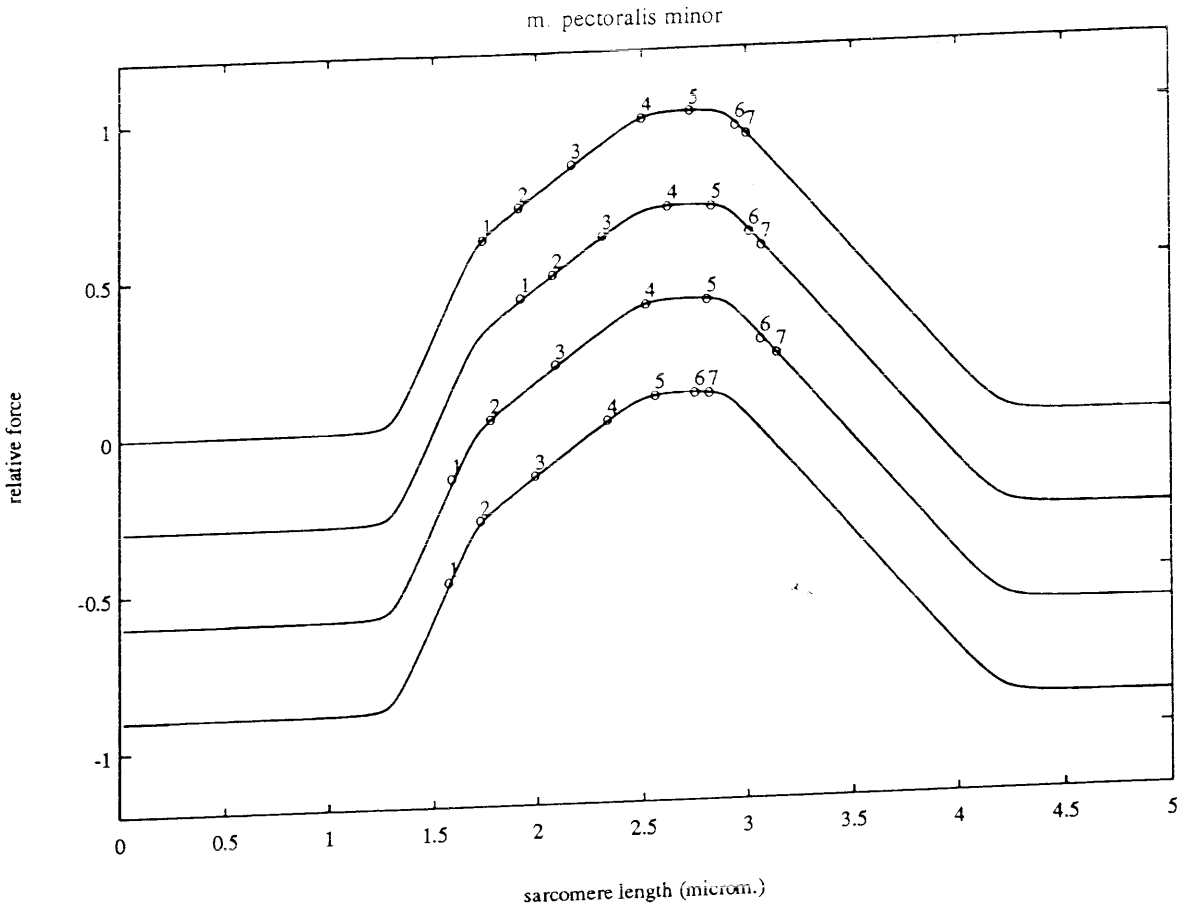

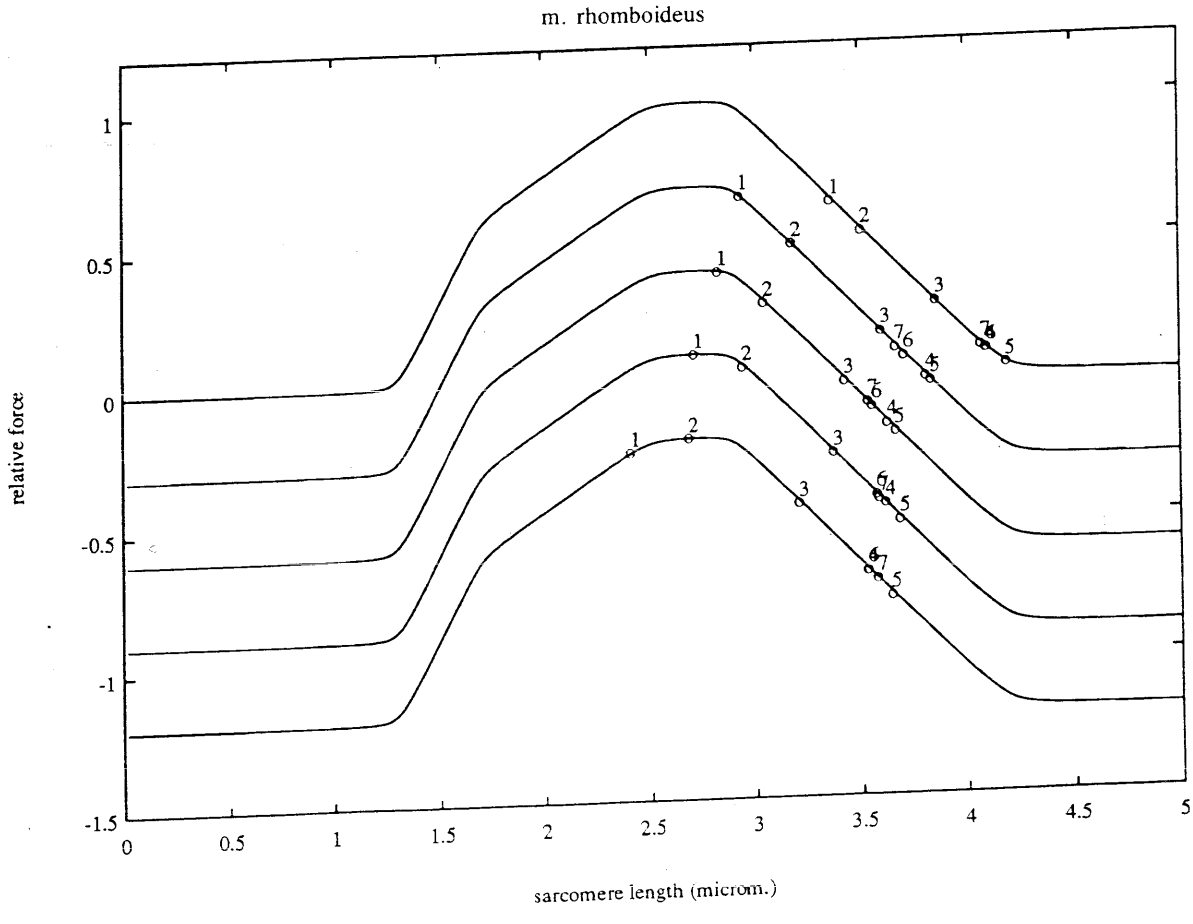

Figure D5, continuation. An anteflexion.

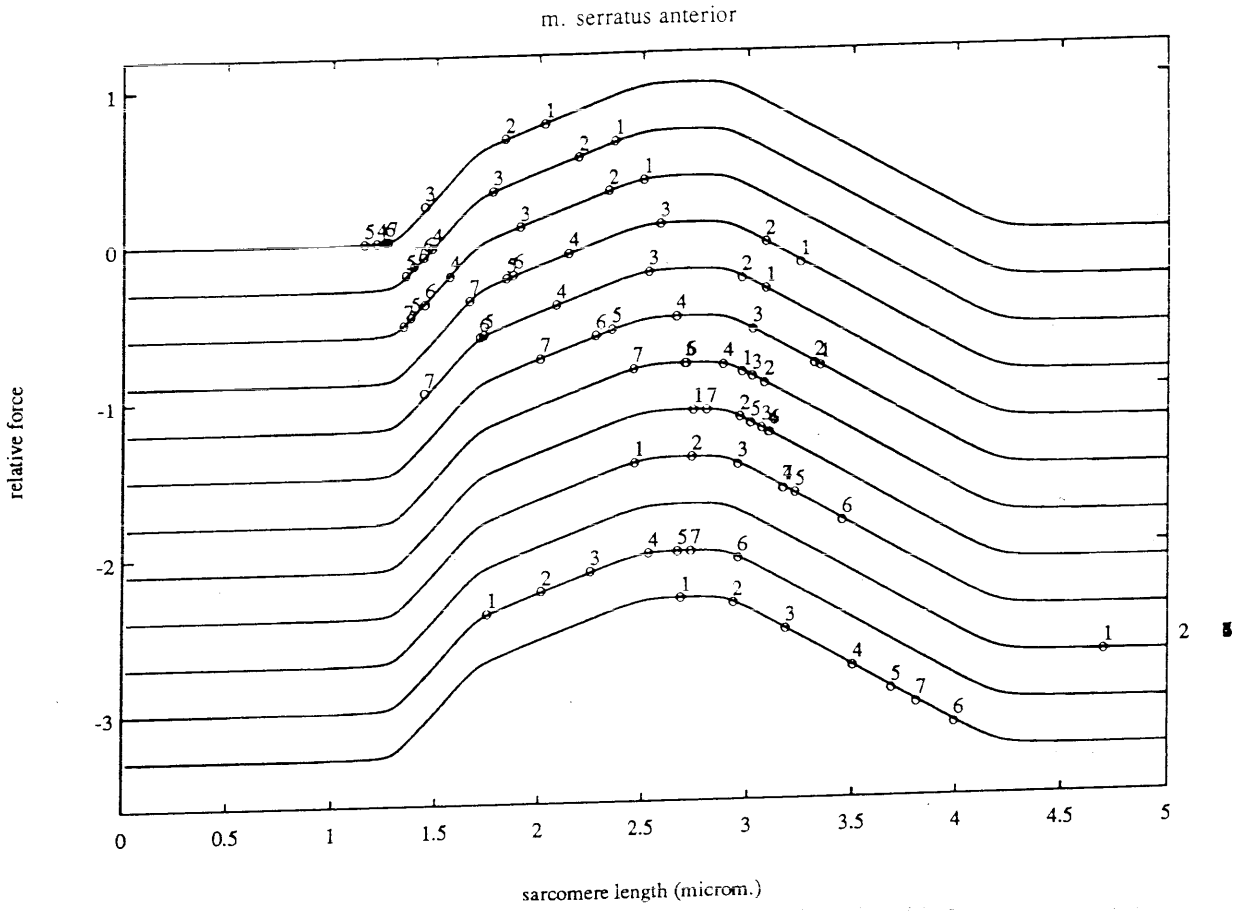

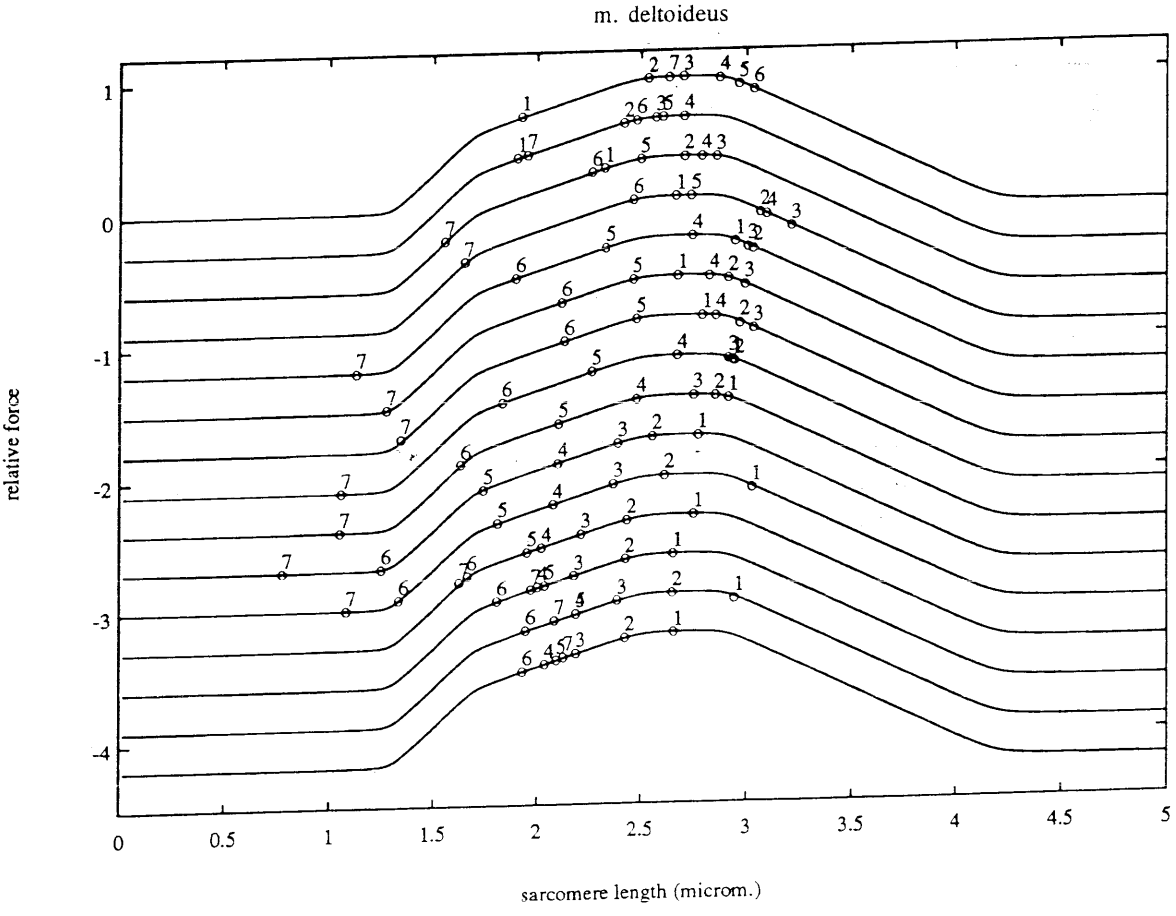

Figure D5, continuation. An anteflexion.

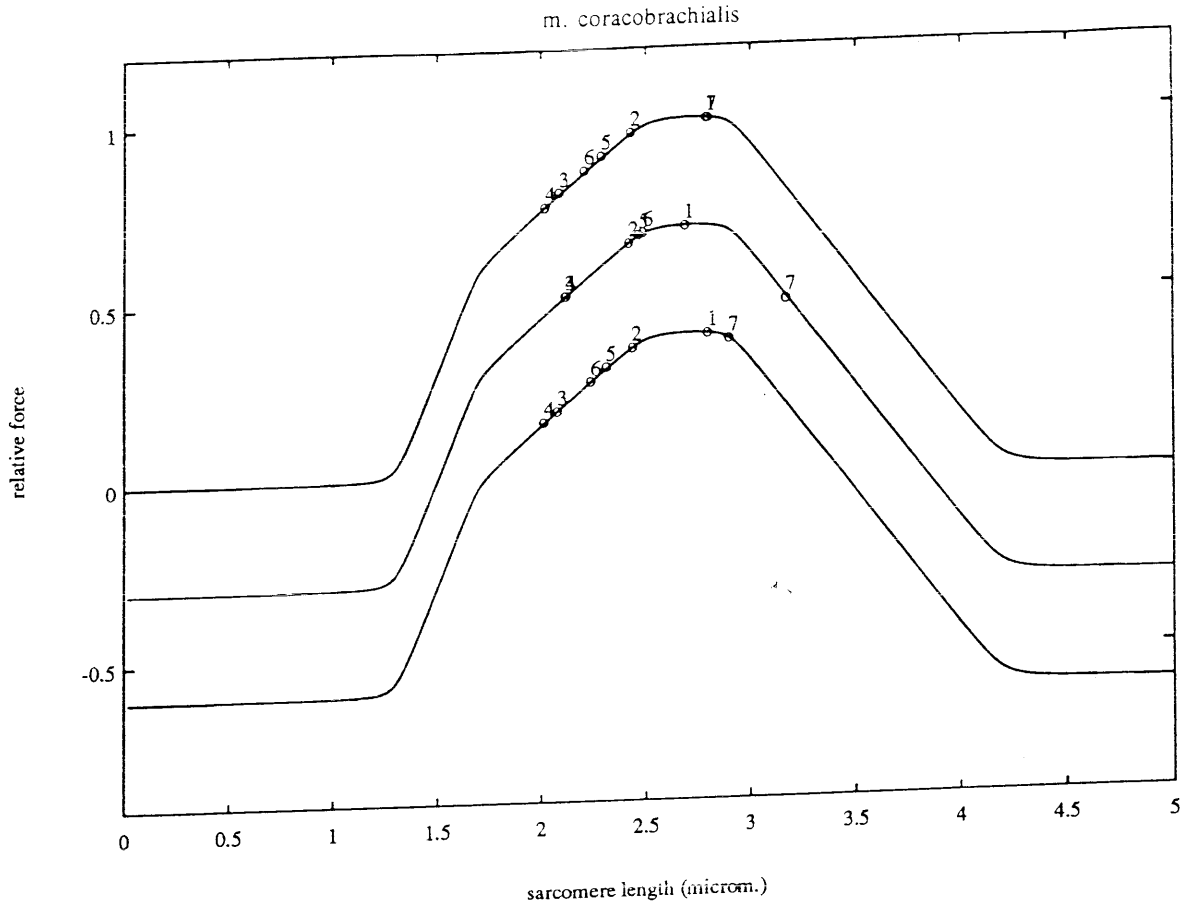

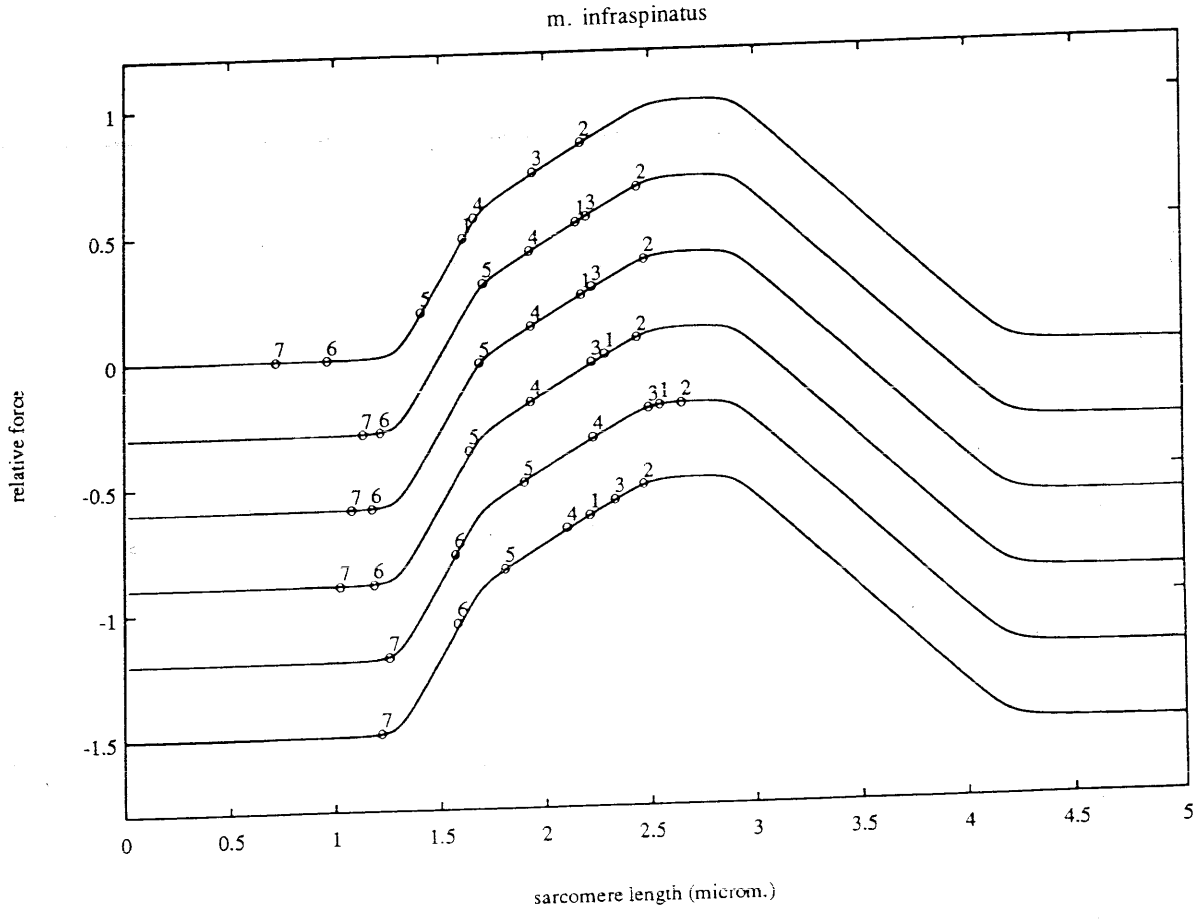

Figure D5, continuation. An anteflexion.

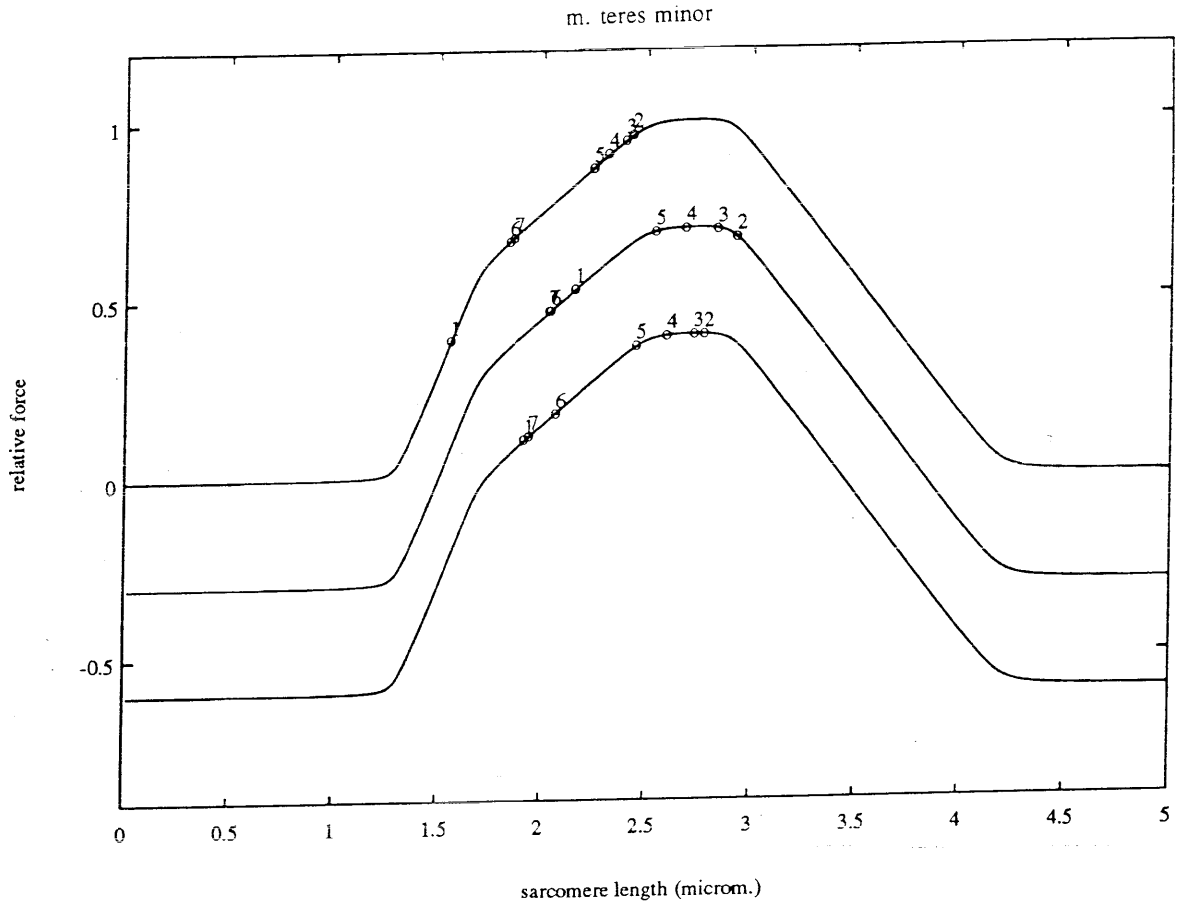

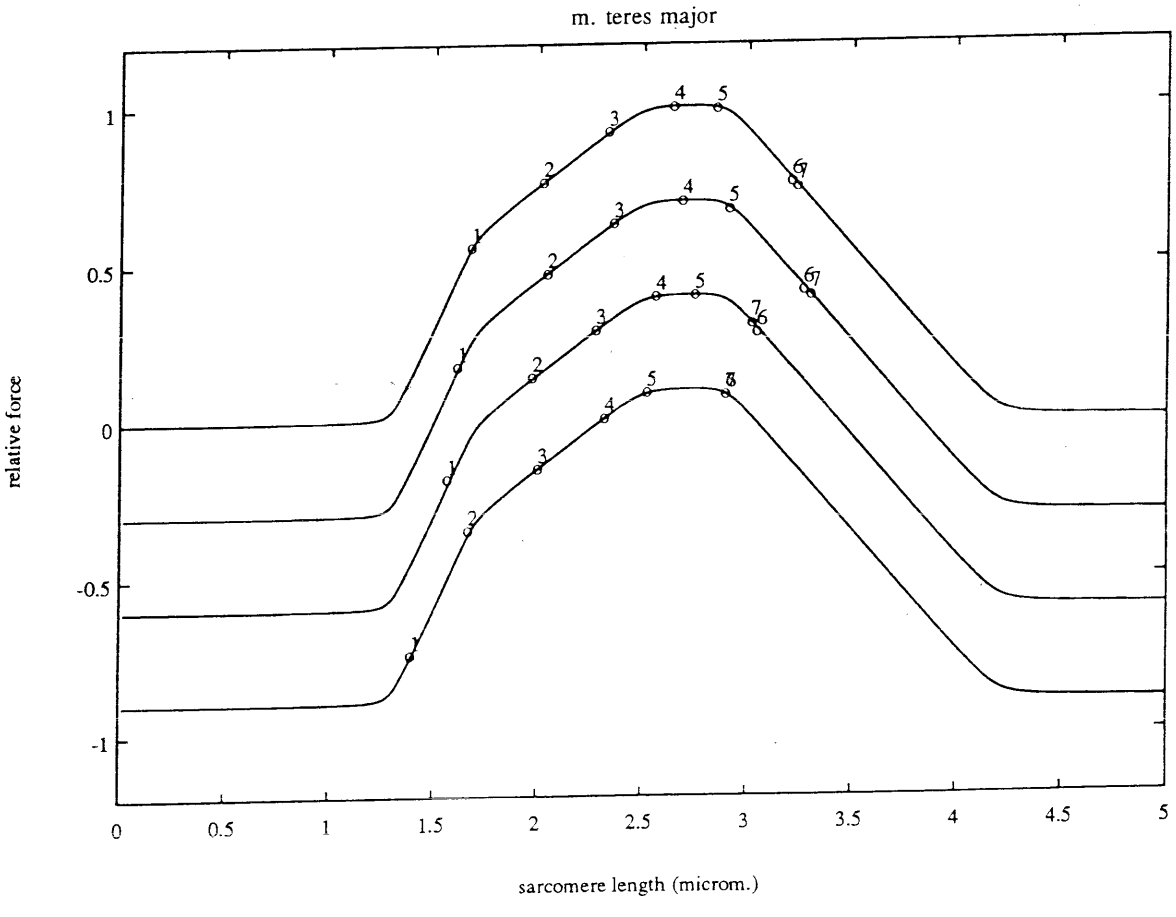

Figure D5, continuation. An anteflexion.

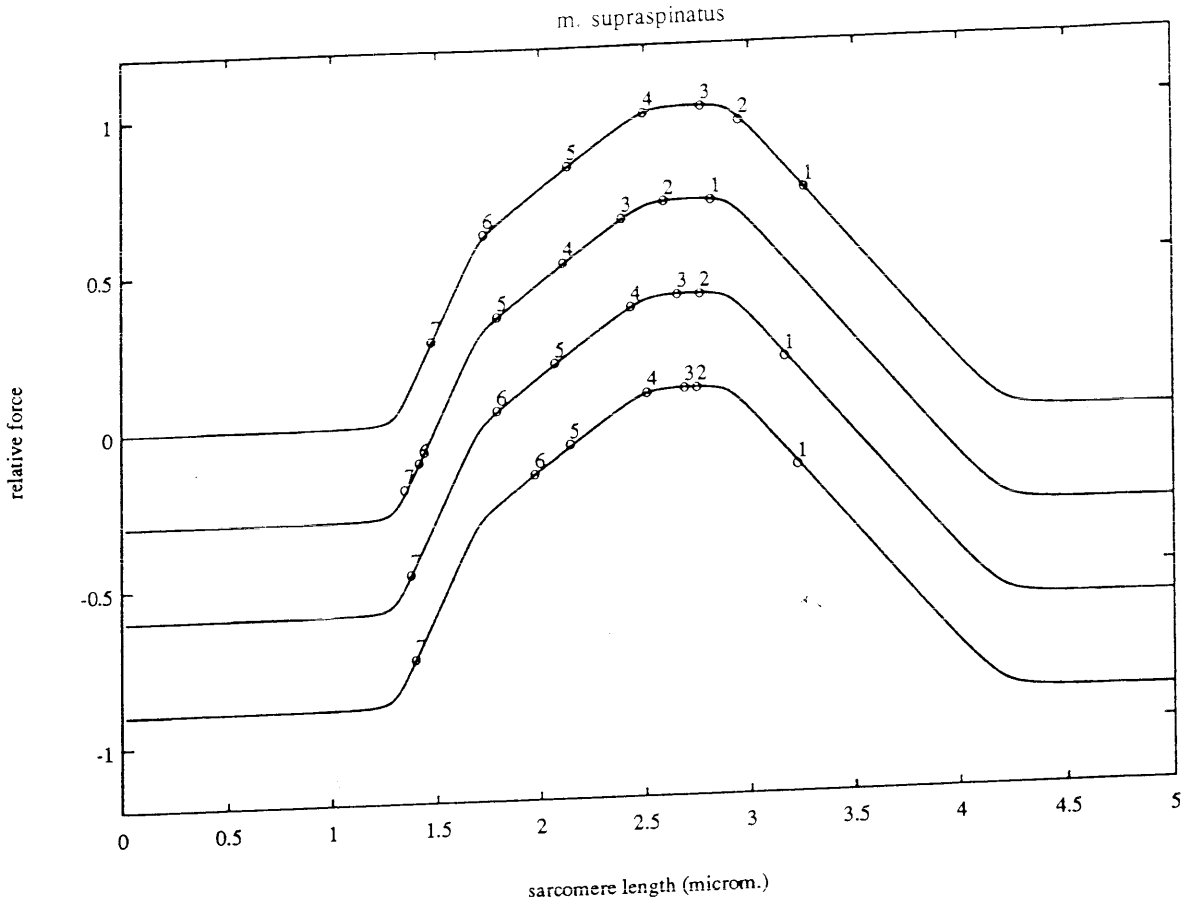

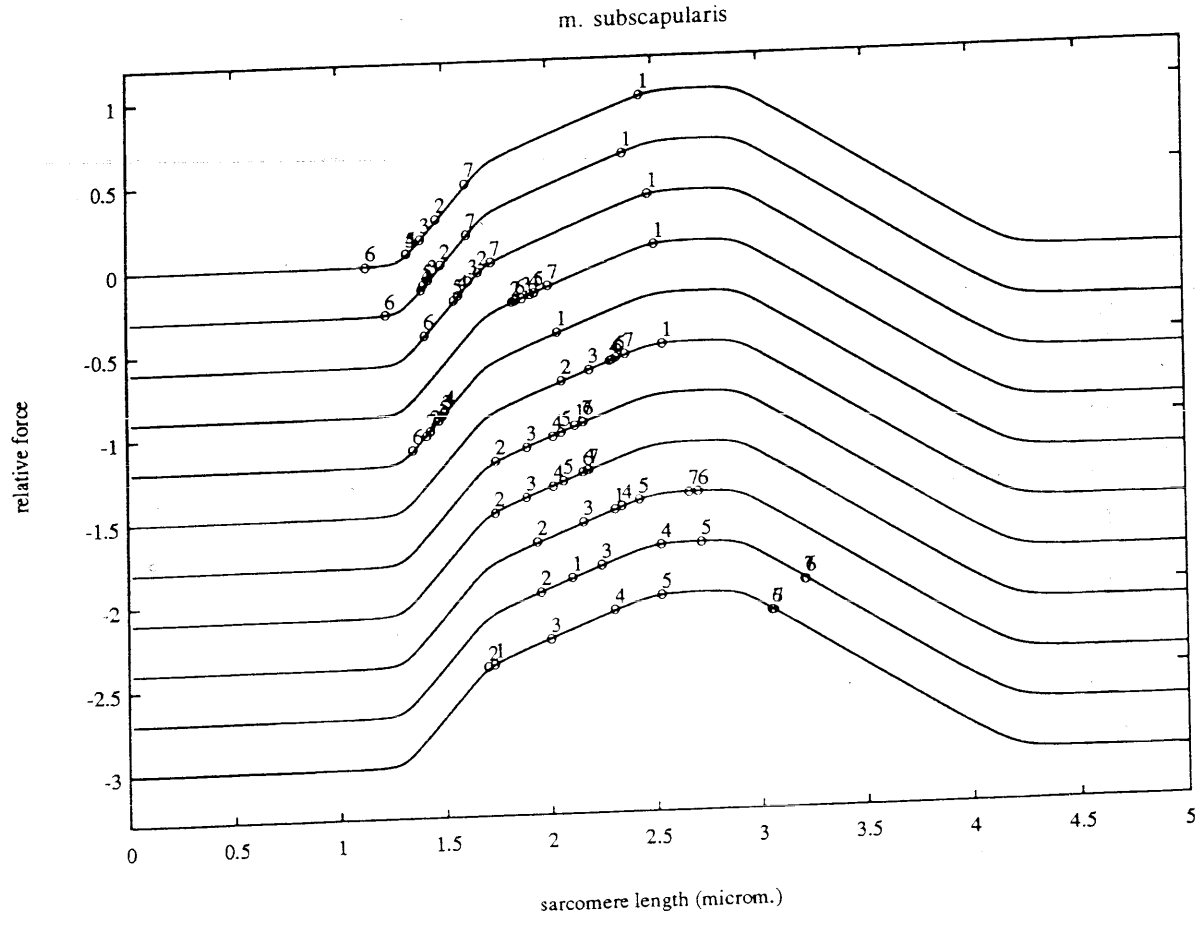

Figure D5, continuation. An anteflexion.

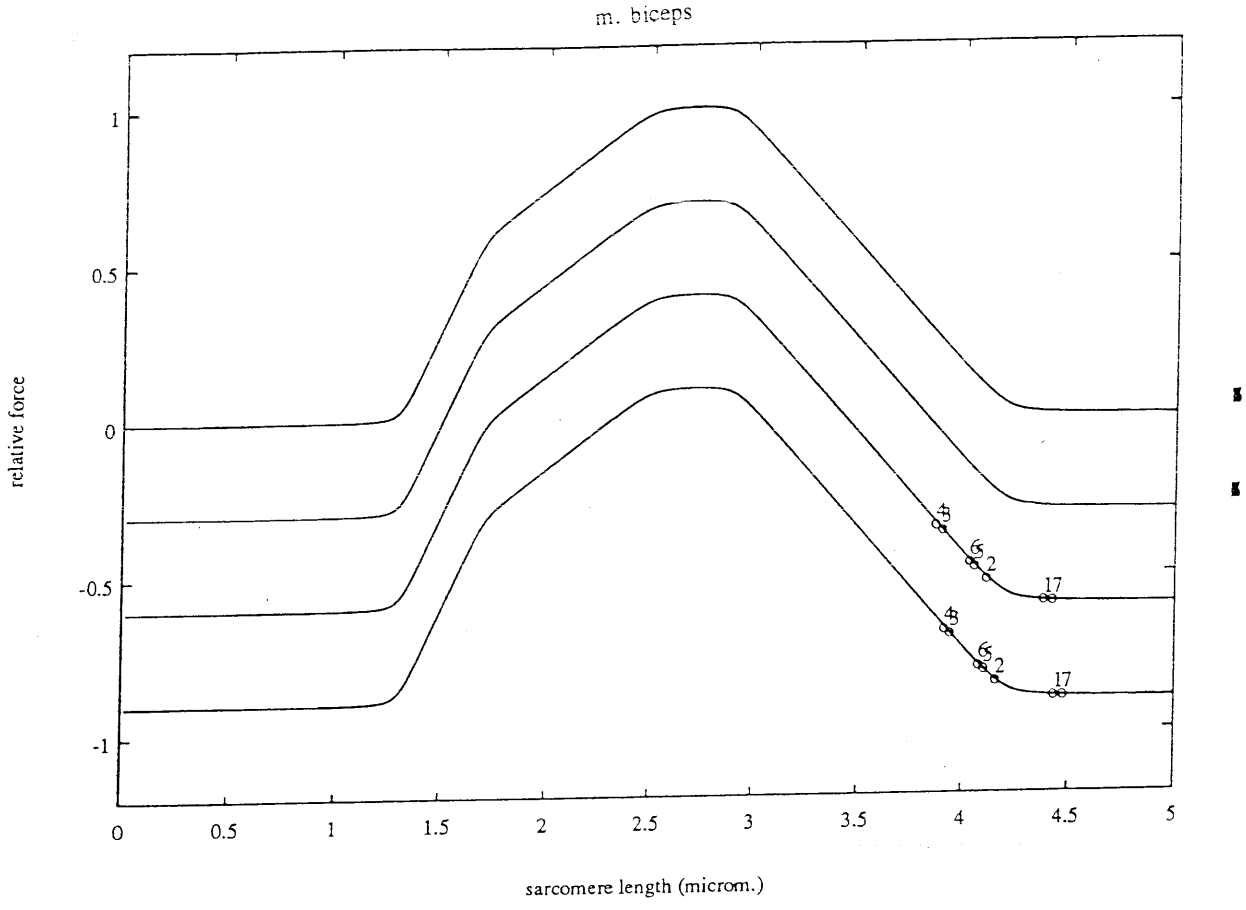

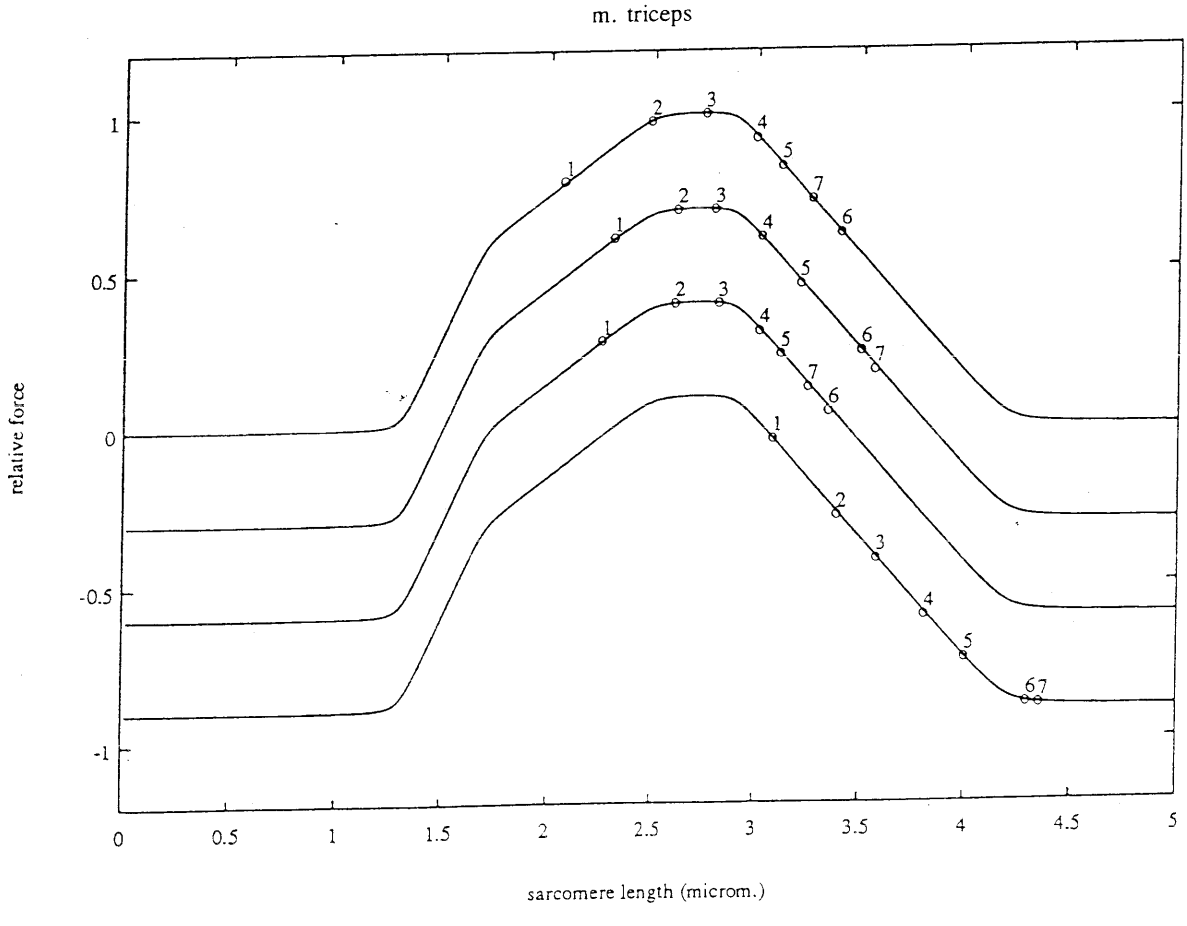

Figure D5, continuation. An anteflexion.

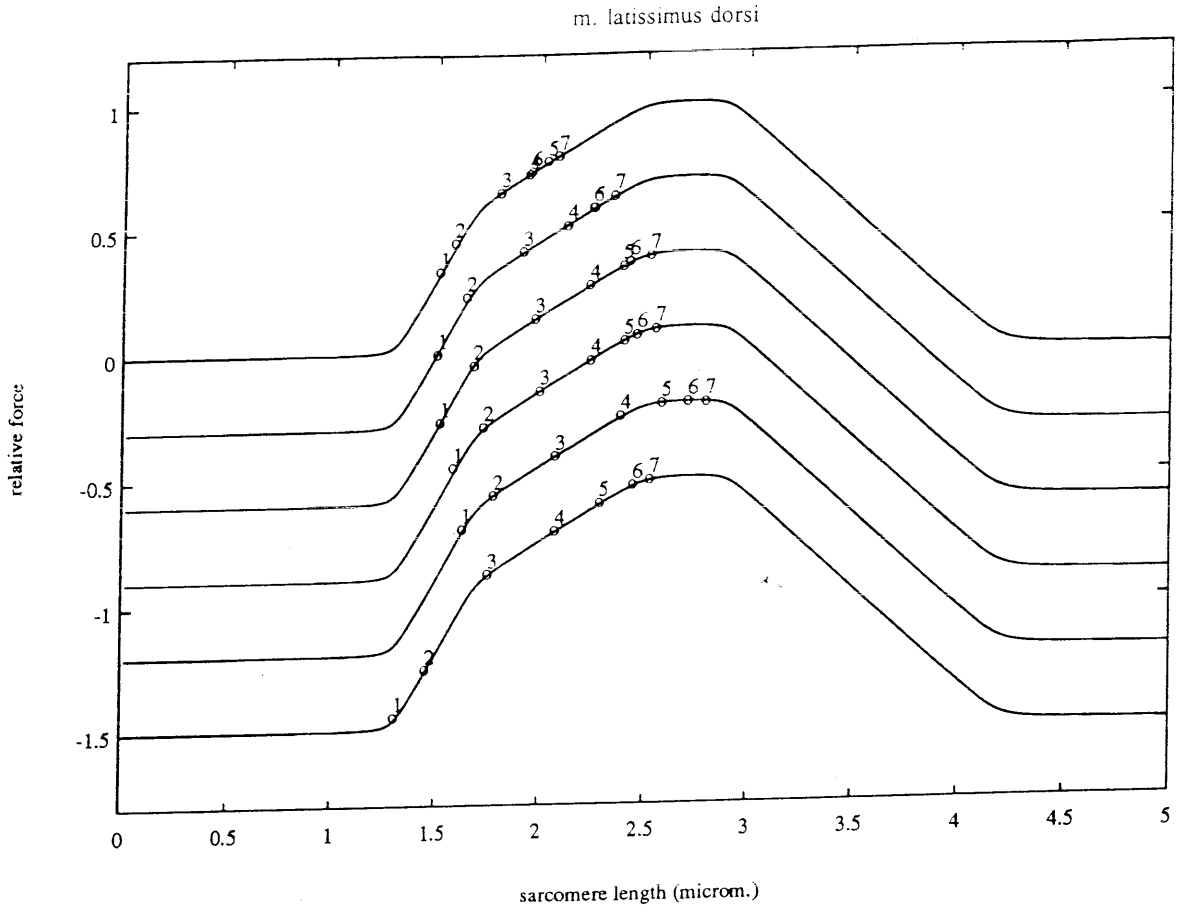

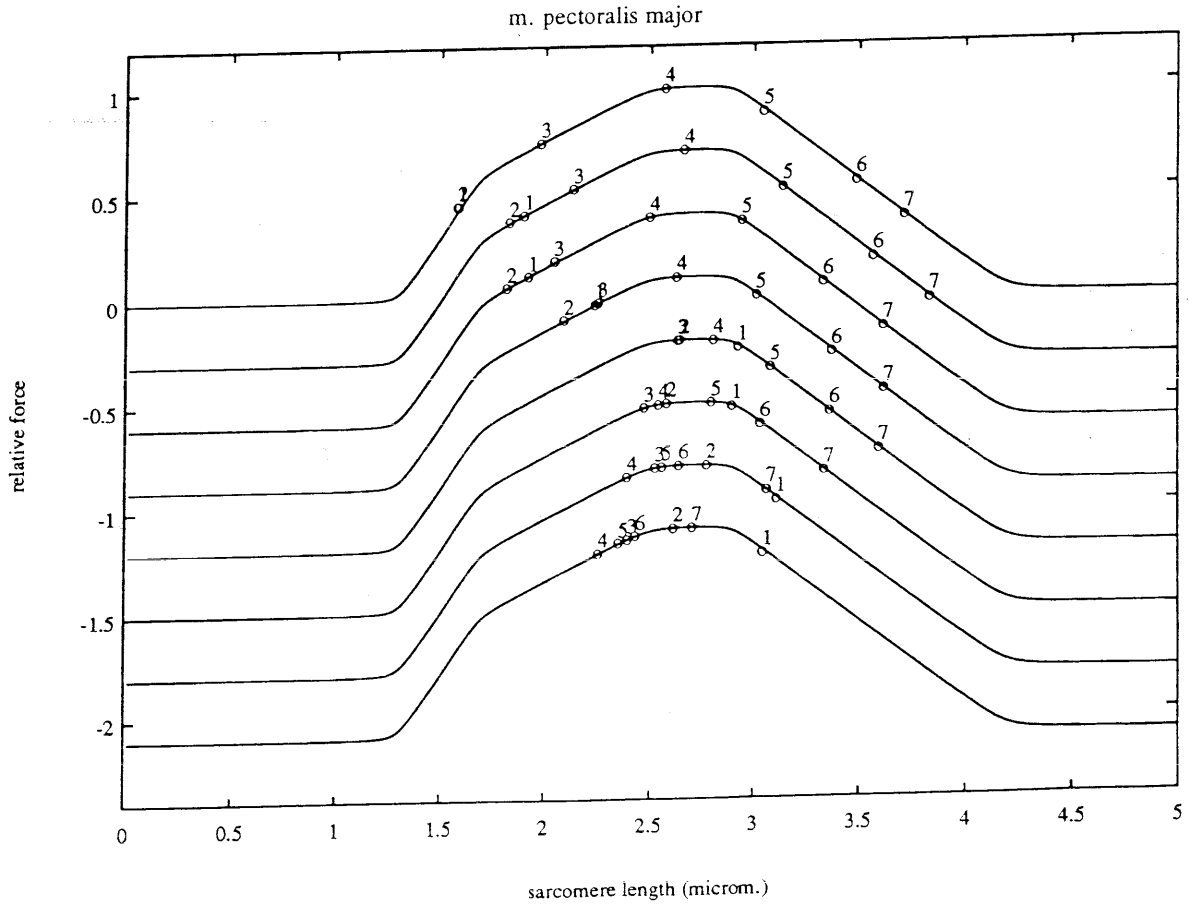

Figure D5, continuation. An anteflexion.